



Master Thesis

Polymer-derived ceramic layer structures with multi-scale porosity

Technische Universität Wien
Institute of Chemical Technologies and Analytics
Getreidemarkt 9/164-CT
1060 Wien

under supervision of Univ.Ass Dr. Thomas Konegger
and Ao.Univ.Prof. Dipl.-Ing. Dr.techn. Roland Haubner

Christina Drechsel BSc
Bleichergasse 1/15, 1090 Vienna

Vienna, 12.09.2016

Abstract

Layered $\text{Si}_3\text{N}_4/\text{SiCN}$ structures with multi-scale porosity were prepared with the future aim of using them as a membrane. The focus was set on finding a method to produce a dense selective layer on a macroporous support via dipcoating with a solution of a preceramic polymer. The planar (disk-shaped) supports were prepared in two different ways, on the one hand via slipcasting (resulting in Si_3N_4) varying the slip loadings and sintering temperatures, on the other hand using the polymer derived route (resulting in SiCN) including the use of polyethylene as a sacrificial filler.

It was necessary to put an intermediate layer on top of the support, which was prepared by dip coating/slip casting with a Si_3N_4 /preceramic polymer solution. Producing a dense top layer was then tested on these two-layered structures without any further treatment and in following experiments with additionally using masking techniques. The permeation behaviour of the structures was measured.

Additional experiments were conducted to set up a model for the relation between withdrawal speed and resulting layer thickness of the dipping solutions that were used to prepare the selective layer. These experiments were carried out on dense substrates. Properties like viscosity and surface tension of the dipping solutions were measured to see if the existing model by Landau-Levich fits the experimental data or has to be adapted.

On both support structures, the slip cast type and the polymer derived ceramic (PDC) type, an intermediate layer (with a thickness of $\sim 30 \mu\text{m}$) could be successfully deposited. A surface modification (silanisation) of the silicon nitride powder of the intermediate layer slip was necessary. The PDC-supports had to be ground to yield a homogenous layer. Using polystyrene as sacrificial mask for the intermediate layer (and the support structure), a fully covering top layer was achieved in the crosslinked stage on both of the support types. The porosity of the underlying layers was preserved after pyrolysis. The results of the planar samples were successfully adapted to the tubular samples.

Kurzfassung

Schichtstrukturen aus $\text{Si}_3\text{N}_4/\text{SiCN}$ mit multiskalärer Porosität wurden mit dem Ziel, sie zukünftig als Membran verwenden zu können, hergestellt. Das Hauptaugenmerk wurde dabei darauf gelegt, eine Methode zu entwickeln, um eine dichte Schicht auf eine makroporöse Gerüststruktur aufzubringen. Dies sollte mittels Tauchbeschichtung mit präkeramischem Polymer geschehen. Die zur Methodenentwicklung beschichteten Gerüststrukturen sind planar und tablettenförmig und wurden auf zwei verschiedene Arten hergestellt: Zum einen über Schlickerguss (Si_3N_4), wobei die Feststoffbeladung des Schlickers und die Sinteremperatur variiert wurden, zum anderen über die polymerabgeleitete Route (SiCN) unter Verwendung von UHMW-PE als Opferfüllstoff.

Es stellte sich heraus, dass eine Zwischenschicht auf die Gerüststruktur aufgebracht werden muss, die über Tauchbeschichtung/Schlickerguss mit einem Schlicker aus Si_3N_4 -Pulver und dem präkeramischem Polymer hergestellt wird. Auf die so hergestellten zweischichtigen Strukturen wurden dann zuerst ohne weitere Behandlung und in folgenden Experimenten unter Verwendung einer Maskierungstechnik versucht, die dichte Schicht aufzubringen. Die Permeabilität wurde bestimmt.

Außerdem wurde in Vorversuchen ein Modell aufgestellt, um den Zusammenhang zwischen Ziehgeschwindigkeit und Schichtdicke der Tauchbeschichtungslösungen, die für die dichte, oberste Schicht verwendet werden, darzustellen. Diese Versuche wurden auf dichten Substraten, nämlich Glasplatten, durchgeführt. Sowohl Viskosität als auch Oberflächenspannung dieser Lösungen wurden gemessen, um zu überprüfen, ob das bestehende Landau-Levich-Modell hier verwendet werden kann, oder angepasst werden muss.

Sowohl auf die über Schlickerguss hergestellten als auch auf die PDC-Gerüststrukturen konnte erfolgreich eine Zwischenschicht (~30 μm dick) aufgebracht werden. Allerdings war die Silanisierung des Siliziumnitridpulvers und die Oberflächenbehandlung der PDC-Gerüste nötig. Außerdem gelang es mit Hilfe der Maskierung der Zwischenschicht (und darunterliegender Gerüststruktur) mit Polystyrol in beiden Fällen im vernetzten Zustand eine deckende selektive Schicht herzustellen und die Porosität der darunterliegenden Schichten (nach der Pyrolyse) zu erhalten. Die Ergebnisse der planaren Proben konnten erfolgreich auf tubulare Proben übertragen werden.

Acknowledgements

First of all, I want to thank Dr. Thomas Konegger and Prof. Roland Haubner for giving me the opportunity to do my master thesis in the research group of high performance ceramics. A special thanks to Thomas for instructing and helping me, always in a kind and dedicated way.

I also want to thank the whole research group of high performance ceramics (especially Arne Ziebell and Dominik Brouczek) and generally the members of the institute of chemical technologies for providing a nice atmosphere during the time of practical work.

I am thankful for my family and friends, who supported me through my whole time of studying. Especially Bettina Ritt, because of sharing all the ups and downs at the university with me during the last five years, making it a great time.

Finally, I want to thank the Institute of applied synthetic chemistry, especially Dr. Christian Gorsche, for the possibility of measuring the rheological behaviour and surface tension using their facilities.

TABLE OF CONTENTS

1	Introduction	3
1.1	Motivation – Membranes for Gas separation	3
1.2	Aims of this thesis	4
2	Theoretical background	5
2.1	Silicon nitride	5
2.2	Polymer derived ceramics.....	5
2.2.1	Preceramic polymers	6
2.2.2	Crosslinking	7
2.2.3	Polymer-to-ceramic-conversion	7
2.2.4	Applications of polymer derived ceramics PDCs	9
2.3	Manufacturing of porous ceramics.....	10
2.3.1	Slip casting	11
2.3.2	Pressing	11
2.3.3	Extrusion	11
2.3.4	Sacrificial templating	12
2.3.5	Blowing/ Foaming	14
2.3.6	Freeze casting	15
2.3.7	Aerogels	16
2.3.8	Emulsions	16
2.4	Coating of porous substrates	18
2.4.1	Use of an intermediate layer	18
2.4.2	Masking	18
2.4.3	Latex barrier	19
2.4.4	Aerosol assisted deposition	20
2.4.5	Spin coating	20
2.5	Dip coating	20
3	Experimental Procedure	22
3.1	Preparation of the macroporous supports.....	23
3.1.1	Slip casting	23
3.1.2	Polymer derived ceramics	27
3.1.3	Warm Pressing	31
3.2	Preparation of the intermediate layer	33
3.2.1	Preparation of the slip	33
3.2.2	Dip coating	36
3.2.3	Crosslinking and pyrolysis	37
3.2.4	Characterization	38
3.3	Preparation of the top layer.....	39
3.3.1	Preliminary tests	39
3.3.2	Dip coating	40
3.3.3	Crosslinking and pyrolysis	40
3.4	Masking	41

3.4.1	Preparation of the dipping solution	41
3.4.2	Dip coating	41
3.4.3	Consequences for the preparation of the top layer	41
3.5	Preparation of tubular samples	42
3.5.1	Slip cast supports	42
3.5.2	Polymer derived supports	43
3.6	Permeability testing	44
4	Results	46
4.1	Support structure	46
4.1.1	Slip casting	46
4.1.2	Polymer derived ceramic supports	49
4.2	Intermediate Layer	51
4.2.1	Preliminary tests	51
4.2.2	Intermediate layer on the slip cast supports	53
4.2.3	Intermediate layer on the polymer derived supports	56
4.3	Top layer	61
4.3.1	Preliminary tests	61
4.3.2	Direct coating of the support structures	67
4.3.3	Coating of support structures with an intermediate layer	69
4.3.4	Coating of masked samples	71
4.4	Tubular structures	84
4.4.1	Structures using slip cast supports	84
4.4.2	Structures using polymer derived supports	87
4.5	Permeation behaviour	89
5	Discussion	92
5.1	Support structures	92
5.2	Intermediate layer	93
5.3	Top layer	95
5.4	Comparison of planar and tubular samples	97
5.5	Permeation behaviour	98
6	Summary	99
7	References	103

1 INTRODUCTION

1.1 MOTIVATION – MEMBRANES FOR GAS SEPARATION

Because of the excellent mechanical and thermal properties and the chemical stability of non-oxide ceramics, their use as membrane material becomes more and more interesting. One big reason is the production of hydrogen, which is usually performed by steam reforming of methane:



As one can see, the reaction is endothermic, which leads to high temperatures necessary for the conversion (approximately 1073 K). To shift the equilibrium to the product-side, it would be helpful to remove the hydrogen from the reaction-mixture continuously using a membrane reactor. That would, in addition, lower the required temperature. Polymer and metal membranes or ones out of oxide ceramics aren't stable under the conditions mentioned above. As a result, the separation of hydrogen has to be carried out separately and is currently complicated and therefore expensive. [1], [2], [3], [4]

An asymmetric porous membrane, which is wanted in this case, consists of several layers with different structures and pore sizes. The top layer is the actual membrane with micropores (by definition < 2nm); it is responsible for the separation. There has to be a support structure for stability reasons. It provides the mechanical strength, but has to be of higher porosity to provide enough gas permeation. The pores are in the macroporous range, which means larger than 50 nm. Usually there has to be a third layer, the so called intermediate layer, bridging the pore size gap between support and membrane. [5], [6]

There are already several approaches using Al_2O_3 supports, which are industrially available in combination with top layers of non-oxide ceramics. [7]

As mentioned above, oxide ceramics have limited properties in comparison to non-oxide ceramics, and in addition, the use of different materials for each layer could lead to problems in case of temperature change because of different thermal expansion. For that reason, it is desired to make the whole structure, including the support, out of non-oxide ceramic and more the less similar material, for example SiC or Si_3N_4 .

1.2 AIMS OF THIS THESIS

Regarding the previously mentioned interest in non-oxide ceramic membranes, the following goals have been targeted:

- A method should be found to prepare a fully covering layer on top of a macroporous support structure.
- Dip coating should be used to deposit the top layer. Optimal parameters for the dip coating process should be found in preliminary tests.
- The whole module is supposed to consist of Si_3N_4 and SiCN based ceramic.
- The disc shaped support structure should be manufactured in different ways to provide different substrates for the additional layers.
- The best results of the toplayer preparation should be tested on tubular support structures.
- Permeation behaviour has to be investigated for the disc-shaped as well as for the tubular structures.

2 THEORETICAL BACKGROUND

2.1 SILICON NITRIDE

Silicon nitride is a non-oxide ceramic with a very good combination of properties:

- Low density (~3,21 g/cm³)
- High fracture toughness (7 MPam^{1/2})
- Good flexural strength (850 MPa)
- Good thermal shock resistance
- Thermal and chemical stability; maximum operating temperature in oxidizing/neutral atmosphere: 1300°C/1600 °C
- High creep resistance

Because of these properties it is typically used as cutting and forming tool, balls and rolling elements for high-precision bearings, engine moving and wear parts, etc. [8]

Generally there are two modifications of silicon nitride: α -Si₃N₄ which is stable at temperatures up to 1400-1600 °C and β -Si₃N₄; both are hexagonal crystal structures.[9]

It is difficult to produce pure dense silicon nitride, due to the strong covalent bondings. It decomposes to silicon and nitride at approximately 1800 °C and can't be sintered to a sufficient degree without the use of sintering aids or high pressures and temperatures. There are three main types of silicon nitride regarding fabrication: reaction bonded silicon nitride (RBSN), hot pressed silicon nitride (HPSN) and sintered silicon nitrides (SSN; pressureless but with sinter additives, eg. Al₂O₃ + Y₂O₃), the properties of which differ a little. Reaction bonded silicon nitride is formed through nitridation of silicon; if the reaction isn't fully completed, lower densities are achieved than for HPSN and SSN. [10]

2.2 POLYMER DERIVED CERAMICS

Ceramics formed through pyrolysis of - typically silicon based - polymers have become more and more important over the last decades. This is due to several advantages compared to the common powder based route, for example the flexibility in shaping the polymers previous to conversion, enabling the production of, for example, fibers and coatings.

2.2.1 Preceramic polymers

As mentioned above, mostly silicon based polymers are used as precursors. By modifying the backbone and the side groups of the polymer, the resulting ceramic and its properties can be influenced. The carbon-content can be regulated through the chain length and type of the side groups, which are usually responsible for the cross linking. The general structure of an organosilicon polymer can be seen below (Figure 1).

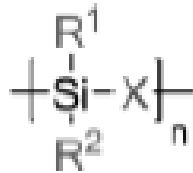


Figure 1: General structure of an organosilicon polymer [11]

The resulting ceramic system depending on the used polymer class can be read from Figure 2. The polymeric precursors have to fulfill some requirements to be suitable for that process. To avoid the loss of volatile compounds, the molecular weight has to be high enough. Rheological properties and solubility are important for the shaping process, crosslinking has to be possible.

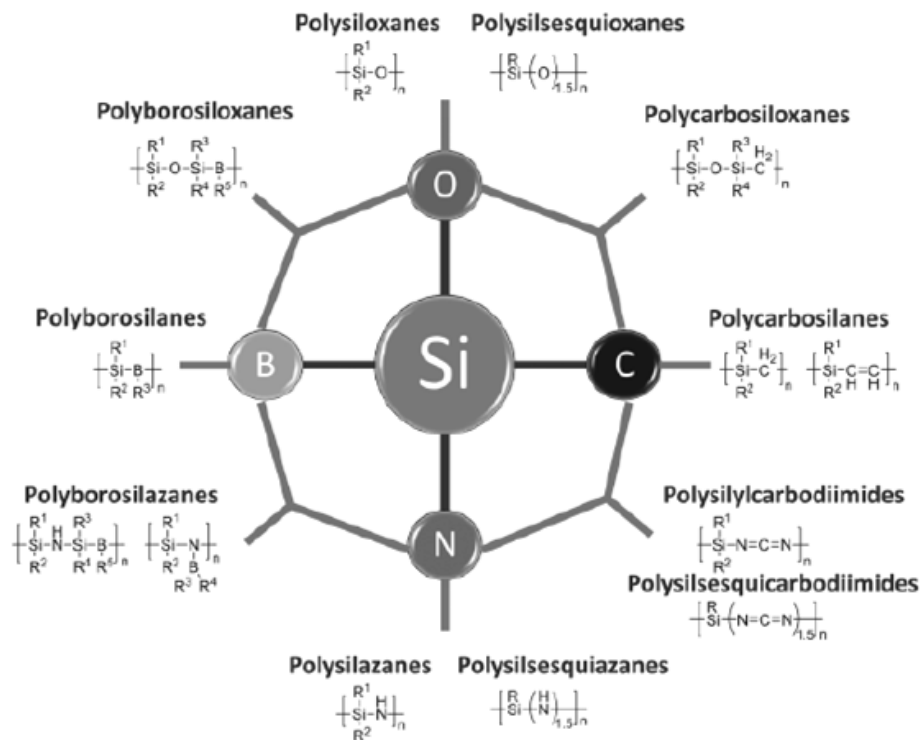


Figure 2: Overview of preceramic polymer classes [11]

2.2.2 Crosslinking

The preceramic polymer is either a meltable or soluble solid or a liquid. In the latter case, the desired form has to be stabilized after the shaping step. This is done by crosslinking of the polymer to form a stable network.

Several Si-sidegroups like vinyl-groups or just H-atoms or hydroxy-groups enable crosslinking via condensation or addition reactions which take place at increased temperature. By the use of catalysts, the necessary temperature can be decreased.[11]

In Figure 3, the crosslinking process is shown for a poly(vinyl)silazane.

Not only thermo-crosslinking is possible but also oxidative curing, UV-curing, curing using a laser beam, a radiation beam or an e-beam can be done depending on the shape and requirements of the product.[11]

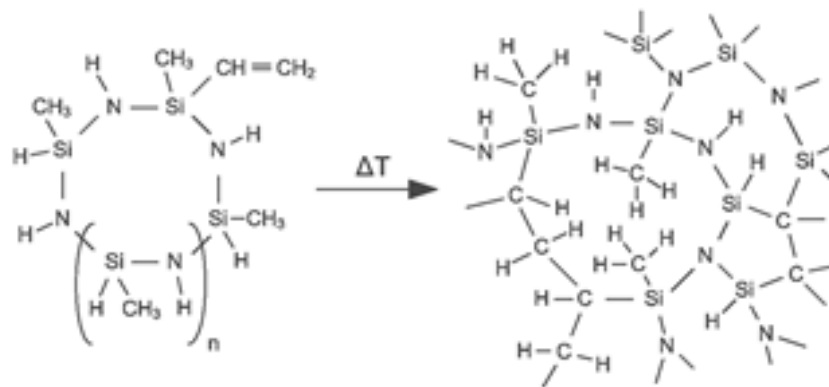


Figure 3: Crosslinking of a poly(vinyl)silazane [12]

2.2.3 Polymer-to-ceramic-conversion

The final step is the conversion of the polymer into the ceramic by pyrolysis (usually oven pyrolysis). Temperatures needed are usually lower than for sintering of the corresponding ceramic powder. The organic compounds are thermally decomposed, leaving back an amorphous ceramic-like residue. This is shown for the same poly(vinyl)silazane as in 2.2.2 in Figure 4.

Due to the decomposition of the organic compounds, gaseous products have to leave the material, shrinkage takes place and micro- and sometimes macropores are formed (Figure 5a). This leads to defects in the resulting material.

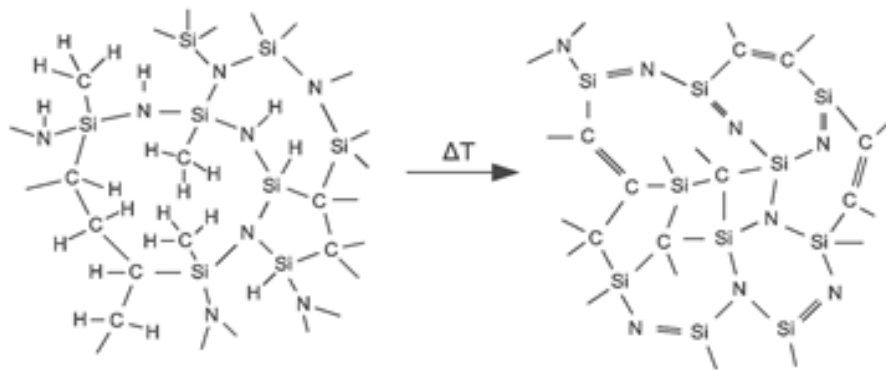


Figure 4: Polymer-ceramic-conversion [12]

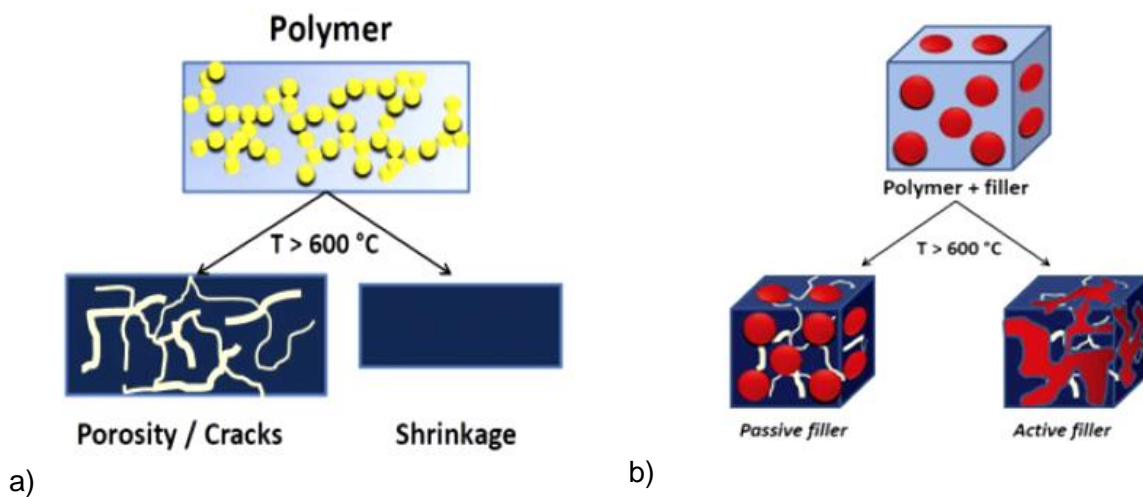


Figure 5: (a) dimension change during pyrolysis
(b) mode of action of passive and active fillers [11]

A way to avoid cracks and shrinkage is to use fillers. They can either be inert (passive fillers) or reactive (active fillers) and of various materials and shapes.

Inert fillers are typically ceramic powders, which decrease the shrinkage and in addition make gas release easier.

Active fillers react in some way with the ceramic or the gaseous byproducts during the conversion under huge volume expansion leading to less shrinkage. With reactive fillers the

ceramic composition can be changed during pyrolysis; remaining metal particles can influence magnetic and electric properties.[11]

The effects of both active and passive fillers can be seen in Figure 5b.

2.2.4 Applications of polymer derived ceramics PDCs

Due to their easy processing the use of preceramic polymers is the favourable way to manufacture ceramic fibers or coatings as well as complex microcomponents to name a few.

2.2.4.1 Fibers

Ceramic fibers are mainly used for (ceramic matrix) composites, due to their high strength and oxidation and corrosion stability, when commonly carbon fibers, which have excellent mechanical properties but are sensible towards oxidation, fail. [13] Preceramic fibers are usually prepared using melt-spinning or electrospinning, followed by curing and pyrolysis. [14]

2.2.4.2 Coatings

The use of metal parts, for example turbines, becomes possible under temperatures higher than the melting point of the metal and aggressive environments through the use of environmental/thermal barrier coatings made of ceramics. They can be deposited via PVD/CVD or thermal spraying, but these processes have several drawbacks like the structure of the resulting films or the complexity of the manufacturing process. An easy approach is the dip coating with a preceramic polymer, which is converted into ceramic afterwards. [15], [16]

2.2.4.3 Porous ceramics

Due to their unique combination of properties like low density, high thermal and chemical stability and low thermal conductivity, high specific strength, etc. porous ceramics are suitable for structural and functional applications under conditions where other materials fail. They can be used for example as support for catalytic or membrane applications or for liquid metal filtration. [2], [13], [17], [18], [19]

2.2.4.4 Micro/Nanoelectro mechanical systems MEMS/NEMS

Using the polymer derived route, it is possible to fabricate MEMS/NEMS made out of non-oxide ceramics, which can be used in harsh environments due to their excellent properties. The powder based route isn't suitable for this application, because of the small dimensions of the parts; the formation of complex moulds is too expensive, adequate tools for green body shaping can't be prepared, etc.

The preceramic polymers on the contrary can be shaped for example using lithography. [20], [21]

2.3 MANUFACTURING OF POROUS CERAMICS

Porous ceramics are of high interest for engineering applications like filtration, absorption and membrane modules to only name a few. They can either be prepared via conventional routes or using preceramic polymers.

Although PDCs are generally not fully dense due to their manufacturing, there has to be another pore structure and/or a higher porosity for most of the engineering applications, which led to several techniques to achieve such products.

A rough overview of methods to produce (macro-)porous ceramics is given in Figure 6; the methods will be discussed in more detail afterwards. Most of them are suitable for the powder based as well as for the PDC route, some only for one of them.

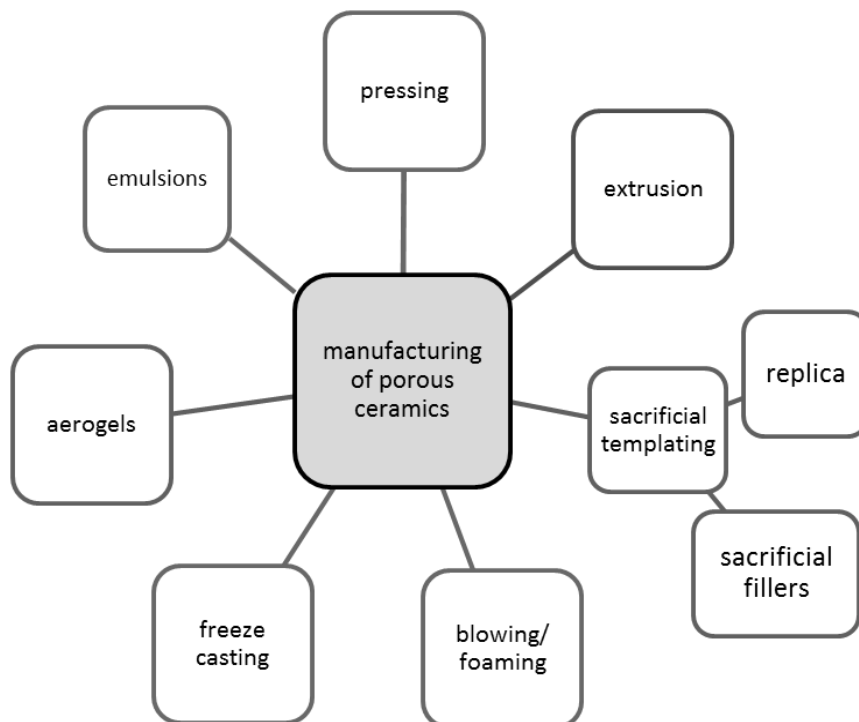


Figure 6: Overview of processing strategies for porous ceramics

2.3.1 Slip casting

Mori prepared porous silicon nitride supports via slip casting. A water based slurry was used containing the silicon nitride powder and a dispersant but no sintering additives (to obtain an oxide free structure). The resulting supports were dried and partially sintered. [22]

2.3.2 Pressing

A conventional way to produce ceramics is to shape them through pressing, followed by sintering to achieve consolidation. By adjusting the parameters in an adequate way, the porosity can be controlled.

Tubular macroporous SiC-supports were prepared using a mixture of two different SiC-powders (and sintering aids). They were dry pressed using little amounts of pressing aids and sintered. [2]

Porous SiC-disks were prepared by Fukushima et al. using cold isostatic pressing CIP. [3]

Tsubaki et al. combined silicon nitride powder with a preceramic polymer which yields a SiCN based ceramic. The powder was dispersed in a slurry containing the polysilazane. After drying, the mixture was pressed isostatically after uniaxial compression; the polysilazane serves as a binder for the powder and is pyrolysed afterwards.[23]

2.3.3 Extrusion

One common way to form tubular ceramic structures is to extrude a powder/binder mixture followed by dewaxing and sintering. By adjusting the sintering temperature and additives, porous ceramics can be achieved through partial sintering.

For example porous SiC-tubes were made using SiC-powder with alumina as sintering additive and a cellulose binder. [1]

2.3.4 Sacrificial templating

In this method, the material which is used to form the pores is removed during or after the heat treatment, depending whether it's a soft or a hard template. In the latter one, further treatment is necessary after the polymer-ceramic conversion using, for example, etching.

2.3.4.1 Replica technique

As the name already indicates, one gets a replica of a porous structure. A solid structure is coated with the preceramic polymer and after crosslinking the polymer-ceramic-conversion is induced by heat treatment. The template is either removed during that process or afterwards as already mentioned above. The process is shown schematically in Figure 7.

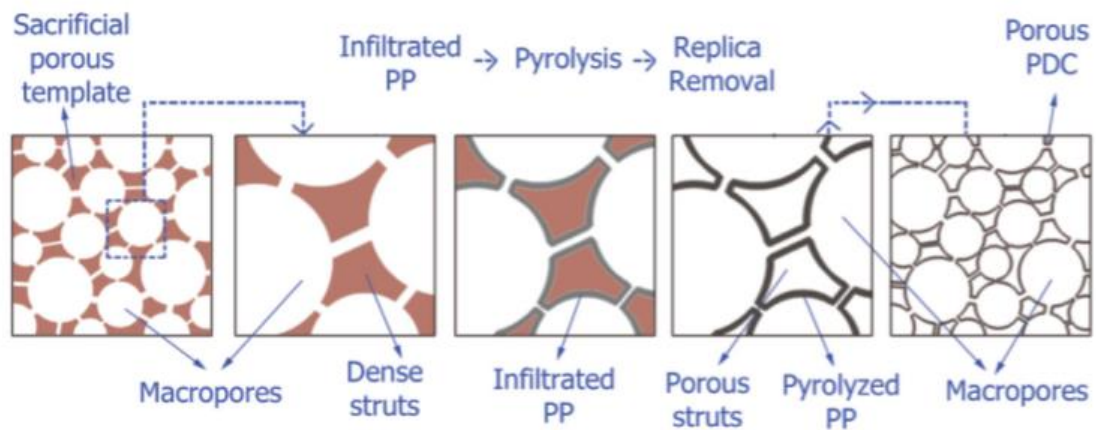


Figure 7: Schematic replica technique process [24]

Usually the resulting ceramics are unstable, because the removal of the template yields in hollow struts. The stability can be improved a little by coating not only once, but several times.

Another approach is the use of a polymer sponge instead of a rigid template. If a suitable solvent is used for the preceramic polymer, it can penetrate the template and therefore result in dense struts.

Various materials can be used as templates (Table 1).

Table 1: Examples of templates (HT...hard template, ST...soft template)

Material	Type	Comment	reference
polymeric sponge/foam	ST	hydroxyapatite scaffold for bone regeneration using a polyurethane sponge as replica template	[25]
corals	ST	Calcium phosphate ceramics can be obtained by thermal treatment of the calcium carbonate skeleton of algae or corals	[26, 27]
glass	HT	Porous glasses of various pore size were prepared; infiltration with silicon carbide precursor (+solvent); removing the glass template by etching with HF	[28]
Cancellous bone	ST	hydroxyapatite (HA) and β -tricalcium phosphate (β -TCP) to be used as bone replacement; negative mold of the bone formed with wax and filled with ceramic slurry	[29]
starch	ST	Corn starch microspheres flake as template; tetrabutyl titanate TBOT transported by scCO ₂ , gelling and drying, removing of the template via calcination	[30]
wood	ST	Amorphous carbon template formed by pyrolysis of wood (oak); calcium phosphate scaffold with the same pore structure as the template	[31]
urea crystals	ST	Crystallization of urea in a water-alumina suspension by cooling down to room temperature and using gravitation; removal of urea by heating up	[32]
silica	HT	mesoporous silica SBA-15 and KIT-6 as template, polycarbosilane yielding in SiC nanowire arrays	[33]
carbon	HT	mesoporous carbon CMK-8 as hard template; polycarbosilane as preceramic polymer was applied via solvent evaporation induced impregnation; PCS-silicon nitride-conversion with ammonia, carbon was removed with ammonia	[34]

2.3.4.2 Fillers

Contrary to the replica technique, a template is used for the pores and not for the ceramic itself. Usually spherical polymer particles are mixed with the preceramic polymer until they are homogeneously dispersed. The preceramic polymer is crosslinked and pyrolysed. During pyrolysis, the filler is burned out and leaves pores in the range of the original particle size.

The process is shown schematically in Figure 8 and some examples of sacrificial fillers are given in Table 2.

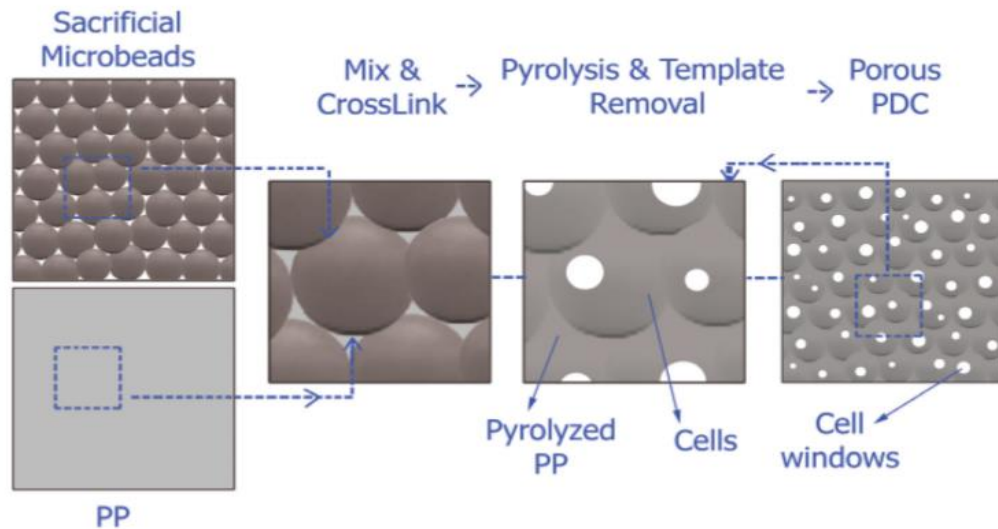


Figure 8: Schematic process for porous ceramic production using sacrificial fillers [24]

Table 2: Examples of sacrificial fillers

Filler- Material	comment	Reference
PMMA	PMMA microbeads were used as sacrificial fillers to produce SiC from Allylhydridopolycarbosilane AHPCS	[35]
PE	UHMW-PE as sacrificial filler for a liquid poly(vinyl)silazane (or polycarbosilane) resulting in porous SiCN (or SiC) ceramic	[18], [19]
	UHMW-PE as sacrificial filler for a solid, meltable polysilazane resulting in porous SiCN ceramic	[36]
PS	Polystyrene/silica sphere array formed by MIMIC; infiltration of preceramic polymer (polyvinylsilazane or allylhydridopolycarbosilane for SiCN or SiC), crosslinking and pyrolysis(PS removal), HF etching to remove silica	[37]
silica		

2.3.5 Blowing/ Foaming

Another possible process is to insert gas in the preceramic polymer solution (or even a slurry containing solid particles) while still liquid and starting the crosslinking process. This can either be done by blowing gas (for example CO₂) through the liquid or by adding a liquid that evaporates at low temperatures (physical and chemical blowing agents), which both can be seen in Figure 9. In some cases self-foaming occurs; small molecules abstracted during polycondensation reactions act as in situ foaming agents.

For example macroporous SiC-foams were produced using a polycarbosilane and an azodicarbonamide as chemical blowing agent. [38]

Konegger et al. prepared mullite based cellular ceramics by self foaming of a poly(silsesquioxane) in a mixture with either alumina or alumina/aluminum during crosslinking. [39]

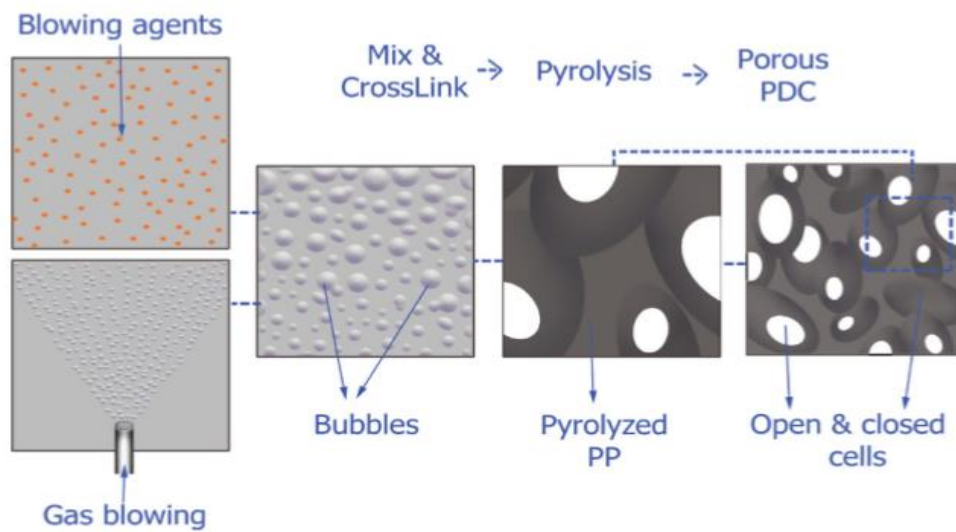


Figure 9: Schematic illustration of pore generation using blowing [24]

2.3.6 Freeze casting

The thought behind this method is to form aligned and therefore anisotropic pores by freezing the solvent of a slurry or solution and thus forcing the particles to assemble along the frozen solvent. To get aligned frozen parts, a temperature gradient is applied. The frozen solvent, which served as template, is removed via freeze drying afterwards and the ceramic is sintered. [24]

The temperature gradient is produced from a metallic rod which is cooled down by liquid nitrogen or an ice bath. By varying the metal and therefore the thermal conductivity of the rod, the freezing velocity can be influenced.

Freeze casting can be used for almost every ceramic powder. There are three main solvents: water (resulting in lamellar pores), camphene (dendritically pores) and tert-butyl alcohol (prismatic pore-shape). [40]

When using a polar solvent, the crystal growth can be influenced by applying an electric field. The growth direction is preferentially along the external field. If the direction of the electric field is the same as the freezing direction, an increase in mechanical stability can be observed due to increasing alignment of the pores. [41]

When using water as solvent, the lamellar shape of the pores can be changed using ice structuring proteins/agents.[42]

Freeze casting can be used for preceramic polymers too. A solution of the polymer is prepared. After partially crosslinking the polymer to increase its stability, the steps are similar to those of processing a ceramic slurry. The polymer is pyrolysed in the end to get the porous ceramic. [43]

The freeze casting process can be seen in Figure 10 a) for a ceramic slurry and in Figure 10 b) for a preceramic polymer.

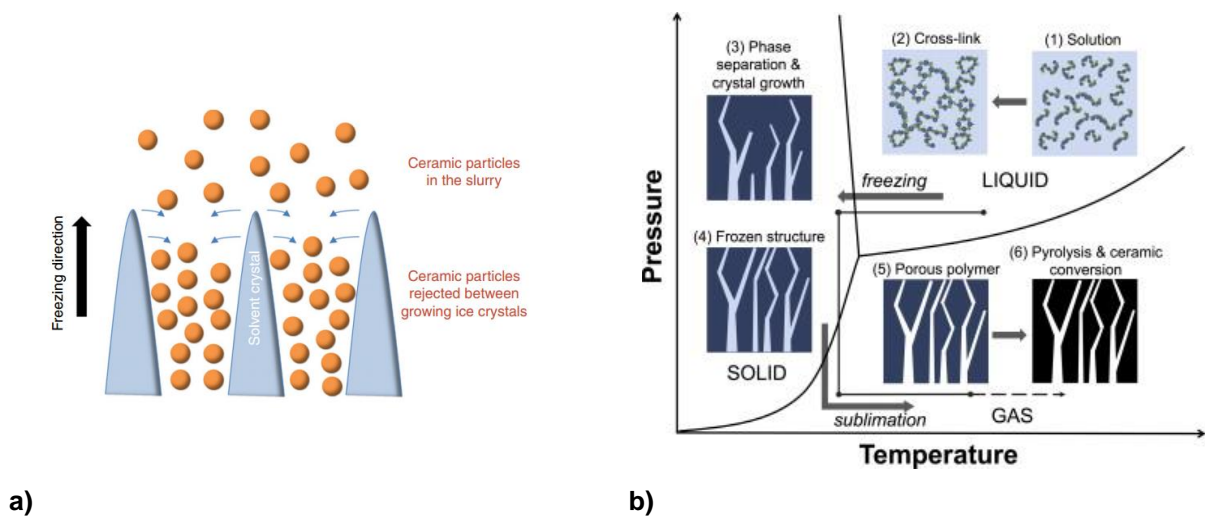


Figure 10: Freeze casting of (a) a ceramic slurry [40]
(b) a preceramic polymer solution [43]

2.3.7 Aerogels

Aerogels can be roughly defined as gels, in which the liquid is replaced by air. They have an extremely low density and are therefore good thermal insulators. Their structure also results in increased transparency and reduced sound velocity compared to the bulk material.

The wet gels are obtained via sol-gel-process. After aging the liquid is removed through supercritical drying SCD. Due to the very fragile solid network, drying would lead to fractures caused by capillary pressure. If the liquid reaches a supercritical state, capillary forces no longer occur because there's no vapor-liquid interface in the pores anymore. [44],[45]

2.3.8 Emulsions

Another possible way to produce porous ceramics is to use a stable emulsion of an oil phase and a water phase (generated using surfactants and ultrasound sonication or magnetic stirring), followed by crosslinking of the preceramic polymer, which is dissolved in the oil

phase, removal of the surfactant, removal of water and polymer-ceramic-conversion (yielding, e.g., SiC(O) ceramics) [46],[47]

Besides using surfactants to stabilize the emulsion, particles can be used for the same purpose (solid-stabilized emulsion). A big difference when compared to surfactants used to stabilize the emulsion is that the particles stay adsorbed to the droplet and are not underlying a dynamic ad- and desorption process. Thus, they hinder Ostwald-ripening and coalescence. [48]

For example nanosized silica particles can be used to produce macroporous silica material. Depending on their surface modification (silanisation), an oil in water or water in oil emulsion forms. In both of them excessive particles stay in the continuous phase and form the pore walls. [49]

2.4 COATING OF POROUS SUBSTRATES

For some applications it is necessary to produce a dense layer on a macroporous substrate. A ceramic coating can either be produced via the gas phase using chemical vapor deposition/infiltration [50] or using preceramic polymers, which are converted into ceramics after the shaping step.

The focus of this work is on the PDC route. Thus, only this route is described in more detail. When using a method involving a liquid – as it is the case when using preceramic polymers - capillary effects usually result in the liquid penetrating the support and therefore not forming a crackfree, homogenous coating. Several ideas came up to solve that problem.

2.4.1 Use of an intermediate layer

With a macroporous substrate and a desired microporous top layer the formation of an intermediate layer, which lies inbetween those two considering pore structure/size and chemical composition, is a logical first step.

Elyassi et al. prepared membrane modules consisting of a tubular porous SiC support (prepared by pressing), an intermediate layer prepared via slip casting of a dispersion of SiC-particles in same solution of a preceramic polymer that is also used for the top layer. [7] They also tested SiC-fibers as fillers for the intermediate layer; this time the top layer was deposited using another strategy which is described in 2.4.2. [51]

Mori et al. used an intermediate layer to provide a better substrate for a dense top layer. The macroporous Si₃N₄ support was prepared via slipcasting. To enhance the surface quality of the support and achieve a barrier against penetrating of the top layer dipping solution, an intermediate layer was formed by dipcoating/slipcasting of silicon nitride powder dispersed in a polysilazane/toluene solution. The top layer was prepared using a solution of the same polysilazane in toluene. [22]

2.4.2 Masking

Another approach is penetrating the pores of the support on purpose for the duration of the coating process and removing the used material after stabilization of the coating.

Hedlund et al. used wax to close the pores of the support structure, hence providing a dense substrate for the deposition of the top layer. To make sure that only the pores and not the surface of the support are masked, first a PMMA layer is applied on the surface, followed by infiltration of the wax, removal of the PMMA, adsorption of zeolithe crystals on the surface and crystal growth forming a film. Finally the wax is molten out. [52]

Elyassi et al. prepared membrane modules (as mentioned in 2.4.1) made of SiC using an intermediate layer to provide a better substrate for the top layer deposition. In addition, they used polystyrene to fill the pores of the intermediate layer. This is done by simply dip coating the substrate in a polystyrene solution followed by drying. The top layer is prepared via dip coating too, using a solution of preceramic polymer in a solvent which doesn't dissolve the polystyrene (n-hexane is used here). The polystyrene is burned out during pyrolysis. Multiple coating runs are necessary to get a dense top layer. [53] The whole process is shown schematically in Figure 11.

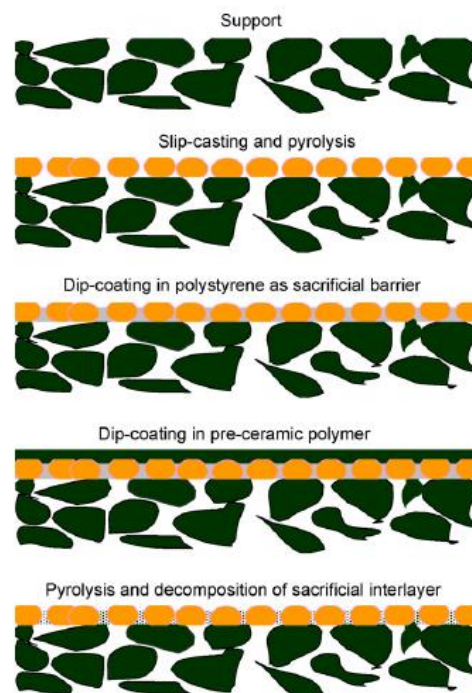


Figure 11: PS-masking of the intermediate layer [53]

Wang et al. prepared carbon membranes on alumina supports by dipcoating in furfuryl alcohol followed by carbonization. To enhance the quality of the alumina support and prevent penetration, they decorated the surface using a conventional pencil. [54]

2.4.3 Latex barrier

In this case the coating is formed from particles. A dispersion of latex particles of the desired polymer is applied via dip coating. The solvent evaporates, the particles deform and change to the energy favourable state of a thin film if parameters like particle size, temperature, etc. are adequate. This worked well for soft polymers, which means that their glass transition temperature is beneath room temperature, whereas the hard polymers tested in this work group didn't show film formation. [55]

2.4.4 Aerosol assisted deposition

Xomeritakis et al. formed a mesoporous silica membrane on a coarse porous alumina substrate by use of aerosol formation. As shown schematically in Figure 12, droplets of a sol are formed by ultrasound sonication and carried by N_2 -gas to a funnel, in which the substrate was placed. Above the substrate, an aerosol cloud forms, the sol condenses and forms a film on top of the substrate. [56]

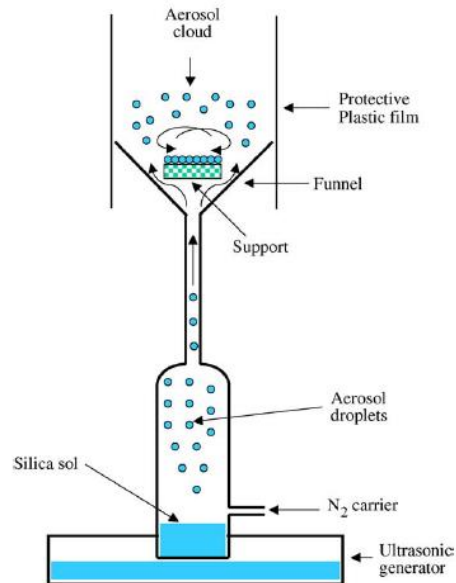


Figure 12: Aerosol assisted deposition of a membrane on a porous support [56]

2.4.5 Spin coating

Tseng et al. used spin coating to get a polyetherimide-derived carbon molecular sieve layer on a porous alumina support. [57]

Wach et al. prepared a SiC based membrane on top of a porous alumina support by spin coating. [58]

2.5 DIP COATING

Dip coating is a simple process to apply a layer onto a substrate.

The process consists of three steps: first the immersion step, where the substrate is moved into the solution at a constant speed, secondly the dwell time, where it is held motionless and fully immersed, and finally the withdrawal step, in which it is removed with a constant speed. The faster the substrate is withdrawn, the less time remains for the solution to drip off again, which results in a thicker layer. [59]

A model showing the relation between layer thickness and withdrawal speed was set up by Landau and Levich [60], valid for Newtonian liquids (equation 1).

$$h_0 = 0.944 \times \sqrt[6]{\frac{\mu U}{\sigma}} \times \sqrt{\frac{\mu U}{\rho g}} \quad (1)$$

h₀... thickness

μ... viscosity

U... withdrawal speed, mm/min

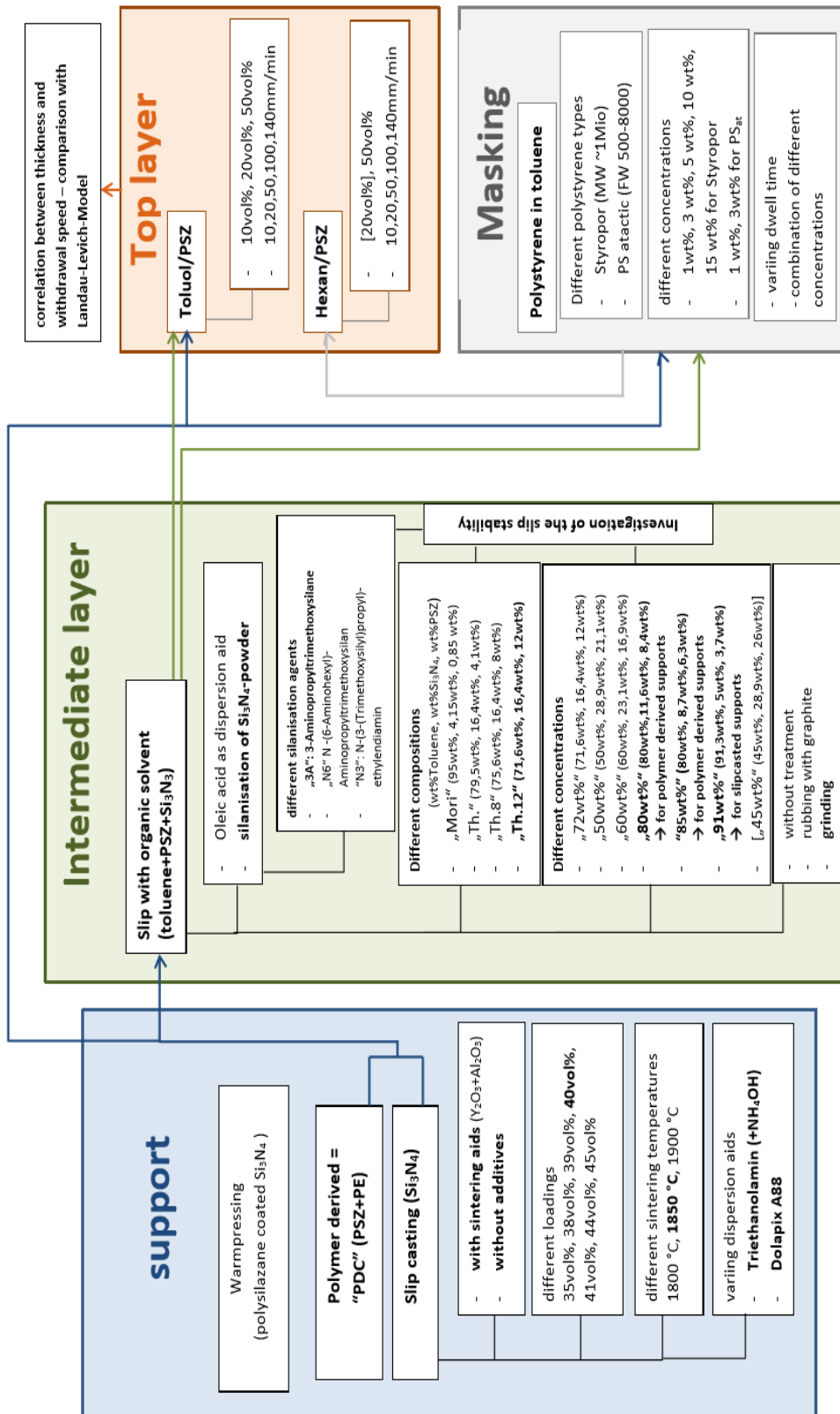
σ... surface tension

g...gravitational acceleration =9.8 m/s²

ρ... density

3 EXPERIMENTAL PROCEDURE

An overview of the experiments made during this thesis can be seen in below and is described in more detail in the following sections.



3.1 PREPARATION OF THE MACROPOROUS SUPPORTS

The first part of this work was the preparation of macroporous supports on which the following layers with decreasing pore size should be applied. Three methods were chosen: slip casting of silicon nitride, polymer derived ceramics using polysilazane as preceramic polymer and warmpressing of polysilazane-coated silicon nitride.

3.1.1 Slip casting

The first method to prepare the substrates was the traditional powder based route – slip casting.

3.1.1.1 Preparation of the slips

Following Mori et al. [22], slips with different loadings were prepared. The goal was to reach a loading as high as possible which was supposed to result in a final porosity of about 30-40 % without using sintering aids. The experimental procedure followed that of Mori with one extra step – the adjustment of the pH.

First the correct amounts of water and triethanolamine (98+%, Alfa Aesar), which was used as dispersion aid (1 wt% with respect to Si_3N_4), were mixed in a HDPE-bottle (125 ml or 250 ml depending on the volume prepared in total) containing milling balls (silicon nitride, 1/2" or 5/16") and the pH was adjusted to approximately 10 using 25% NH_4OH . Then the silicon nitride powder (SN-E10, Ube) was added little by little. After each step the bottle was shaken by hand until the dispersion appeared homogenous (reaching higher loadings the shaking step was necessary to get a „fluid“ again). The amount added per step was decreasing due to the increasing loading which made it more difficult to disperse the powder. It showed that it helped to not fully adjust the pH at the beginning but to add ~ 2 drops of the NH_4OH after adding the vast amount of the powder. The resulting mixture was milled on a ball mill for about 8 hours. The balls were removed and the slip was degassed using vacuum. This turned out to be a critical step, because a pressure below 40 mbar led to evaporation of water causing additional bubbles instead of removing them and slightly changing the composition of the slip.

The slips and their loadings are listed in Table 3.

Table 3: Si₃N₄ loading of the aqueous slips prepared using 1wt% TEA

slip	loading, vol%
A	35
B	35
C	35
D	38
E	39
F	38
G	40
H	38
I	41
J	40

Another dispersion aid, so called Dolapix A88 (Zschimmer & Schwarz GmbH&Co KG), was used in later experiments and slips with even higher loadings were prepared. The procedure was quite the same except for not adjusting the pH. This time 0,5 wt % of the dispersion aid were used with respect to Si₃N₄.

The following slips were prepared (Table 4):

Table 4: Si₃N₄ loading of the aqueous slips prepared using 0.5 wt% DolapixA88

slip	loading, vol%
K	41
L	45
M	45
N	44
O	40

3.1.1.2 Casting of the slips

Due to the planar shape of the samples, a simple setting was chosen for the slip casting. Hollow cylinders out of silicone rubber were placed on a plaster plate. After filling in the slip, the cylinders were covered by a fitting silicone top to hinder water from simply evaporating and to make sure the water is mainly removed by the plaster. After 24 hours at room temperature the green samples were removed from the forms and dried for an additional 24 hours at 60 °C. Diameter, height and mass were measured and the density was calculated. Measuring the correct height was difficult because a meniscus formed at the top side of the samples. The green bodies had to be handled carefully because of their poor mechanical properties.

3.1.1.3 Sintering

Sintering was carried out in a hot press (KCE Sondermaschinen GmbH) using an *Infratherm Meßumformer* IP1 (Gulton GmbH) for temperature measurement. The influence of the sintering temperature on the resulting porosity was tested using temperatures of 1800 °C, 1850 °C and 1900 °C. These temperatures were held for 4 hours, the heating and cooling rate were set to 10 K/min. The sintering process was carried out under flowing nitrogen, slightly above ambient pressure. In Table 5 one can see the slips tested at each temperature. Every other sample was sintered at 1850 °C.

Table 5: Slips tested at each sintering temperature

temperature, °C	slip	Si ₃ N ₄ loading, vol%
1800, 1850	A	35
	B	35
	C	35
	D	38
	E	39
1900	B	35
	C	35
	D	38
	E	39

Silicon nitride doesn't melt but it decomposes. This process already starts at the temperatures used here which made it necessary to put the samples in a bed of a 50:50 wt% mixture of silicon nitride powder and hBN. The samples were neither allowed to touch each other nor the crucible (graphite).

The resulting samples were cleaned with compressed air and in distilled water in an ultrasonic bath. After drying, diameter, height and mass were measured again and the density was calculated.

3.1.1.4 Characterization

The immersion test method was used to investigate the porosity. Following DIN EN 1389 the samples were dried at 100 °C, cooled down in a desiccator while applying vacuum to prevent water from being adsorbed again. The dry mass was measured by weighing the samples as quickly as possible. The samples were put in the desiccator again and the pressure was held at the lowest reachable value, which was approximately 30 mbar, for at least 15 minutes. Distilled water was added until the water level was about two

centimeters above the samples while keeping the pressure at 30 mbar. After leaving the setup like that for at least 30 minutes the beaker was taken out of the desiccator and the apparent mass in water was investigated using the Archimedes method. To get the wet mass, the excessive water was removed with a wet paper towel.

Three values could be calculated through this method: the raw density ρ_b (equation 2), the apparent density ρ_s (equation 3) and the apparent porosity Π_a (equation 4).

$$\rho_b = \frac{m_1 \times \rho_{H_2O}}{m_3 - m_2} \quad (2)$$

$$\rho_s = \frac{m_1 \times \rho_{H_2O}}{m_1 - m_2} \quad (3)$$

$$\Pi_a = \frac{m_3 - m_1}{m_3 - m_2} \quad (4)$$

m₁...dry mass, g

m₂...mass under water, g

m₃...wet mass, g

The appearance of the support structure as well as the influence of the sintering temperature on the neck-formation were investigated via scanning electron microscopy (Quanta 200, FEI). To reduce electrostatic charging, the sample surface was sputtered with gold. Sufficient results were reached with a sputtering time of 75 s at 10 mA. Only one sample of the 35 vol% (lowest loading) and the 39 vol% (highest loading at that time) slip and of each temperature was analysed.

3.1.2 Polymer derived ceramics

Besides the traditional way of producing ceramics, the supports were also prepared via pyrolysis of preceramic polymers using sacrificial fillers to generate the desired pore structure.

3.1.2.1 Preparation of the polysilazane

The first step was to add 1 wt% of the initiator, which is dicumylperoxide DCP (>97,0%, Fluka), to the polysilazane (Durazane HTT 1800, durXtreme GmbH). Cross linking of the polysilazane doesn't require an initiator but it lowers the necessary temperature.

The correct amount of DCP was weighed in and the mixture was stirred until it dissolved and the solution appeared clear. Due to the instability of polysilazanes towards hydrolysis this step was carried out under nitrogen. This was followed by a degassing step; while still stirring the solution, vacuum was applied carefully in a desiccator until no more bubble formation took place (~15 min). The volume above the solution was filled with nitrogen and the sealed bottle was stored in the fridge. Before using it, degassing is necessary every time, to remove decomposition products like NH_3 .

3.1.2.2 Preparation of the polyethylene

The polyethylene (Mipelon PM-200, Mitsui Chemicals America) had to be completely dry. It was weighed in a glass bottle, the top was closed with a paper towel to prevent dusting and the bottle was put in a vacuum furnace at 50 °C overnight.

3.1.2.3 Preparation of the silicone rubber molds

The polymer which was used is liquid and was therefore formed by casting it into silicone molds, of which it could easily be removed after crosslinking took place.

A two component rubber, so called MoldMaxII, was mixed in a ratio 10:1.

There were two original molds for the cylindrical forms and one for the top. To fill these three at a time 29,70 g of the first (white) and 2,97 g of the second (blue) component were mixed with a glass-stick until the color became a homogenous light blue. To remove the dissolved gas, vacuum was applied until the foam formed due to the gas bubbles going up, broke down. The mass was cast in the Teflon molds and cured for 24 hours at room temperature.

After curing the molds had to be held at 110 °C for several hours (usually overnight) to make sure the curing is complete and again for about one hour before using them. It was shown in previous work of the research group that bubble formation in the samples occurs if this isn't

done. Each form could be used about three times, until the silicone becomes dry and crack formation can be seen. Tops can be used more often.

The molds can be seen in Figure 13.



Figure 13: Silicone molds used for casting of the PDC supports

3.1.2.4 Preparation of the actual supports

As mentioned above, polysilazane isn't stable in presence of water, so the next steps took place in a glovebox. The polysilazane was degassed again if it hadn't been used for some time. It was mixed with UHMW-polyethylene (30:70 vol% which equals 28.4:71.6 wt%) in a beaker while applying vacuum (20 mbar). After stirring for at least 15 minutes, the mixture was cast in the silicone molds, about 2.5 ml each. There's enough space for 13 forms in the furnace, the mixture was prepared for 12 forms which means about 24 g in total: 6.816 g UHMW-PE and 17.184 g polysilazane. The scale inside the glovebox doesn't show correct values, which was tested using 4 different hard-metal pieces – it was a systematic error that could be corrected by making a calibration, which can be seen in Table 6 and Figure 14.

Table 6: Masses measured to calibrate the scale inside the glovebox

	correct mass, g	measured mass, g
1	2.15	2.14
2	9.39	9.36
3	52.31	52.17
4	105.08	104.74

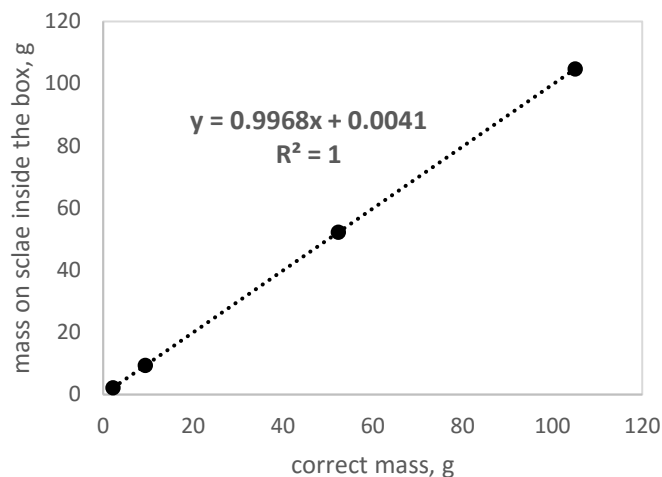


Figure 14: Calibration of the scale inside the glovebox

The molds were closed with a top, taken out of the glovebox and put in a furnace (nitrogen atmosphere) immediately. To initiate the crosslinking in presence of DCP 105 °C are needed. The heating rate was 1 K/min, 105 °C were held for 16 hours. After cooling, the samples were demolded and the temperature program was repeated to be sure that the cross linking was complete.

The top and bottom of the disc-shaped samples were cut off and ground (SiC paper #320 → #600) to reach a height between 2.5 and 3 mm. The whole surface was ground with SiC paper #2000 including chamfering the edges. They were cleaned with compressed air and height, diameter and mass were measured.

3.1.2.5 Pyrolysis of the supports

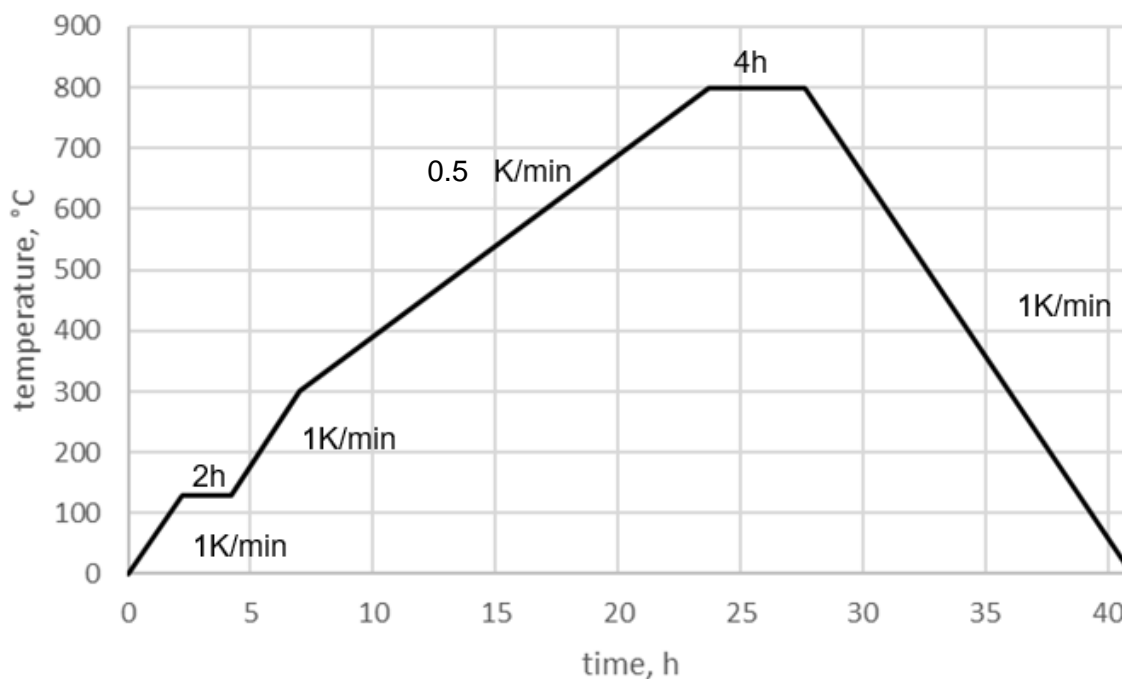
To transform the crosslinked polymer into ceramic, it has to be pyrolysed.

The furnace was purged with nitrogen and the flow was regulated to 0.8 l/min.

The following temperature program was used (Table 7). The dwell time at 130 °C was supposed to definitely complete the crosslinking. The temperature program can also be seen in Figure 15.

Table 7: Temperature program for the pyrolysis of PDC-supports

0 – 130 °C	1 K/min
130	2h
130-300	1K/min
300-800 °C	0.5K/min
800 °C	4 h
800 – 0 °C	1 K/min

**Figure 15: Temperature program for the pyrolysis of PDC-supports**

3.1.2.6 Characterization of the supports

Immersion test method was tried for the polymer derived samples too, but due to lacking wetting behaviour the results weren't reproducible. The density of the pyrolysed polymer was investigated using He-pycnometry, the porosity could then be calculated using the dimensions, mass and the just measured skeletal density, which was assumed to be approximately the theoretical density.

Again, scanning electron microscopy was used to investigate the pore structure and overall looks of the support (conditions as in 3.1.1.4).

3.1.3 Warm Pressing

The third method chosen for producing the support structure was warm pressing of polysilazane coated silicon nitride.

3.1.3.1 Coating of the silicon nitride

The polysilazane was used as a binder for the powder with a polymer content of 20 vol%. The equal mass fraction was calculated using equation 5.

$$M_f = \frac{V_f \times \rho_f}{V_p \times \rho_p + V_f \times \rho_f} \quad (5)$$

M_f...mass fraction of the ceramic filler

V_f...volume fraction of the ceramic filler

V_p...volume fraction of the crosslinked polymer

ρ_f...density of the ceramic filler, g/cm³

ρ_p...density of the crosslinked polymer, g/cm³

With a density of the crosslinked polymer of $\rho_p=1.12 \text{ g/cm}^3$ and the theoretical density of silicon nitride $\rho_f=3.21 \text{ g/cm}^3$, a mass fraction of 92 wt% filler was calculated. A total of 30 g was prepared – 27.6 g Si_3N_4 and 2.4 g polysilazane.

The powder was dried in a three neck flask in a water bath (50-60 °C) while applying vacuum. 92 ml of dry cyclohexane were added and the slip was stirred mechanically in a N_2 atmosphere. After three hours the right amount of polysilazane (degassed before use) was added and the stirring continued for 60 minutes. Then the solvent was removed by applying vacuum. A solid layer formed at the top of the slip, it was destroyed with a spatula. The stirring was slowed down with increasing viscosity of the slip.

Due to a stuck joint plug, not the total yield could be removed from the flask. The drying was completed in a furnace at 60 °C. Only 18.71 g powder (= 62 % of the theoretical yield) were left. It was ground in an agate mortar and sieved through a 200 μm and a 63 μm sieve. 14.78 g could be obtained.

3.1.3.2 Warm pressing

The crosslinking and pressing should be carried out in one step: warm pressing. The goal was to get a disc shaped green body with the following dimensions:

$h = 0.4 \text{ cm}$
$r = 2 \text{ cm}$
$V = 5.03 \text{ cm}^3$

With a mean density of $\rho = 0.2 \times 1.12 + 0.8 \times 3.21 = 2.79 \text{ g/cm}^3$ the mass that was necessary to get such a green body could be calculated: 14.04 g.

A press of the type *P.O. Weber PW 40 S* with a warmpressing tool *P.O. Weber 10 H* and a control unit *TRG1S* was used. The diameter of the stamp was 40 mm. A PTFE-foil was inbetween powder and stamp, PTFE-tape should seal the set up.

A pressure of 35 MPa was applied, which equals a force of 44 kN. The heating rate was 6 K/min from 20 °C to 200 °C, 200 °C were held for 2 hours. When reaching approximately 100 °C during cooling down the pressure was released. The pressure changed while heating starting at 120 °C and reaching a maximum of 50 MPa (=61 kN) during dwell time. After cooling overnight, the green body was removed from the press. It broke on both the top and bottom side, as can be seen in Figure 16. It was decided to not use this method anymore for preparing the supporting structures.



Figure 16: Actual warm pressed sample in the middle, top and lower punch on the sides

3.2 PREPARATION OF THE INTERMEDIATE LAYER

In order to make it possible to put the top layer on the macroporous support, an additional layer – the intermediate layer – is required. The aim was a structure inbetween those of support and top layer regarding pore structure and composition.

The layer was fabricated by a combination of slipcasting and dipcoating.

3.2.1 Preparation of the slip

To get a structure between those of support and top layer, a slip containing polysilazane and silicon nitride powder was prepared.

Two different slips were prepared, using toluene, silicon nitride and the same polysilazane that was already used for the support structure before (containing DCP too). Slip M was the same as Mori et al. used in [22] and one was similar to previous work in the research group (slip R). The concentrations can be seen in Table 8.

Table 8: Slip compositions for intermediate layer

	Slip M (after Mori et al.)		Slip R (after previous work in this research group)	
	vol%	wt%	vol%	wt%
silicon nitride	1,16	4,15	5	16,4
polysilazane	0,73	0,85	4	4,1
toluene	98,11	95	91	79,5

Toluene and polysilazane were weighed in a HDPE-bottle already containing silicon nitride milling balls, and the silicon nitride powder was added. Due to the low amount of powder, this could be done in one step. After replacing the air above the mixture with nitrogen, the slips were ball milled for 3 hours.

Both of them were tested on their sedimentation behaviour. As expected they were very unstable. To get a consistent layer it is necessary to have a stable dispersion. Two strategies were set up to improve the stability. The first and more simple one was the use of dispersion aids, e.g., oleic acid [61]. The second option is surface modification of the silicon nitride powder with silanes. [62]

Oleic acid

The effect of adding oleic acid was tested through preparing slips of both compositions (slip M and slip R) like above but adding 1 wt% oleic acid (in relation to the silicon nitride powder).

Silanisation of the silicon nitride powder

Three silanes were tested on their influence on the stability:

- 3-Aminopropyltrimethoxysilane
- N-(3-(trimethoxysilyl)propyl)ethylendiamine
- N-(6-aminohexyl)aminopropyltrimethoxysilane

They are from now on called 3A, N3 and N6 respectively.

Following [63], the silanisation was carried out in a 95:5 vol% EtOH:water mixture. The concentration of the used silane was supposed to be 2%. The necessary amount to get a monolayer of silane on the silicon nitride surface was calculated (equation 6).

$$silane [g] = \frac{silicon\ nitride [g] \times SSA_{Si_3N_4} [m^2/g]}{SWS_{silane} [m^2/g]} \quad (6)$$

where SSA is the specific surface area of the silicon nitride powder (SSA=11m²/g for UBE SN-E10) and SWS is the specific wetting surface of the silane (listed in Table 9).

Table 9: Specific wetting surface of the silanes [64], [65]

	SWS [m ² /g]
3A	353
N3	358
N6	358 ¹

The silane was weighed in a beaker and the solvent was added. Using acetic acid the pH was adjusted to 4,5-5,5. After 5 minutes of stirring the silicon nitride powder was added little by little and the stirring was continued for another ten minutes. The beaker was put in an

¹ No value was found for that specific silane, but due to the similar values for 3A and N3 that of N3 was used for N6 too.

ultrasonic bath for 3 minutes followed by another 1 minute of stirring with the magnetic stirrer. This was repeated 3 times before centrifuging with 3000 rpm for 4 minutes. After removing the supernatant, the precipitate was (two times) washed with EtOH and again centrifuged. The powder was then dried at 110 °C until reaching constant weight.

Polysilazane showed a positive effect on the appearance of the slip; the concentration of the polymer was increased, first to 8 wt%, then to 12 wt% for the slip similar to that of the previous work of the research group.

Once the best combination of composition and stabilisation aid was found, different concentrations were tested, varying the amount of toluene while keeping the ratio silicon nitride:polysilazane constant.

The slips listed in Table 10 were prepared.

First Th12 was tried on both the supports prepared via slip casting and the polymer derived route. The different pore structure of them resulted in a different layer formation. The coating on the slip cast supports had to be thinner, therefore, 80 wt% and then 91 wt% were tried. 91 wt% was chosen for the following experiments. For the polymer derived supports a problem occurred: the slip didn't wet the surface properly. Therefore, a higher concentrated slip was prepared, first 50 wt% and then even one containing only 45 wt% toluene. Although the concentration was extremely high by then, no homogenous coating could be obtained. Another strategy was pursued: surface treatments before coating. One idea was closing the pores on the surface through rubbing with graphite. Another was grinding the surface with SiC-paper (#600). Both were compared to the layer on an untreated sample. Grinding the surface was chosen for further experiments. The concentration of the used slip was lowered again to get a thinner coating; from 72 wt% to 80 wt% where a few experiments were made, but finally to 85 wt%.

Not only sedimentation tests were carried out to evaluate the suitability of the slips for coating. The quality of a resulting layer was tested on glass plates, by dipping them and crosslinking the layer.

Table 10: Overview of the slips tested for the intermediate layer preparation

		toluene, wt%	Si ₃ N ₄ , wt%	polysilazane, wt%	dispersion aid
Slip M		95	4.15	0.85	-
					oleic acid
Slip R	Th	79.5	16.4	4.1	-
					oleic acid
					modified powder
	Th8	75.6	16.4	8	modified powder
	Th12 ≡ 72wt%	71.6	16.4	12	modified powder
	50 wt%	50	28.9	21.1	modified powder
	60 wt%	60	23.1	16.9	modified powder
	80 wt%	80	11.6	8.4	modified powder
	85 wt%	85	8.7	6.3	modified powder
	91 wt%	91.3	5	3.7	modified powder
45 wt%	45	28.9	26	modified powder	

3.2.2 Dip coating

Dip coating is done with a coater built by members of the research group. The engine was programmed via Arduino. Different files were programmed for withdrawal speeds of 10, 20, 40, 50, 100, 120 and 140 mm/min. The setup can be seen in Figure 17.



Figure 17: Dip coater used for the experiments

The layer is supposed to be as thin as possible. Usually a higher withdrawal speed yields in a thicker layer. But in this case, a porous substrate is used, which causes filtration effects; it's a combination between dip coating and slip casting. The longer the substrate is dipped in, the thicker the layer becomes. Therefore, the highest withdrawal speed was used here, which is 140 mm/min. This hypothesis was once tested using 120 mm/min instead of 140 mm/min.

All samples were cleaned before dip coating, first in acetone, using an ultrasonic bath, then rinsing them with acetone and isopropanol.

Teflon tape was used to make sure only one side is coated and a wire sling made it possible to attach it to the dipcoating set up.

3.2.3 Crosslinking and pyrolysis

The crosslinking procedure was done the same way as for the supporting structure, but was only carried out one time, not two times.

Another temperature program was used for the pyrolysis. Because of the smaller volume and the absence of PE, a higher heating rate can be chosen. The program can be seen in Table 11.

Table 11: Temperature program for the pyrolysis of the intermediate layer

0 – 300 °C	3 K/min
300 – 800 °C	1 K/min
800 °C	4 h
800 – 0 °C	1 K/min

3.2.4 Characterization

The layer-thickness and overall appearance were investigated using a scanning electron microscope, as described in 3.1.1.4.

3.3 PREPARATION OF THE TOP LAYER

The goal of this thesis was finding a method to prepare a dense top layer on a macroporous support structure by dip coating with a preceramic polymer.

3.3.1 Preliminary tests

To evaluate the optimal dipping parameters, glass plates were dip coated with polysilazane solutions of different concentrations and using different withdrawal speeds. Toluene was used as a solvent and mixtures with 10 vol%, 20 vol% and 50 vol% of the polysilazane were prepared. For each concentration five speeds were tested: 10, 20, 50, 100, 140 mm/min. The plates were dipped in approximately 2.5 cm deep, the backside was cleaned and the coating was crosslinked for 16 hours at 105 °C in a nitrogen atmosphere (flowing), in analogy to the polymer derived support structures (3.1.2.4)

The thickness of each layer was measured using profilometry (Dektak II, Sloan). Five or six spots on each plate were measured by scratching off small areas of the coating.

The Landau-Levich-model (equation 1, section 2.5) describes the correlation between withdrawal speed and resulting layer thickness. To apply the model to evaluate the solutions mentioned above, the viscosity and surface tension have to be measured. The density was calculated. The analysed samples were prepared directly before the measurement, but older solutions were tested too, to find out, if there is a change in properties with time.

The viscosity was measured shear-rate-dependent at 25 °C with a cone-plate setup using a Anton Paar MCR 302 WESP with a P-PTD 200/GL Peltier glass plate. A cone with 25 mm diameter and 1° angle (CP25-1) was used. 15 different shear rates (10...250 s⁻¹) were each held for 10 seconds. Before starting the measurement, the sample was sheared for 10 seconds.

The surface tension was measured using a tensiometer (KRÜSS GmbH Germany Model: K6, the ring was an RI0111 type) which can be seen in Figure 18 .

Each of the solutions was filled in a crystallizing dish, the table was moved upwards until the Pt-Ir-wire-sling was about 5 mm beneath the surface.

The lever was moved in the zero-position and force was applied carefully. Then the lever was again brought to zero by moving the table downwards. This was continued under meniscus-formation until the wire abruptly detached from the liquid-surface. The applied force could be directly read off the tensiometer.

Not only the solutions but also the pure components were measured.



Figure 18: Tensiometer [66]

3.3.2 Dip coating

Except for the cleaning step, the dip coating was done the same way as for the intermediate layer (3.2.2).

3.3.3 Crosslinking and pyrolysis

The crosslinking and pyrolysis steps were the same as for the intermediate layer (3.2.3).

3.4 MASKING

Due to capillary effects, the dipping solution penetrates the pores of the support which leads to an inhomogenous top layer. Elyassi et al. [53] tried filling the pores on purpose with a sacrificial polymer which is burned out during pyrolysis but still stable during the crosslinking step. That leads to a support structure that seems dense while applying the following layers, but keeps its macroporous structure in the end.

3.4.1 Preparation of the dipping solution

In this work, polystyrene was used as sacrificial mask. Two different kinds of polystyrene were tried out. One was atactic polystyrene in form of flakes with a known molecular weight (Polystyrene, atactic, flakes, 44416, FW: 800-5000; Alfa Aesar); the other was conventional styrofoam, which was in the first case just supposed to be used for preliminary tests, but turned out to work better.

Toluene was used as a solvent and solutions of different concentrations were prepared in glass bottles using a magnetic stirrer. Elyassi et al. [53] used 1 wt% of polystyrene (GPC grade, MW=2500, Scientific Polymers Products, Inc.), but in our case higher concentrations were needed to see any effect. During the experiments solutions of 1 wt%, 3 wt%, 5 wt%, 10 wt% and 15 wt% were prepared with the styrofoam. For the industrial polystyrene only 1 wt% and 3 wt% were chosen.

3.4.2 Dip coating

As before, a wire sling is necessary to attach the samples to the dip coating set up. Again, 140 mm/min were chosen as withdrawal speed. The time the samples were held in the solution before removing them was either 1 s or 15 s. The longer time was supposed to make sure that the solution could completely penetrate the samples.

The toluene was removed in a furnace at 110 °C (appr. 1 hour).

3.4.3 Consequences for the preparation of the top layer

The pores have to stay filled with the polystyrene during the whole process of applying the top layer, which includes the dip coating step itself as well as the crosslinking of the polysilazane. Due to that, the solvent for the polysilazane has to be changed. In the previous experiments toluene was used as a solvent, but the polystyrene would be dissolved when getting in contact with the dipping solution. Therefore, n-hexane was chosen as new solvent.

Solutions with 20 wt% and 50 wt% were prepared, but only the higher concentrated one was used for further experiments.

For the toluene-polysilazane solutions, preliminary tests were done to evaluate the Lendau-Levich-model and also to get the correlation between withdrawal speed and layer thickness by oneself. This was repeated with the new solutions, but turned out to be more difficult due to the higher vapor pressure of n-hexane. The experiments on the glass plates had to be repeated several times. Also the measurement of the viscosity didn't work well, because during the measurement some hexane evaporated leading to a constant increase in viscosity (4.3.1).

The viscosity of n-hexane is lower than that of toluene which generally results in thinner coatings.

3.5 PREPARATION OF TUBULAR SAMPLES

The results of the experiments on the disc shaped samples were tried for tubular supports too, to prove that they can be adapted.

3.5.1 Slip cast supports

The supports were mainly prepared during another thesis of a member of the research group. The exact procedure is described in the master thesis of Dominik Brouczek.

Tubes with a diameter of about 10 mm and a length of about 55 mm in the sintered stage (6 cm as green body) were slip cast in a plaster mold consisting of two parts, removing the slip after 70 seconds by turning the mold upside down. The samples were left inside the mold for 24 hours, removed, and then dried at 110 °C before sintering. The slip contained sintering aids ($\text{Al}_2\text{O}_3 + \text{Y}_2\text{O}_3$) and therefore lower sintering temperatures were necessary (1550 °C).

For the intermediate layer, additional experiments were conducted with planar, disc shaped samples to find out which slip concentration is needed to yield a layer thickness in the range of those of the previously investigated samples with higher porosity. Disc shaped samples were prepared in the same way as the tubular samples and coated with slips of two concentrations, the "72 wt%" and the "80 wt%" slip; the resulting layer was investigated using electron microscopy.

To be able to apply the intermediate layer without preparing a large amount of dipping slip, shorter samples were needed. The tubular structures were cut in two pieces to get tubes with around 3 cm length. Only one side of the planar samples was coated, using Teflon tape. To manage getting a coating only on the outside and not on the inside of the tubular samples,

top and bottom were closed with small PE-stoppers of glass vials. A wire was attached to the PE piece at the upper side and then attached to the dip coater; the set up can be seen in Figure 19. Crosslinking and pyrolysis were conducted as described in 3.2.3.



Figure 19: Set up for dipping of tubular slipcast supports

Only the best working method should be used for the top layer preparation, but it involved grinding the sample after masking it, which did not work well on the curved surface. The second best method was used: The sample was masked, but only the upper side was closed so that the polystyrene solution can penetrate the whole sample easier. For the application of the top layer, again both sides were closed with the PE-pieces. Crosslinking and pyrolysis were done as in 3.3.3.

3.5.2 Polymer derived supports

All the tubular polymer derived support structures used were prepared by another member of the research group.[67] The procedure was the same as for the disc shaped samples.

The pyrolysed tubular supports were cut in half for the same reason as the slip cast supports; also getting a length of about 3.3 cm.

The surface of the samples was prepared like that of the planar ones, which means grinding the surface and cleaning the samples in acetone and with isopropanol.

Due to the smaller diameter than that of the slip cast supports, the PE-tops didn't fit and parts of the silicone molds used to cast the samples were cut out to close the open ends. The upper end was directly attached to the dip coater. (Figure 20)



Figure 20: Set up for dipping of tubular PDC-supports



Figure 21: Arrangement for pyrolysis of tubular coated supports without touching the crucible

The intermediate layer was prepared with the “85 wt%” slip. Crosslinking and pyrolysis are similar to that of the planar samples. The samples were put in the furnace as shown in Figure 21.

Both the bottom and the top were closed for the masking step as well as for the top layer application. Again crosslinking and pyrolysis were done in the same way as before (see section 3.3.3).

3.6 PERMEABILITY TESTING

A future aim is to use the prepared multi-layered structures as asymmetric membranes for gas separation. Therefore, permeability is one of the most important properties besides selectivity and mechanical as well as chemical stability.

Permeability was measured in two different setups: one for the planar, disc shaped samples that were mostly prepared in this thesis; and a second one which was for tubular samples, where the support was prepared in previous work of the research group, but the coating was added as final experiment of this thesis.

For both set ups, the measurements were carried out at room temperature and with filtered compressed air as fluid. By constructing the setup following DIN EN ISO 4022, an unidirectional, axial flow through the sample can be achieved.

The gas flow Q was recorded using a soap bubble flow meter, while varying the differential pressure between upstream and downstream side of the sample from $\Delta p = 0.25 \text{ bar} \dots 2 \text{ bar}$.

Forchheimer's equation for compressible fluids (equation 7, [68]) was used to determine Darcian (k_1) and non-Darcian permeabilities (k_2).

$$\frac{p_i^2 - p_o^2}{2p_o \cdot l} = \frac{\eta}{k_1} \frac{Q}{A} + \frac{\rho}{k_2} \left(\frac{Q}{A} \right)^2 \quad (7)$$

$p_{i/o} \dots$ absolute pressures on upstream/downstream side

$\eta \dots$ air viscosity ($= 1.84 \cdot 10^{-5} \text{ Pa} \cdot \text{s}$)

$\rho \dots$ air density ($= 1.16 \text{ kg/m}^3$, $p_o = 990 \text{ mbar}$ and $T = 22 \text{ }^\circ\text{C}$)

k_1 and k_2 were calculated by fitting of a quadratic function to $(p_i^2 - p_o^2 / 2p_o l)$ versus Q/A using the least-squares method.

4 RESULTS

4.1 SUPPORT STRUCTURE

4.1.1 Slip casting

The influence of loading and sintering temperature on the porosity was investigated.

One slip with 35 vol% loading and one with 39 vol% loading were analysed using electron microscopy and the immersion testing method.

The measured and calculated values of the immersion testing can be seen in Table 12. Independent on temperature and loading the apparent porosity Π_a is between 52.5 % and 53.9 %. The increasing temperature doesn't have any effect on the porosity, nor has the higher loading.

Table 12: Immersion testing method results

loading, %	sample	m_1 , g	m_2 , g				m_3 , g	ρ_b , kg/m ³	ρ_s , kg/m ³	Π_a , %	Π_a , % mean value	$T_{\text{sintering}}$, °C	
			1	2	3	mean value							
35	C2	1.4228	0.9717	0.9730	0.9707	0.9718	1.9417	1.464	3.147	53.5	53.4	1800	
	C7	1.1559	0.7898	0.7914	0.7900	0.7904	1.5725	1.475	3.155	53.3			
39	E1	1.3274	0.9090	0.9100	0.9110	0.9100	1.7866	1.510	3.172	52.4	52.5		
	E12	1.2337	0.8454	0.8446	0.8452	0.8451	1.6584	1.513	3.166	52.2			
	E13	1.3178	0.9010	0.9016	0.9016	0.9014	1.7792	1.497	3.156	52.6			
	E16	1.3228	0.9052	0.9079	0.9070	0.9067	1.7878	1.497	3.171	52.8			
35	C3	1.3518	0.9312	0.9292	0.9307	0.9304	1.8420	1.480	3.201	53.8	53.7		1850
	C9	1.4551	1.0007	0.9989	1.0000	0.9999	1.9810	1.480	3.189	53.6			
39	E8	1.3908	0.9521	0.9530	0.9524	0.9525	1.8717	1.509	3.165	52.3	52.7		
	E11	1.2764	0.8729	0.8740	0.8743	0.8737	1.7188	1.506	3.161	52.4			
	E17	1.0158	0.6962	0.6945	0.6967	0.6958	1.3776	1.486	3.166	53.1			
	E21	1.1701	0.8024	0.8021	0.8011	0.8019	1.585	1.490	3.169	53.0			
35	C1	1.3928	0.9539	0.9529	0.9552	0.9540	1.9051	1.461	3.167	53.9	53.9	1900	
	C4	1.9483	1.3374	1.3372	1.3364	1.3370	2.6640	1.465	3.180	53.9			
39	E2	2.0042	1.3784	1.3769	1.3773	1.3775	2.7069	1.504	3.190	52.9	53.2		
	E4	1.5610	1.0755	1.0740	1.0745	1.0747	2.1169	1.494	3.201	53.3			
	E14	1.3799	0.9496	0.9494	0.9482	0.9491	1.8723	1.491	3.194	53.3			
	E18	1.316	0.9033	0.9058	0.9068	0.9053	1.7851	1.492	3.196	53.3			

The dimensions of the samples were measured before and after the sintering process and the density was calculated using the mass. By putting the calculated density in relation with the theoretical density of silicon nitride ($\rho=3.21 \text{ g/cm}^3$), the porosity could be estimated.

The data is listed in Table 13.

The change in diameter and height was little, approximately 1 % and without a trend in one direction. The mass loss was about 4 % for all the samples without a special trend depending on loading and temperature. Due to that mass loss and the little change in dimensions the density decreased while sintering too.

Table 13: Change of dimensions and mass loss during sintering

loading, %	sample	d			h			m			ρ			Πa, %	T _{sintering} , °C	
		before, mm	after, mm	Δ, %	before, mm	after, mm	Δ, %	before, g	after, g	Δ, %	before, g/cm ³	after, g/cm ³	Δ, %			
35	C2	17.64	17.56	-0.45	4.35	4.31	-0.92	1.4829	1.4235	-4.01	1.4214	1.3638	-4.05	57.5	1800	
	C7	17.58	17.56	-0.11	3.48	3.44	-1.15	1.2007	1.1555	-3.76	1.4420	1.3870	-3.81	56.8		
39	E1	17.70	17.63	-0.40	3.83	3.79	-1.04	1.3718	1.3278	-3.21	1.4835	1.4352	-3.25	55.3		
	E12	17.62	17.61	-0.06	3.64	3.62	-0.55	1.2745	1.2338	-3.19	1.4462	1.3994	-3.24	56.4		
	E13	17.61	17.60	-0.06	3.90	3.81	-2.31	1.3662	1.3180	-3.53	1.4747	1.4219	-3.58	55.7		
	E16	17.49	17.44	-0.29	4.13	4.12	-0.24	1.3725	1.3232	-3.59	1.3953	1.3445	-3.64	58.1		
35	C3	17.55	17.49	-0.34	4.25	4.18	-1.65	1.4094	1.3517	-4.09	1.4041	1.3460	-4.14	58.1		1850
	C9	17.65	17.50	-0.85	4.45	4.43	-0.45	1.5263	1.4550	-4.67	1.4331	1.3655	-4.72	57.5		
39	E8	17.58	17.52	-0.34	4.46	4.48	0.45	1.4405	1.3907	-3.46	1.3344	1.2876	-3.51	59.9		
	E11	17.49	17.47	-0.11	3.93	3.95	0.51	1.3234	1.2768	-3.52	1.3984	1.3485	-3.57	58.0		
	E17	17.69	17.55	-0.79	3.72	3.76	1.08	1.0595	1.0160	-4.11	1.1654	1.1170	-4.16	65.2		
	E21	17.51	17.53	0.11	4.04	4.00	-0.99	1.2173	1.1705	-3.84	1.2615	1.2124	-3.90	62.2		
35	C1	17.58	17.51	-0.40	4.50	4.30	-4.44	1.4652	1.3931	-4.92	1.4157	1.3461	-4.92	58.1	1900	
	C4	17.75	17.60	-0.85	5.72	5.66	-1.05	2.0525	1.9484	-5.07	1.4913	1.4157	-5.07	55.9		
39	E2	17.55	17.54	-0.06	4.08	4.16	1.96	1.4450	1.3798	-4.51	1.4383	1.3734	-4.51	57.2		
	E4	17.59	17.60	0.06	5.05	4.95	-1.98	1.6369	1.5607	-4.66	1.3599	1.2966	-4.66	59.6		
	E14	17.64	17.64	0.00	5.88	6.00	2.04	2.0803	2.0040	-3.67	1.4194	1.3673	-3.67	57.4		
	E18	17.72	17.50	-1.24	4.31	4.43	2.78	1.3756	1.3154	-4.38	1.2916	1.2351	-4.38	61.5		

As mentioned before, the neck formation and the overall appearance of the samples were investigated using electron microscopy. The fracture surface was studied. No difference depending on loading or sintering temperature could be observed. Almost no neck formation can be seen in all the pictures, which confirms the assumption that sintering didn't take place properly due to the lack of sintering aids. The SEM-pictures can be seen in Figure 22.

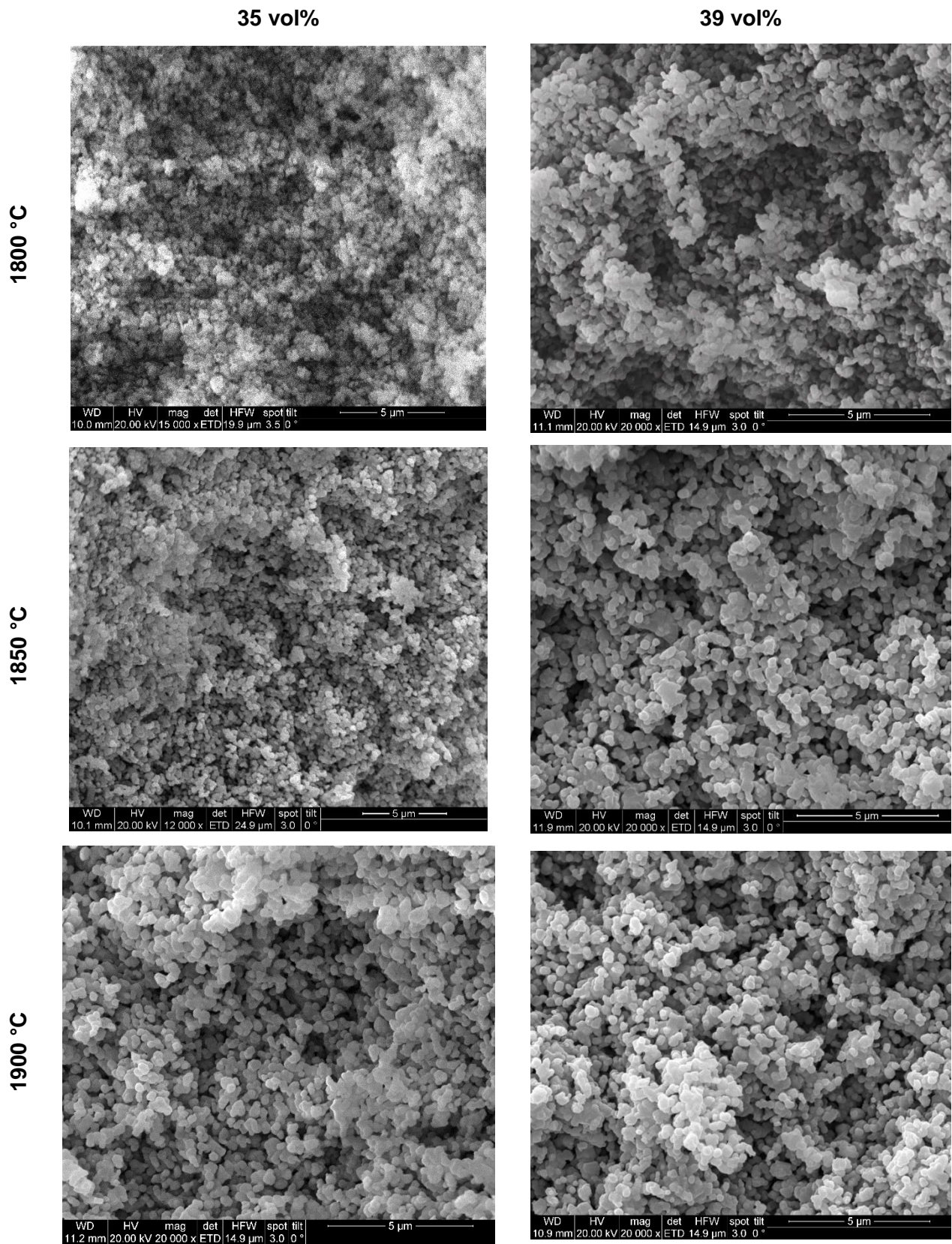


Figure 22: Fracture surface of slip cast Si_3N_4 -supports with different loadings and sintering temperatures

The mass loss during sintering is caused by the vaporization of remaining water and decomposition of the dispersion aid.

The increasing height and diameter of some of the samples occurs because of the previously mentioned problems while measuring, especially for the height, due to meniscus forming and instability of the samples. When trying to grind them to make a more accurate measurement possible, fragments broke out of the sample. But as mentioned above, no trends could be found. The absence of any influence of loading and sintering temperature was also confirmed by the results of the immersion testing method.

4.1.2 Polymer derived ceramic supports

Despite the calculation of the density, no further investigations were made to characterize the supports, because the process was already used in former work of the research group. The scanning electron microscope picture shown in Figure 23a is taken from [19] (Figure 4b) to show the structure of the PDC-supports. One can see the large spherical pores. resulting from decomposition of the sacrificial PE-fillers, connected by small channels due to gas release. The overall appearance of such a support can be seen in Figure 23b.

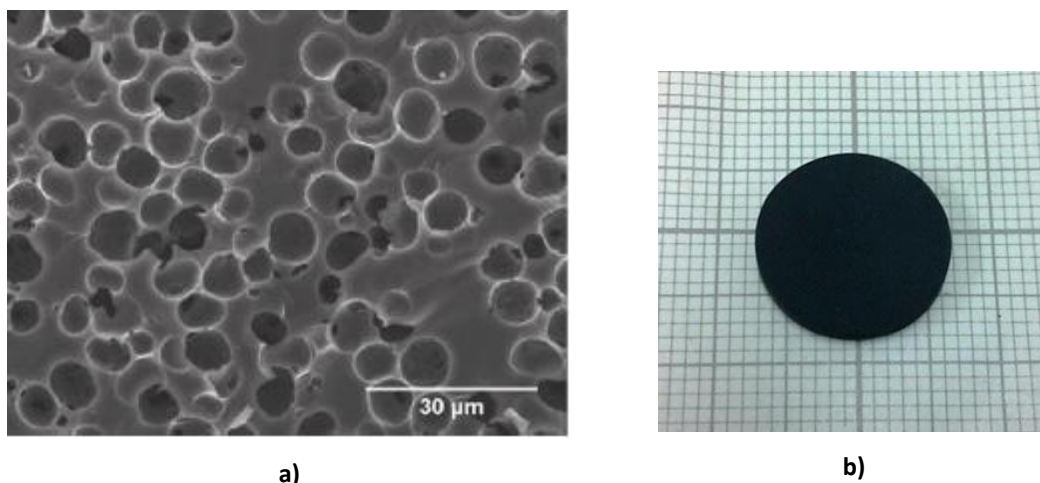


**Figure 23: PDC-support (a) pore structure
(b) overview**

The skeletal density of the pyrolysed material was investigated using He-pycnometry, resulting in a value of 2.11 g/cm³.

The porosity of the produced samples was calculated using the density of the samples compared to that value.

Seven batches of such PDC supports were prepared. The mass loss, change in dimensions, and the density before and after sintering is listed in Table 14.

Batches I and II showed slightly higher porosity compared to the following batches. In addition they looked brown instead of black/grey and showed large cracks all over the surface. These two were the first samples pyrolysed in a new furnace. Apparently the gas pipes weren't leak tight, leading to oxygen contamination of the atmosphere and oxidation of the samples.

Batch VII also shows higher porosity than expected. The gas outlet was partly closed by decomposition products of the PE during the pyrolysis process, leading to a decreased gas flow.

The rest of the batches all had calculated porosities of about 45 %, which was expected.

Table 14: Mass loss, dimension change and calculated porosity of the PDC-supports

Batch	sample	d			h			m			ρ			porosity [%]
		before, mm	after, mm	Δ, %	before, mm	after, mm	Δ, %	before, g	after, g	Δ, %	before, g/cm ³	after, g/cm ³	Δ, %	
I	1	17.74	14.19	-20	2.91	2.36	-19	0.74	0.40	-60	1.03	1.06	3	50
	2	17.44	13.86	-21	2.92	2.31	-21	0.73	0.38	-62	1.05	1.08	3	49
II	1	17.67	13.55	-23	2.90	2.23	-23	0.73	0.36	-64	1.03	1.12	9	47
	2	17.51	13.30	-24	2.94	2.28	-22	0.71	0.35	-65	1.01	1.11	10	48
III	1	17.65	13.71	-22	2.97	2.22	-25	0.73	0.36	-64	1.00	1.11	11	47
	2	17.77	13.64	-23	2.86	2.14	-25	0.74	0.37	-63	1.04	1.17	13	44
IV	1	17.68	13.71	-22	2.96	2.20	-26	0.76	0.38	-62	1.05	1.16	11	45
	2	17.65	13.64	-23	2.82	2.10	-26	0.72	0.36	-64	1.04	1.17	12	44
V	1	17.85	13.52	-24	2.94	2.24	-24	0.76	0.37	-63	1.03	1.15	11	46
	2	17.90	13.50	-25	2.66	2.10	-21	0.69	0.33	-67	1.03	1.11	8	47
VI	1	17.57	13.15	-25	2.87	2.16	-25	0.70	0.34	-66	1.00	1.15	15	45
	2	17.33	13.16	-24	2.86	2.16	-24	0.70	0.34	-66	1.04	1.15	12	45
VII	1	17.51	13.83	-21	2.88	2.30	-20	0.73	0.36	-64	1.06	1.04	-2	51
	2	17.32	13.68	-21	2.90	2.30	-21	0.72	0.36	-64	1.05	1.06	1	50

4.2 INTERMEDIATE LAYER

4.2.1 Preliminary tests

Two different compositions were tried in the first place, slip M following Mori et al. [22], and slip R similar to one done in the research group. Two strategies were tried to increase the stability of the slips used for the preparation of the intermediate layer. For slip M only oleic acid was tested.

In Figure 24 one can see the sedimentation test results for slip M without any dispersion aid and with about 5 wt% auf oleic acid. The amount was supposed to be 1.2 wt% but because of the little total volume of the slip, such a small amount wasn't possible to be weighed in correctly. Both curves go down rapidly, the one with the dispersion aid even more than the untreated one. After half an hour slip M+ OA already reaches nearly the final value. Due to the poor results, it was decided to not continue with further experiments using slip M.

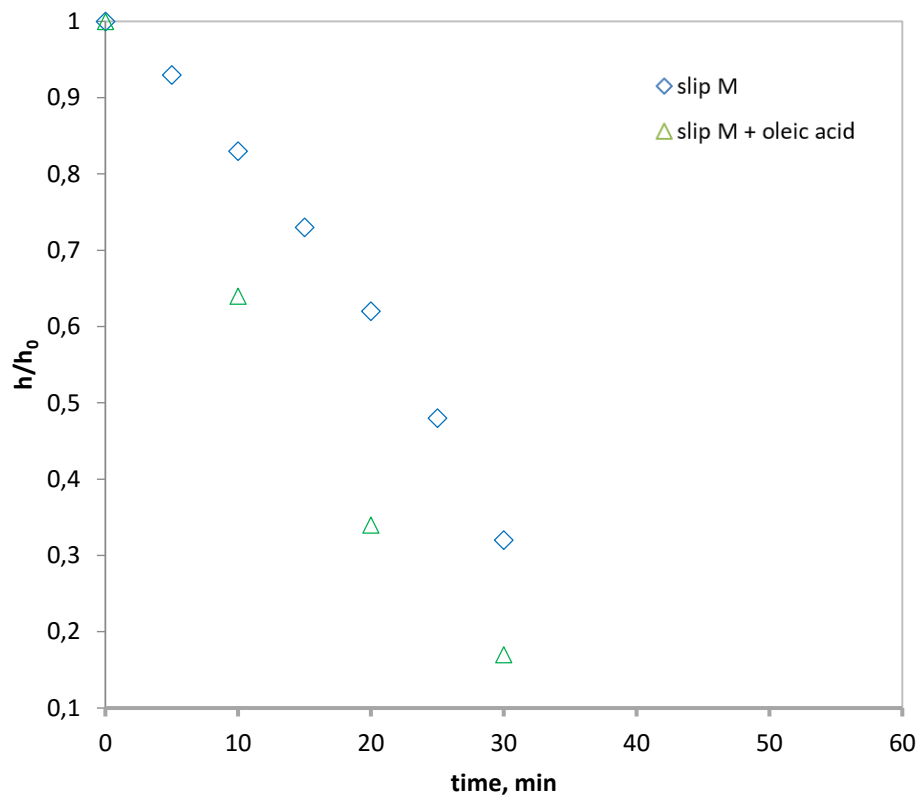


Figure 24: Sedimentation behaviour of slip M with and without oleic acid as dispersion aid

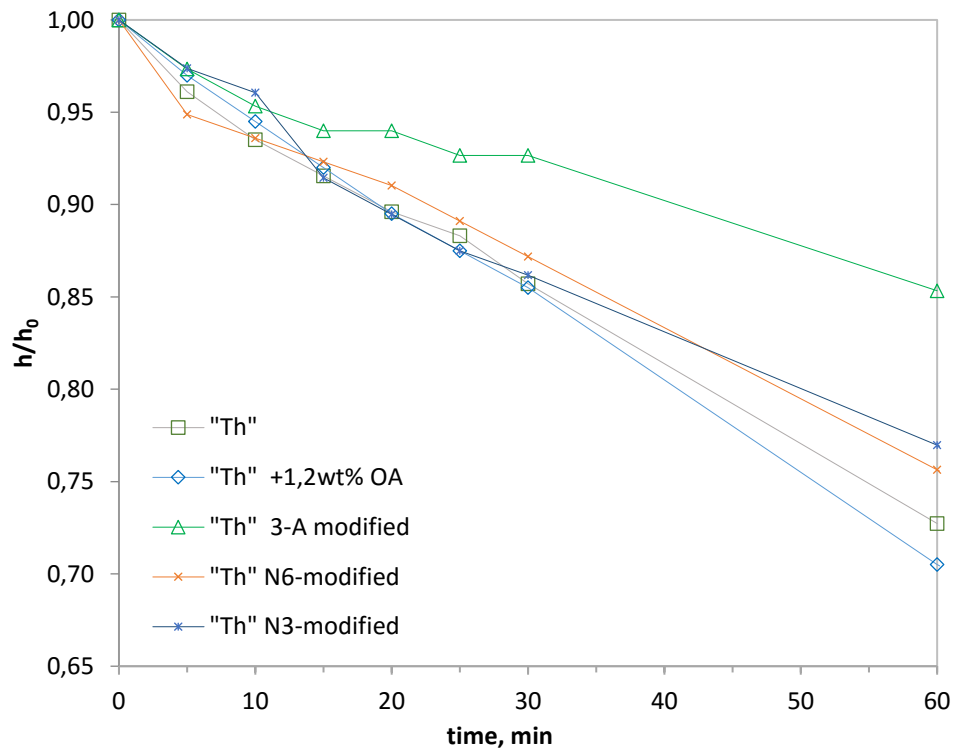


Figure 25: Sedimentation behaviour of slip R ("Th") using different stabilisation strategies

In Figure 25 the results for the slip "Th" (79.5 wt% toluene, 16.4 wt% Si_3N_4 , 4.1 wt% polysilazane) can be seen. First on the effect of oleic acid for this slip, looking at the two lowest curves: As for the Mori slip, oleic acid even has a negative effect on the stability.

For this composition also modified silicon nitride powders were tested, which can be seen in the same figure. After five minutes the 3-A and the N-3-modified ones are head to head the most stable ones, but already after 15 minutes the 3-A one clearly outmatches the other ones, while they are yielding quite the same values.

It was decided that the 3-A modified powder should be used for further experiments.

If comparing slip M and slip R ("Th"), there's a significant difference: whereas slip M reaches the final h/h_0 value after half an hour, Th needs more than twice the time.

The polysilazane fraction is higher in the "Th" slip which led to the assumption that the polymer itself works as dispersion aid for the silicon nitride. While preparing the slips, it was observed that they were extremely instable before adding the polymer, huge agglomerates formed and couldn't be destroyed through milling until the polymer was added. For that reason, higher contents of polymer were tried: 8 wt% and 12 wt% instead of 4 wt%.

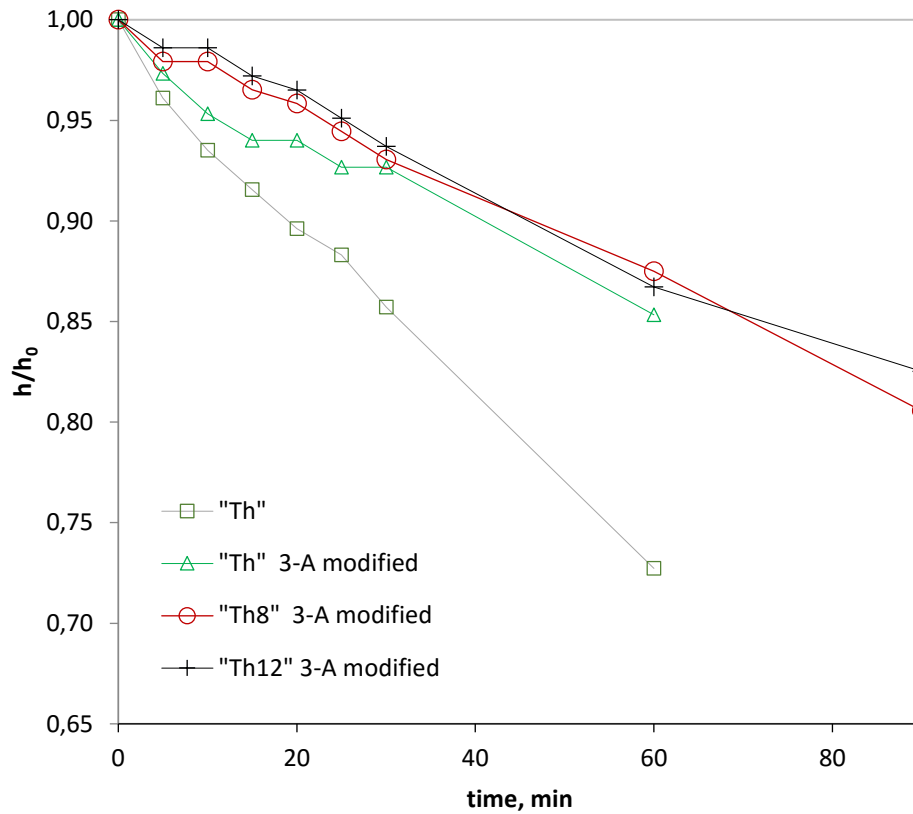


Figure 26: Sedimentation behaviour of “Th”-slips with increasing polymer content

The results are shown in Figure 26.

The sedimentation tests were carried out an additional 30 minutes for the slips with higher polysilazane content. It can be seen that with an increasing content, the stability increases too, although the effect becomes smaller when reaching higher contents (4 wt% → 8 wt% bigger difference than 8 wt% → 12 wt%).

The slip “Th12” was chosen for the dip coating experiments on the support structures.

4.2.2 Intermediate layer on the slip cast supports

As the porosity didn’t differ much between the batches, all of the supports were treated the same.

The first experiment was done with the “50wt%” slip, the withdrawal speed was 140 mm/min, the dwell time inside the slip was 1s. Because the resulting layer was too thick, it cracked while drying. Therefore, experiments with “60wt%”, “72wt%” (≡ “Th12”), “80wt%” and finally “91wt%” were done in that order. Only in the last experiment, the resulting layer stayed crack free during crosslinking and pyrolysis. The layer thickness was estimated via electron microscopy. It is listed in Table 15 and can be also seen in Figure 27.

Table 15: Intermediate layer thickness on slip cast supports (determined by SEM)

wt% toluene	h, μm
50	290
60	223
72	170
80	130
91	23

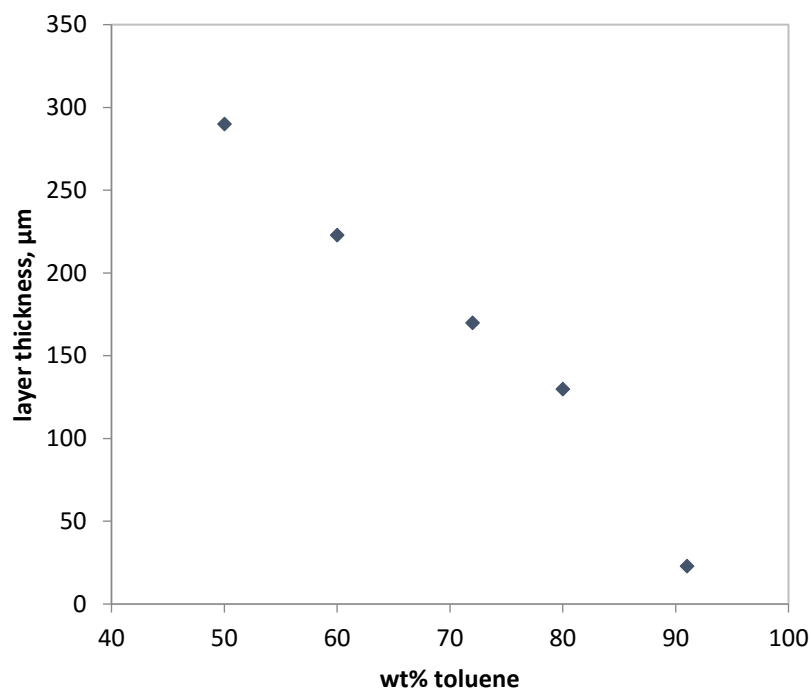


Figure 27: Intermediate layer thickness depending on slurry concentration on slip cast supports

In Figure 28 one can see the coated samples with “50 wt%” and the final “91 wt%” in the crosslinked stage. Where in the first experiments cracks can be observed and the surface is wavy, it is homogenous and smooth in the final one.

As mentioned above, the theory that a longer time inside the slip results in a higher layer thickness, was tested using a withdrawal speed of 120 mm/min instead of the usual 140 mm/min. A layer of approximately 32 μm was obtained (140 mm/min: 23 μm).

For the following experiments the intermediate layer was prepared using the “91 wt%” slip and a withdrawal speed of 140 mm/min. The resulting surface and fracture surface can be seen in Figure 29.

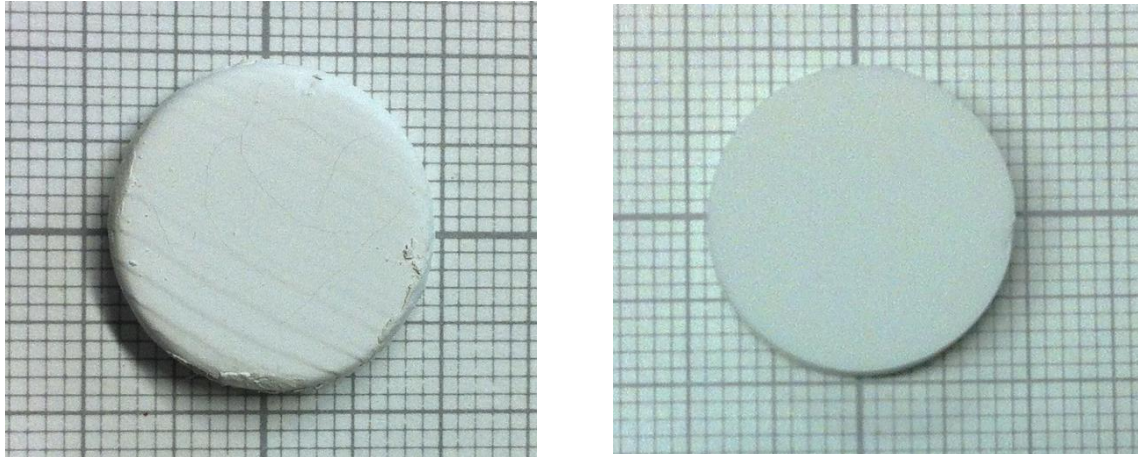


Figure 28: Slip cast supports coated with intermediate layer 50 wt% (left) and 91 wt% (right) in the crosslinked stage

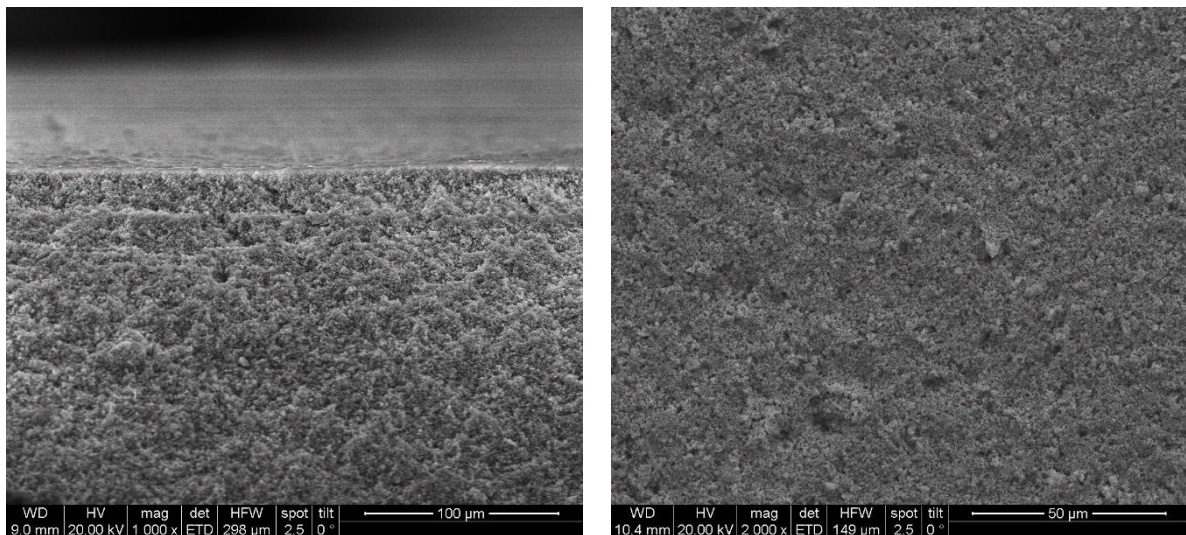


Figure 29: Intermediate layer 91 wt% on slip cast supports, fracture surface (left) and surface (right)

4.2.3 Intermediate layer on the polymer derived supports

The first experiments were done using the “50 wt%” slip. The coating was inhomogenous, the surface was extremely wavy. This may be caused by insufficient wetting.

The first thing that was tried to coat the surface completely was the higher concentrated slip “45 wt%”. In addition to that, two strategies were processed: rubbing graphite on the surface to close the pores, which was inspired by [54], and grinding the sample surface with SiC paper.

The electron microscopy pictures of the fracture surface are shown in Figure 30 in two different magnifications. There are also pictures which show the whole coated samples in the crosslinked stage.

One can clearly see, that the quality of the coating is best for the ground samples. The one spot where the coating is missing is due to removing the wire sling after the coating process. When looking at the electron microscopy pictures of the untreated sample, one can see the wavy surface, resulting in extreme differences of layer thickness within the sample.

For the graphit-treated ones, the wetting becomes better, but it looks as if the coating isn't connected well to the support structure. The best results were yielded by grinding the sample – the waves were reduced to a high extent and the coating is homogenous all over the sample. A possible explanation would be that decomposition products of the polyethylene-filler couldn't be removed quick enough by the nitrogen flow and condensed on the surface.

The layer didn't endure the pyrolysis – cracks formed because of the high thickness. Fracture surface and surface of the ground, coated, crosslinked and pyrolysed sample can be seen in Figure 31.

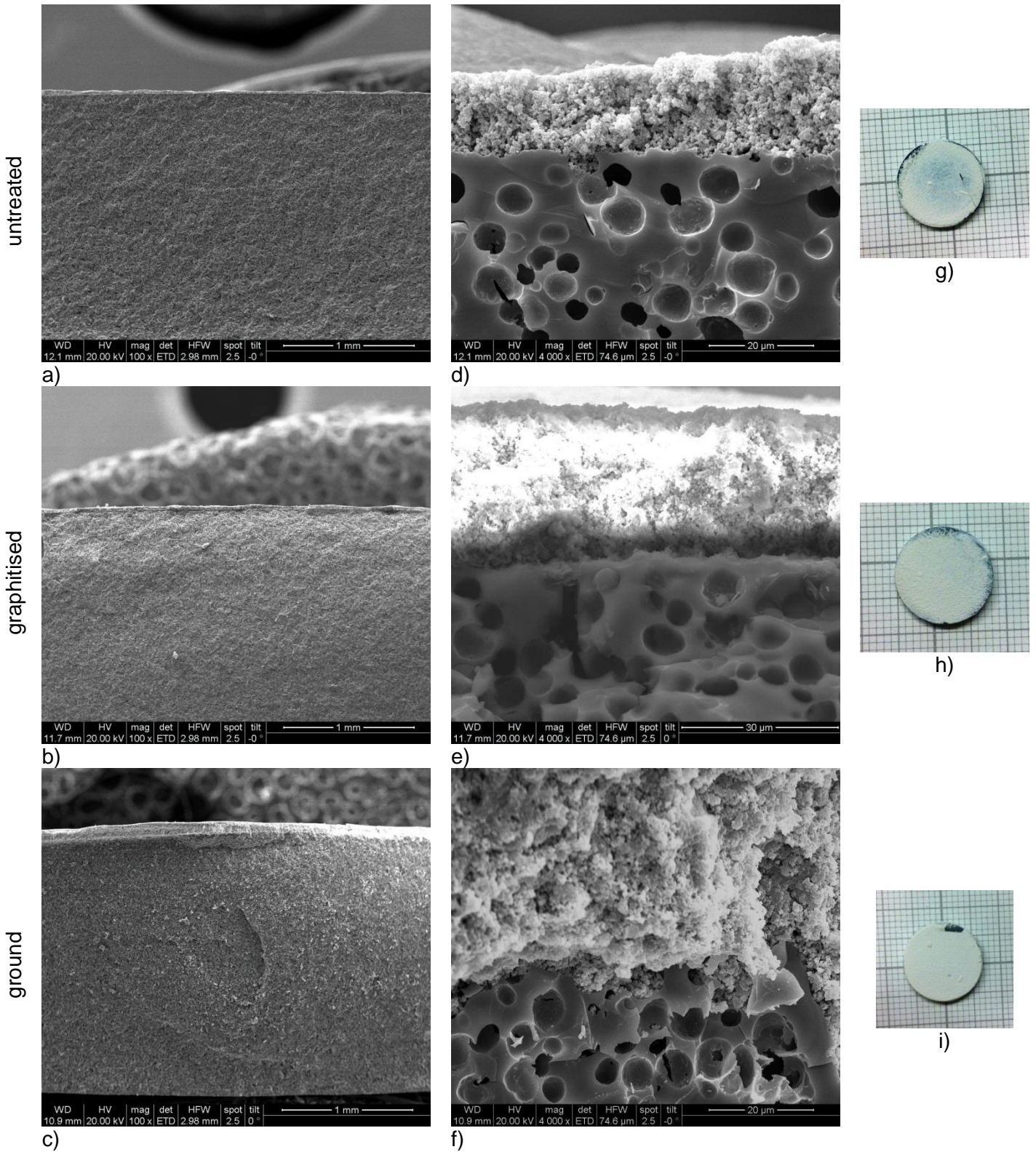


Figure 30: The fracture surfaces of PDCs with crosslinked 45 wt% intermediate layer for the untreated, graphitised and ground supports are shown in figure a, b and c respectively; higher magnifications are shown in figures d-e. The whole samples are shown in figures g-i.

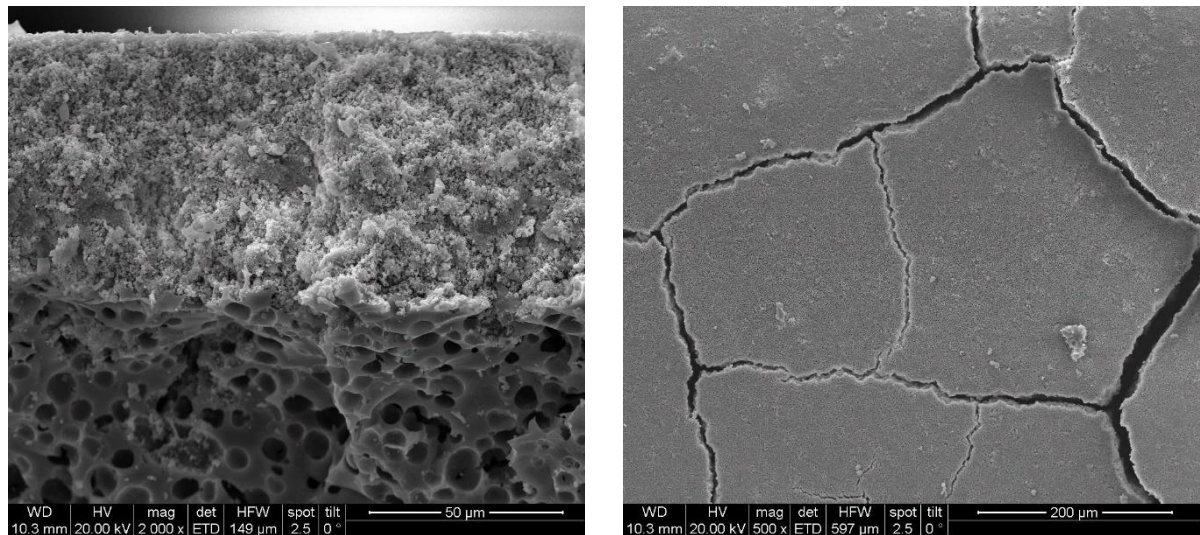


Figure 31: Ground support + intermediate layer 45 wt% in the pyrolysed stage, fracture surface (left) and surface (right)

The concentration of the slip was reduced step by step: “Th12” which equals “72 wt%”, then “80 wt%” and after problems with “80 wt%” an additional slip with “85 wt%” was prepared and samples were coated. The resulting layer thickness can be seen in Table 16 and Figure 32.

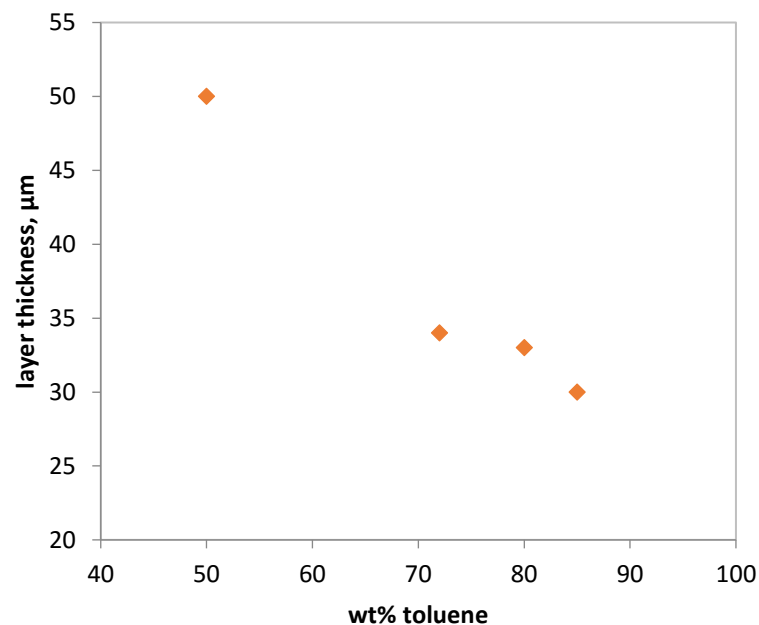


Figure 32: Intermediate layer thickness on PDC-supports dependant on slurry concentration

**Table 16: Intermediate layer thickness on PDC-supports
(determined by SEM)**

wt% toluene	h, μm
50	50
72	34
80	33
85	30

In the following pictures one can see the fracture surface of a sample coated with “80 wt%” in two magnifications as well as the surface after pyrolysis. The coating is homogenous over the whole sample. (Figure 33)

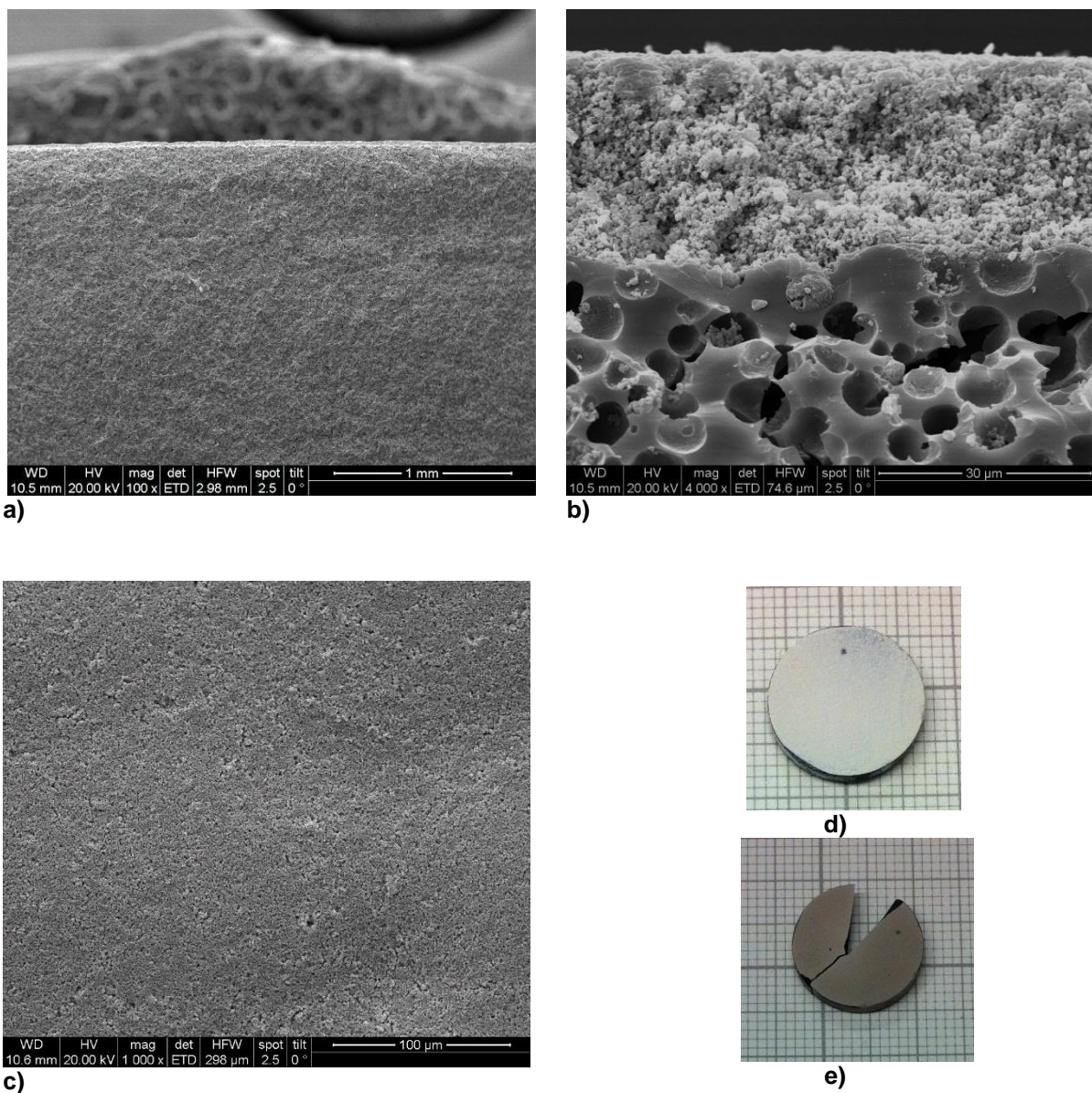


Figure 33: PDC support + intermediate layer 80 wt% in the pyrolysed stage; fracture surface (a & b), surface (c), sample in the crosslinked (d) and in the pyrolysed stage (e)

The first samples coated like that were crack free, but some of the following showed crack formation. Another batch was prepared again without cracks, while having approximately the same thickness according to SEM. The concentration seems to be too close to the critical value.

Coating the polymer derived supports with the “91 wt%” slip was tested, but the layer becomes too thin (Figure 34). Therefore, the slip with 85 wt% was prepared and used for further investigations.

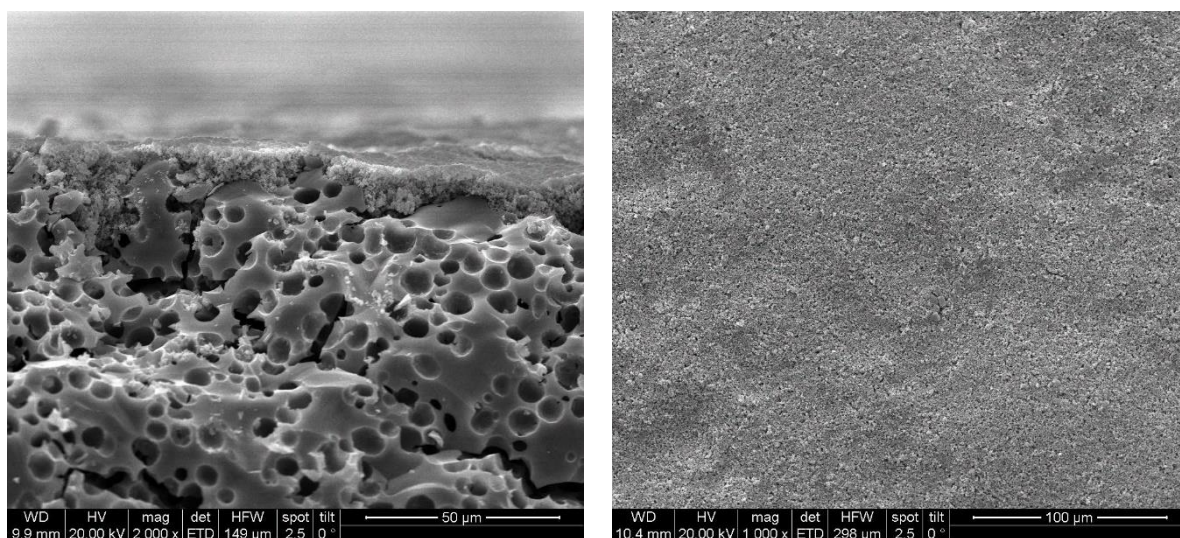


Figure 34: PDC support + intermediate layer 91 wt% in the pyrolysed stage, fracture surface (left) and surface (right)

4.3 TOP LAYER

4.3.1 Preliminary tests

The correlation between layer thickness and withdrawal speed for each solution was investigated using glass plates as substrates. The results for the toluene-polysilazane-solutions are shown in Figure 35 and listed in Table 17.

The curves for the 10, 20 and 50 vol% solutions and withdrawal speeds from 10 to 140 mm/min are shown. With increasing concentration, the layer becomes thicker, a higher withdrawal speed resulting in higher values. Depending on the combination of speed and concentration thicknesses between 0.1 and 3 μm can be achieved.

The height was measured on 5 to 6 different spots all over the coating. The high standard deviation of the two highest speeds for 50 vol% may be caused by the slightly changing thickness from the upper to the lower end of the glass plate, being extremer for higher concentrated solutions of course.

The Landau-Levich model was evaluated for the used solutions. Herefore, the viscosity and the surface tension had to be measured. The results of the viscosity measurements are shown in Figure 36.

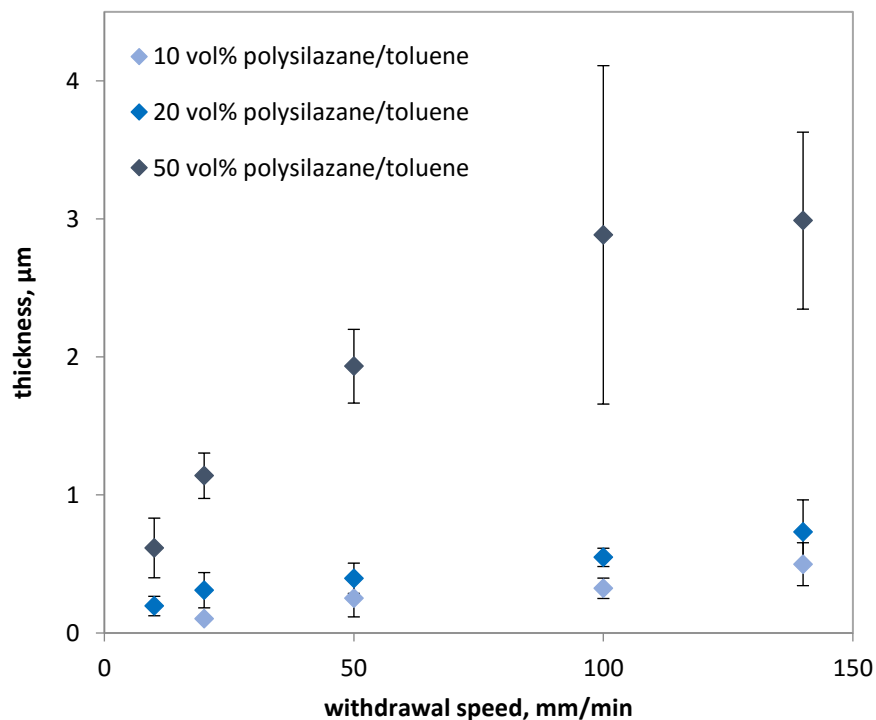
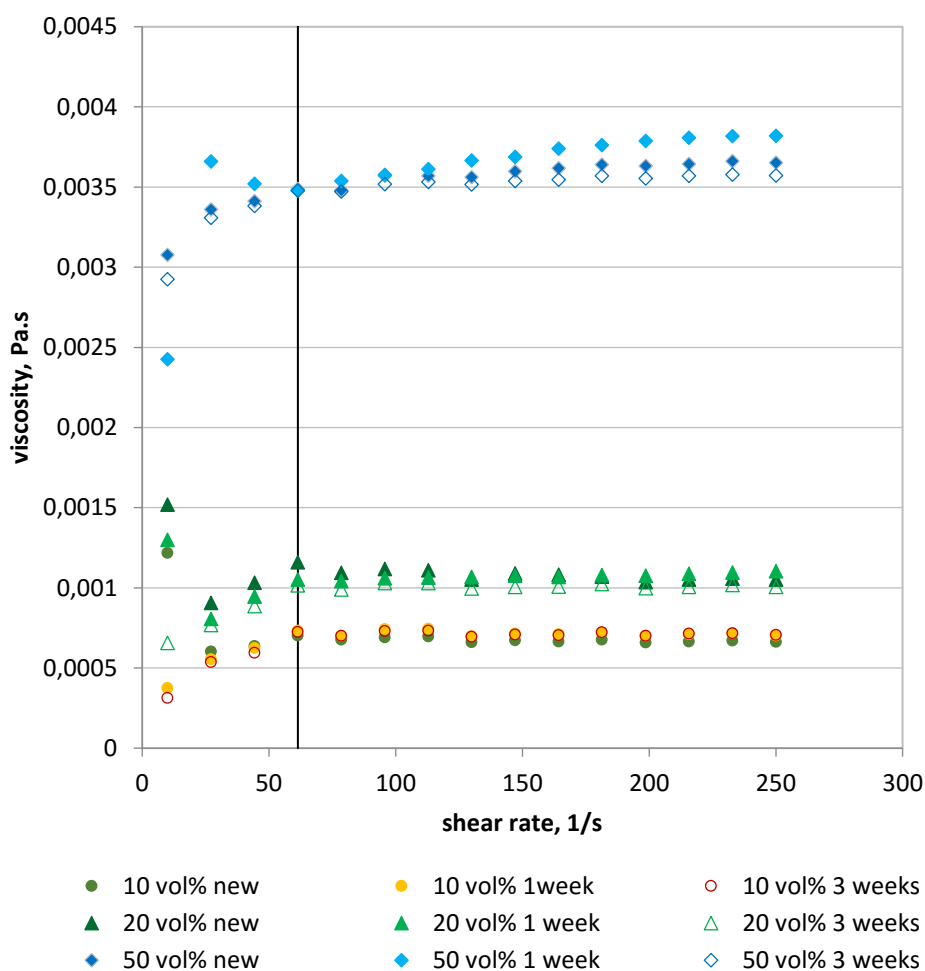


Figure 35: Relation between layer thickness and withdrawal speed for PSZ/toluene solutions on glass plates

Table 17: Measured layer thickness of polysilazane coatings on glass plates (using profilometry)

withdrawal speed, mm/min	thickness, μm		
	10 vol%	20 vol%	50 vol%
10	too low to measure	0.20 ± 0.07	0.62 ± 0.22
20	0.10 ± 0.02	0.31 ± 0.13	1.14 ± 0.16
50	0.25 ± 0.13	0.40 ± 0.11	1.93 ± 0.27
100	0.32 ± 0.07	0.55 ± 0.07	2.88 ± 1.23
140	0.50 ± 0.16	0.73 ± 0.23	2.99 ± 0.64

**Figure 36: Shear rate and age dependent viscosity of the PSZ/toluene solutions; after the vertical line an almost constant value is reached**

The different concentrations are represented by different colours and symbols, the older the solution was, the lighter is the colour. The vertical line shows the point where the viscosity reaches an almost constant value. The shear rate independent behaviour indicates a Newtonian fluid.

With increasing concentration, the viscosity increases too.

The age of the solution doesn't seem to have a profound impact on the viscosity. Although there are little differences there is no trend in one direction when comparing the different concentrations. For the 10 vol% solution, the viscosity increases with time, for 20 vol% it decreases and for the 50 vol% solution it first increases and then decreases.

The mean values behind the vertical line in Figure 36 can be seen in Table 18.

Table 18: Viscosity of the differently concentrated PSZ/toluene solutions

solution		μ , mPa.s
10 vol%	new	0.67 ± 0.01
	1 week	0.72 ± 0.02
	3 weeks	0.71 ± 0.01
20 vol%	new	1.08 ± 0.04
	1 week	1.07 ± 0.02
	3 weeks	1.01 ± 0.01
50 vol%	new	3.59 ± 0.06
	1 week	3.69 ± 0.12
	3 weeks	3.54 ± 0.04

The measured values for the surface tension are listed in Table 19.

Again a change with time was investigated and again the properties stayed the same for the older solutions. With increasing polymer content, the surface tension decreases, which seems logical, since the surface tension of pure polymer is lower than that of toluene.

Table 19: Surface tension of the differently concentrated PSZ/toluene solutions and the pure components

solution		σ , mN/m			
		1	2	3	mean value
10 vol%	new	29.0	29.5	29.5	29.3
	1 week	29.5	29.5	29.5	29.5
	3 weeks	29.5	29.5	29.5	29.5
20 vol%	new	29.0	29.0	29.0	29.0
	1 week	29.0	29.0	29.0	29.0
	3 weeks	29.0	29.0	29.0	29.0
50 vol%	new	28.5	28.5	28.5	28.5
	1 week	28.5	28.5	28.5	28.5
	3 weeks	28.0	28.5	28.5	28.3
pure	polysilazane + DCP	27.5	27.0	27.5	27.3
	toluene	28.5	28.5	28.5	28.5

Using the measured/calculated values in Table 20 and the gravitational acceleration $g = 9.8$ m/s² the thickness h_0 that is to be expected can be calculated with the already known equation (section 2.5), but by adding two additional parameters A and B:

$$h_0 = 0.944 \times \sqrt[6]{\frac{\mu U}{\sigma}} \times \sqrt{\frac{\mu U}{\rho g}} \times A \times B$$

h_0 ... thickness

μ ... viscosity

U ... withdrawal speed, mm/min

σ ... surface tension

g ...gravitational acceleration =9.8 m/s²

ρ ... density

A ... factor including the evaporation of the solvent

B ... factor including the shrinking during crosslinking

Table 20: Parameters of the PSZ/toluene solutions to calculate the Landau-Levich-model-values

solution	μ , mPas	σ , mN/m	ρ , kg/m ³	A	B
10 vol%	0.67	29.3	0.8844	0.1	0.98
20 vol%	1.08	29.0	0.9028	0.2	0.98
50 vol%	3.59	28.5	0.9580	0.5	0.98

The values in Table 21 were calculated. They are shown together with the previously measured values in Figure 37.

Table 21: Model-values according to the Landau-Levich-Model

speed, mm/min	h_0 , μm		
	10 vol%	20 vol%	50 vol%
10	0.04	0.11	0.58
20	0.07	0.18	0.97
50	0.12	0.33	1.79
100	0.19	0.52	2.84
140	0.24	0.66	3.55

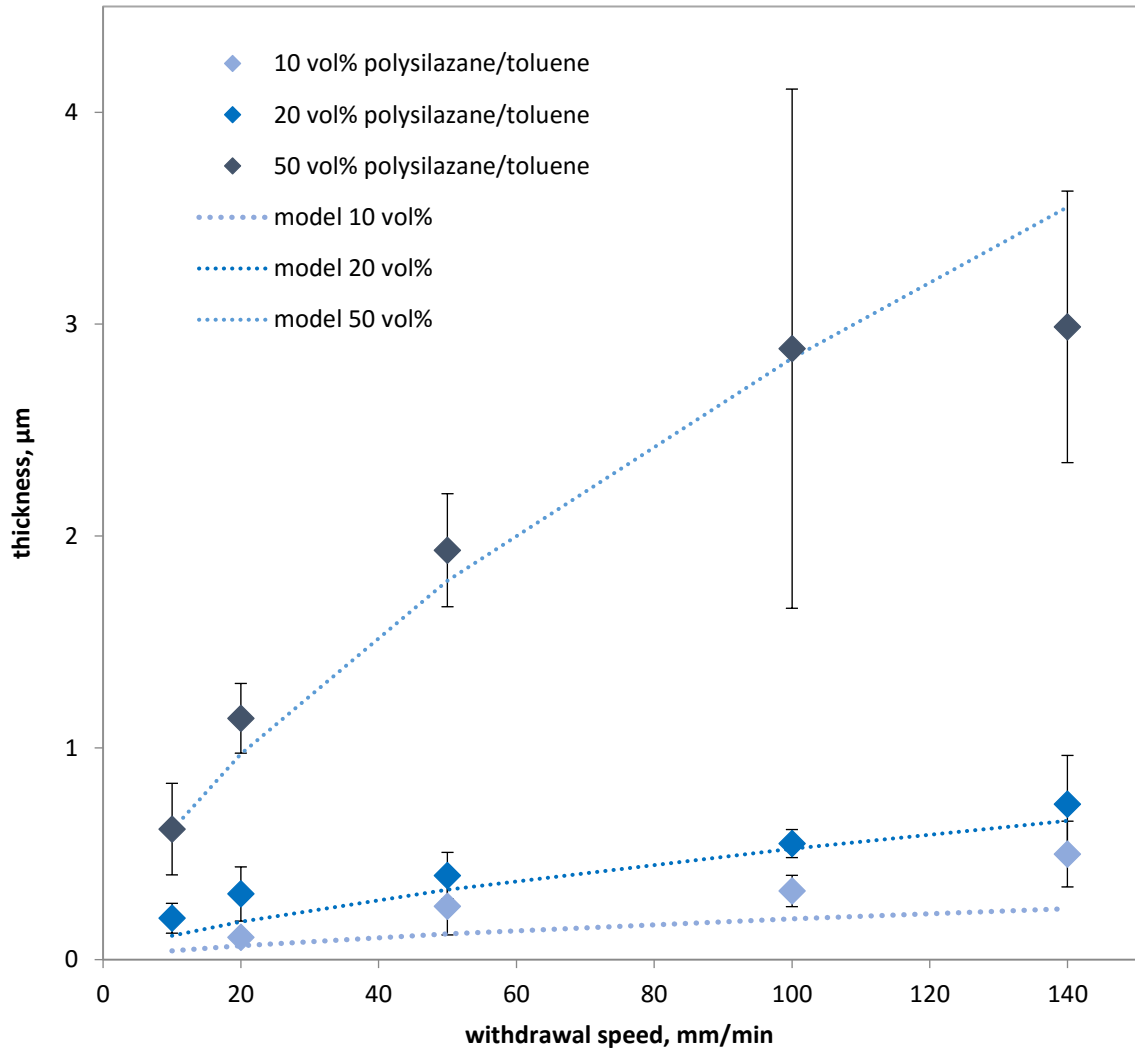


Figure 37: Correlation between measured values and model values for the layer thickness of PSZ/toluene solutions

The data points are the measured values; the dotted lines show the model for the respective concentration. The correlation between the model and the actually measured values is good. The model is slightly below the experimental data; a possible cause is that the solution doesn't have enough time to flow down the substrate while removing it before the solvent evaporates.

Nevertheless, the differences between model and experimental data are small and the model can be used for these systems and be adapted to other concentrations.

The same investigations were done for the system n-hexane/polysilazane for the top layer on masked samples.

The vapor pressure of n-hexane is higher than that of toluene which makes the experiments more difficult and more dependent on the atmosphere and conditions in the room while measuring. N-hexane also has a lower viscosity, which leads to thinner coatings. Solutions with 20 vol% and 50 vol% of polysilazane were prepared, but it was only possible to measure the layer thickness of the more highly concentrated one.

The measurement of the viscosity turned out to be difficult too, because the results were continuously increasing with increasing shear rate, which would indicate a non-Newtonian fluid and that would void the validity of the Landau-Levich- model. But because of the setup, a possible explanation for the increasing values could be the evaporation of n-hexane during the length of the experiment, changing the viscosity because of the change in concentration and not because of the varying shear rate. The lowest measured value was chosen to fit the model.

The surface tension that was measured is listed in Table 22, the parameters used to calculate the model-values are given in Table 23 and the results in Table 24 compared with the experimental values.

Table 22: Surface tension of the PSZ/n-hexane solution

solution	σ , mN/m			
	1	2	3	mean value
50 vol% polysilazane/ n-hexane	22.5	22.5	23	22.7

Table 23: Parameters of the PSZ/n-hexane solution to calculate the Landau-Levich-model-values

μ , mPas	σ , mN/m	ρ , kg/m ³	A	B
1.90	22.67	0.84	0.5	0.98

Table 24: Model values for the layer thickness according to the Landau-Levich-model compared to experimental values for the PSZ/n-hexane solutions

speed, mm/min	h_0 , μm	
	model	experiment
10	0.44	0.59 \pm 0.15
20	0.70	0.66 \pm 0.08
50	1.30	1.13 \pm 0.10
100	2.06	1.47 \pm 0.24
140	2.58	1.99 \pm 0.21

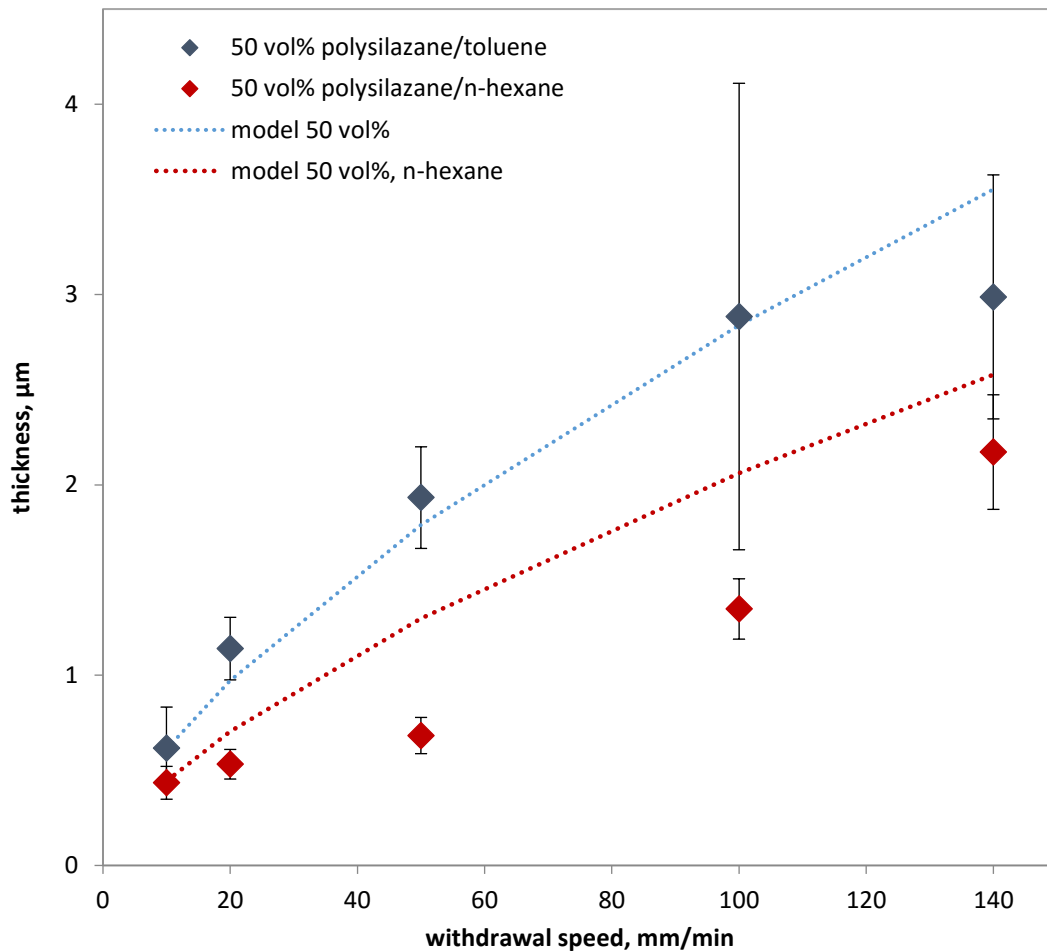


Figure 38: Correlation between measured values and model-values for the layer thickness of the PSZ/n-hexane solution compared to the PSZ/toluene solution

In Figure 38 the results of the 50 vol% polysilazane/n-hexane solution are shown in comparison to those of the polysilazane/toluene solution of the same concentration. The fitted Landau-Levich-model is represented through the dotted lines. The thickness of the coatings prepared with the n-hexane solution is generally lower, because of the lower viscosity. The curve isn't shaped as well as the one of the toluene solution, probably due to the problems while coating the glass plates (as mentioned above). The model doesn't fit the experimental data equally well, for the same reasons.

4.3.2 Direct coating of the support structures

To prove that a direct coating of the support structures without any other treatment isn't possible, a polymer-derived and a slip cast support were dip coated with the 20 vol% and the 50 vol% polysilazane/toluene solution (4 samples in total). After the crosslinking step, they were broken in half and one half was pyrolysed. The SEM images of those samples can be seen in Figure 39.

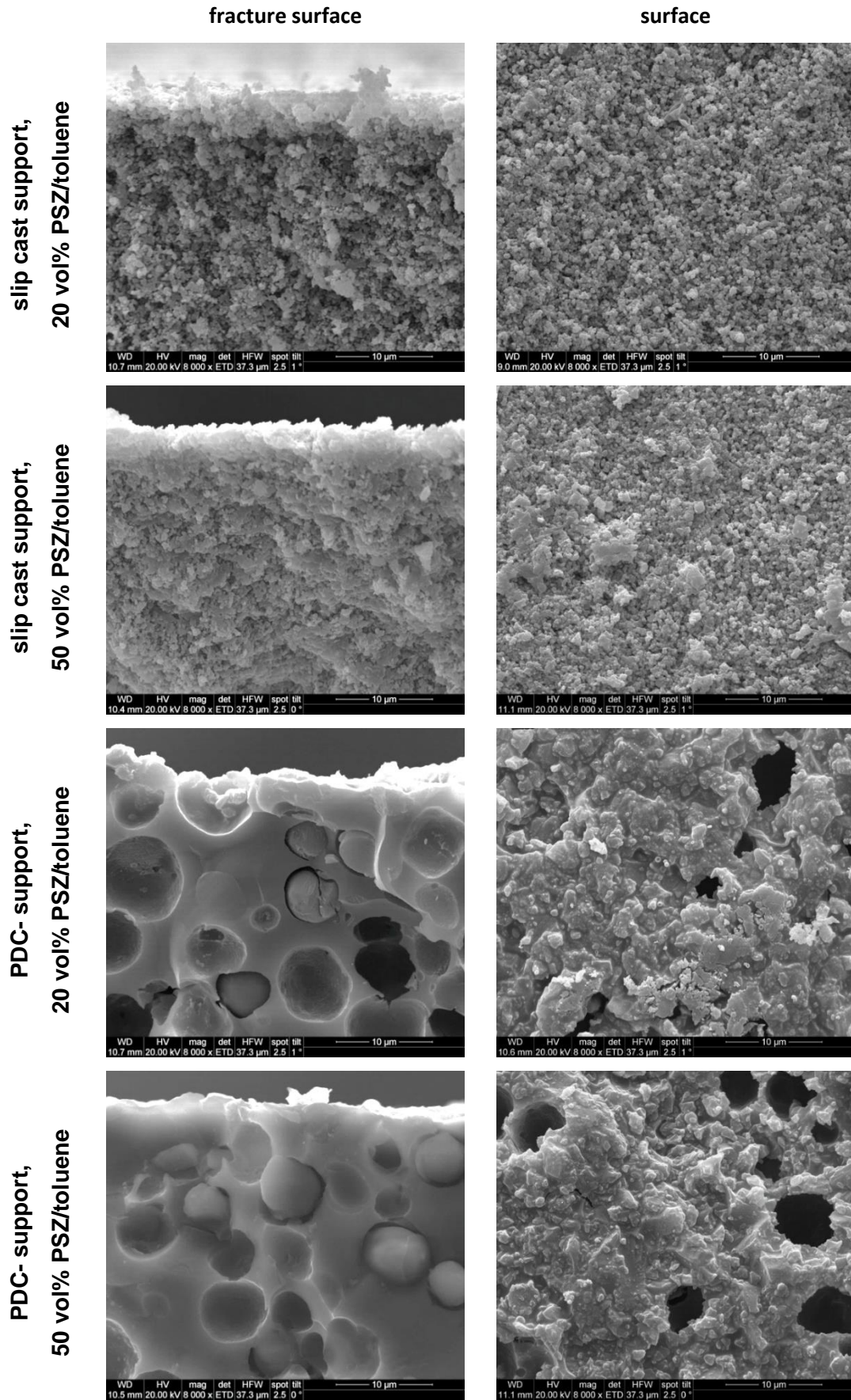


Figure 39: Directly coated supports

In none of the experiments a dense layer was formed.

For the slip cast supports, the polymer seems to constantly fill the whole sample, when comparing the 20 vol% and 50 vol% (fracture) surface. The sample looks generally denser for the more highly concentrated dipping solution. It looks as if a dense layer had formed on top of the sample when just looking at the fracture surface, but the surface itself doesn't look much different from that of the uncoated samples. This could be caused by charging which is more intense on the edge of the sample. Another reason could be that it's hard to identify a concave area/a pore when looking at it from that angle, because of the material behind it.

For the polymer derived supports it can be clearly seen that the dipping solution fills the pores and, after pyrolysis, a spherical particle stays inside the former cavity. Due to the large pore diameter and the shrinking of the polymer while crosslinking and pyrolysis, it is not possible to fill and cover the pores on the surface completely. This can be seen in the pictures of the surface, where for both concentrations some of the original pores can be seen clearly. Even if the surface could be closed via several dipping runs, the porosity of the support structure would be reduced too much by the penetrating polymer to get sufficient permeation properties.

Through these experiments, it was proven that a dense layer on top of the support can't be achieved without additional treatment.

4.3.3 Coating of support structures with an intermediate layer

The aim of the intermediate layer was to create a structure in between those of support and top layer and therefore make it easier to prepare a dense layer.

At this stage the experiments with the intermediate layer weren't fully completed. That's why the coating was tested on samples with an intermediate layer prepared with the "72 wt%" slip. The quality of the intermediate layer was good enough for first experiments to generally see if it could be possible that way. The 50 vol% polysilazane/toluene solution was used; 140 mm/min were chosen as withdrawal speed. Half of the sample was dipped a second time after the crosslinking step.

The SEM-images of the pyrolysed samples are shown in Figure 40.

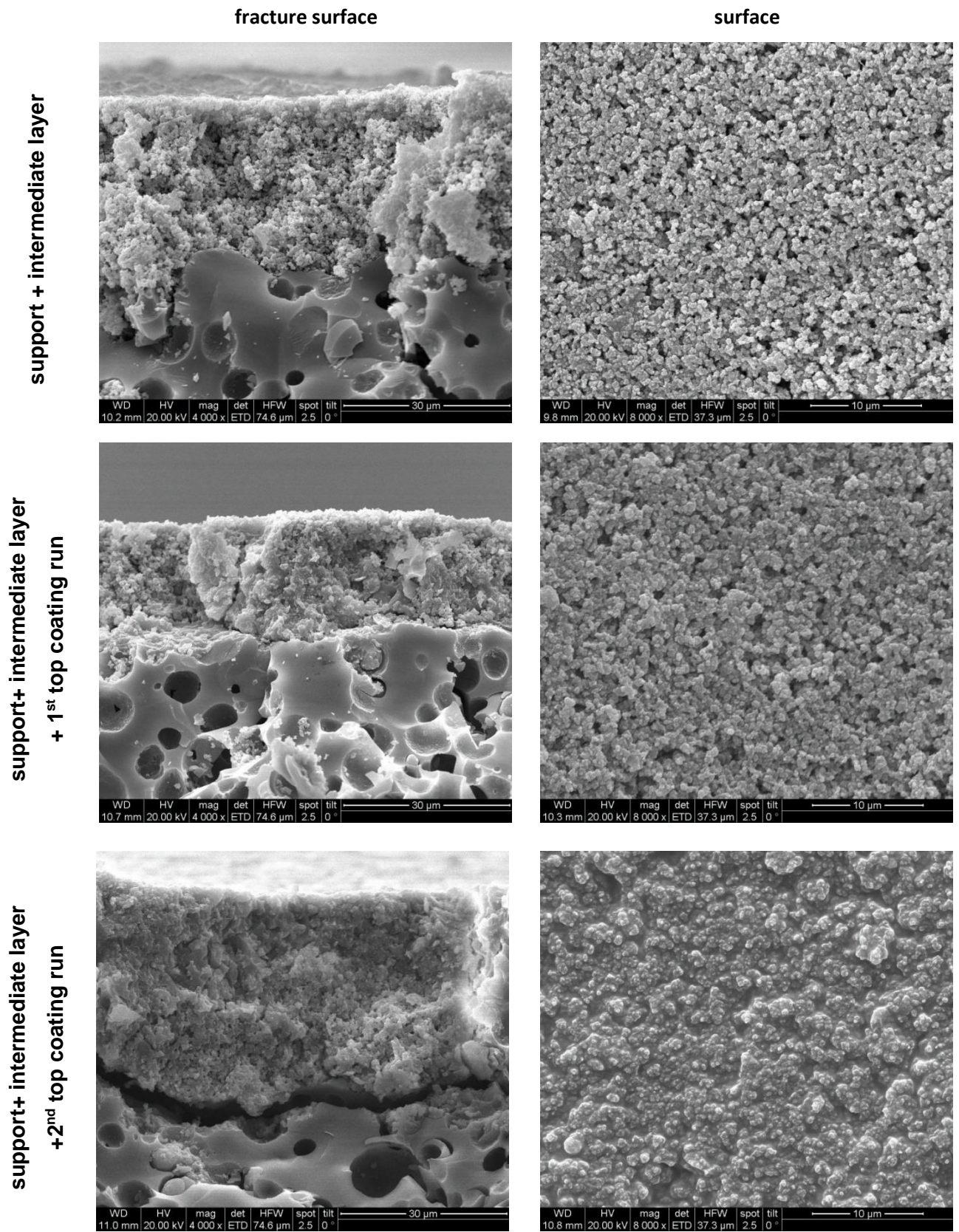


Figure 40: Coating of PDC-supports already having an intermediate layer

After the first coating step, the fracture surface shows that the solution penetrated the intermediate layer and closed nearly all of the pore volume. The surface picture reveals that there is still no dense layer on top.

The piece that was dipped two times shows a dense surface, but only because the whole intermediate layer is already filled.

Although a dense layer formed, which was the aim of this work, it's not a fully satisfactory result, because in this case the whole volume of the intermediate layer serves as selective layer, which means there's a 30 μm thick almost dense layer. This would result in an extremely bad permeability.

4.3.4 Coating of masked samples

A lot of different combinations of concentration, type of polystyrene, dwelling time and multiple runs on most of the samples either with the same combination or with varying ones were tested.

4.3.4.1 Testing of the necessity of the intermediate layer on slip cast supports

For the polymer derived supports the second layer is definitely necessary, because the primary pores are too large to fill them sufficiently with the polystyrene.

The dipping solution penetrated the samples with an intermediate layer too, leading to the question if that layer is necessary when using the masking technique, because of the little structural difference between support and intermediate layer. One sample with and one without intermediate layer were masked with a 1 wt% polystyrene solution (styrofoam), 140 mm/min as withdrawal speed and 1 s dwell time. Then the top layer was applied. The pictures of the pyrolysed samples can be seen in Figure 41.

The surface of the sample with intermediate layer originally looks smoother; through the coating, a denser surface was reached than for the bare support.

Generally, it can be concluded that the smoother the surface, the better the quality of applied coatings. Although the appearance of the top layer is not similar to the desired dense layer for both the experiments, the sample with intermediate layer looks slightly better. For the following experiments, only supports with intermediate layer were used.

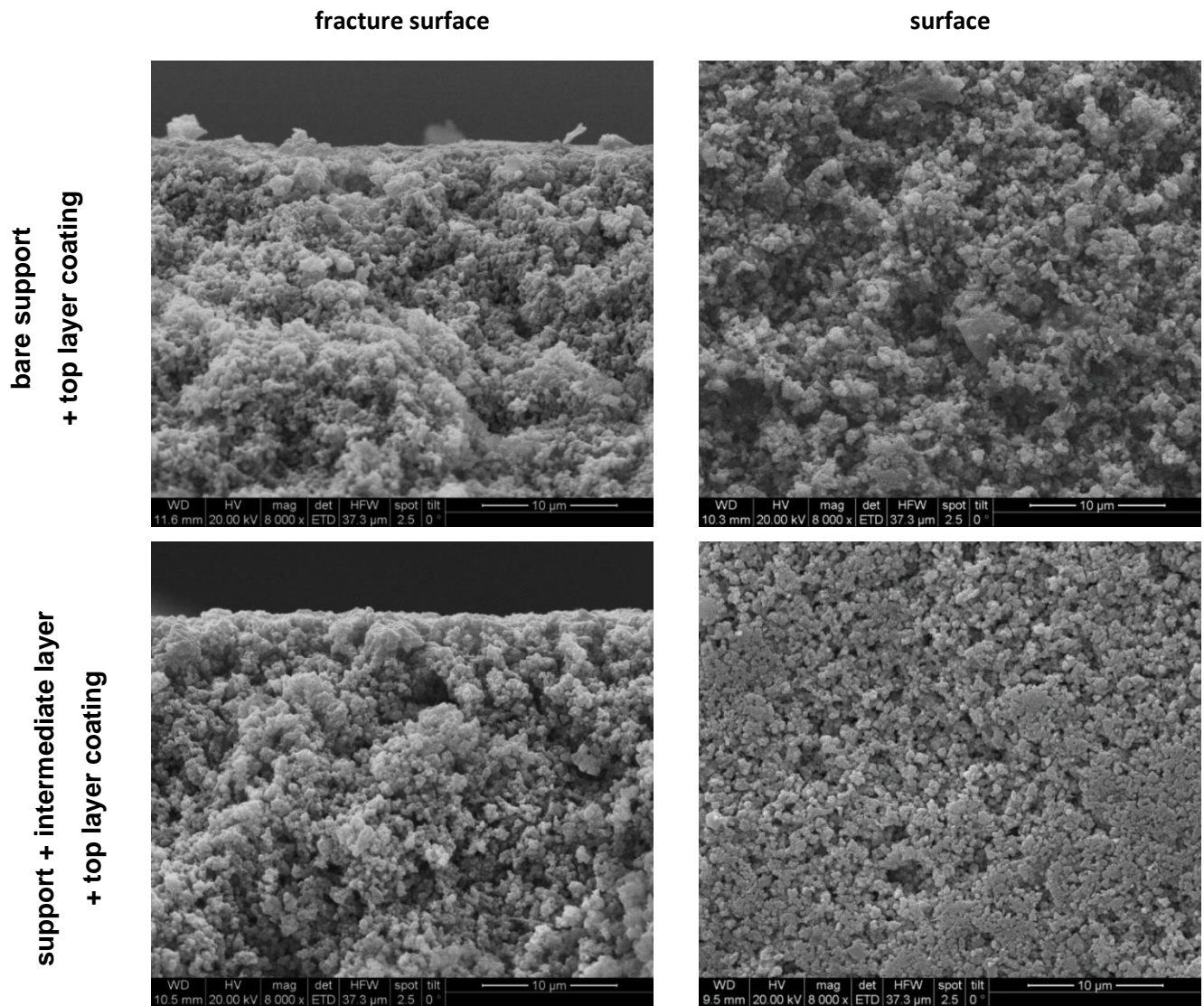


Figure 41: Testing of the necessity of an intermediate layer on the slip cast supports when using the masking technique

4.3.4.2 Comparison of the polystyrene types

Originally, styrofoam was only used to make preliminary test possible until the polystyrene with defined molecular weight arrived. But it turned out to work as least as well as the industrial one. The results of samples masked with 1 wt% of each polystyrene were compared to decide which one should be used for further experiments.

When looking at the SEM-images (Figure 42), at first sight no profound difference between those two can be observed. The intermediate layer is almost completely filled by the polymer derived ceramic, while the surface is still showing porosity. The intermediate layer looks slightly better for the styrofoam masked sample. Since styrofoam is easily available and the results are a little better, it was used for all following experiments.

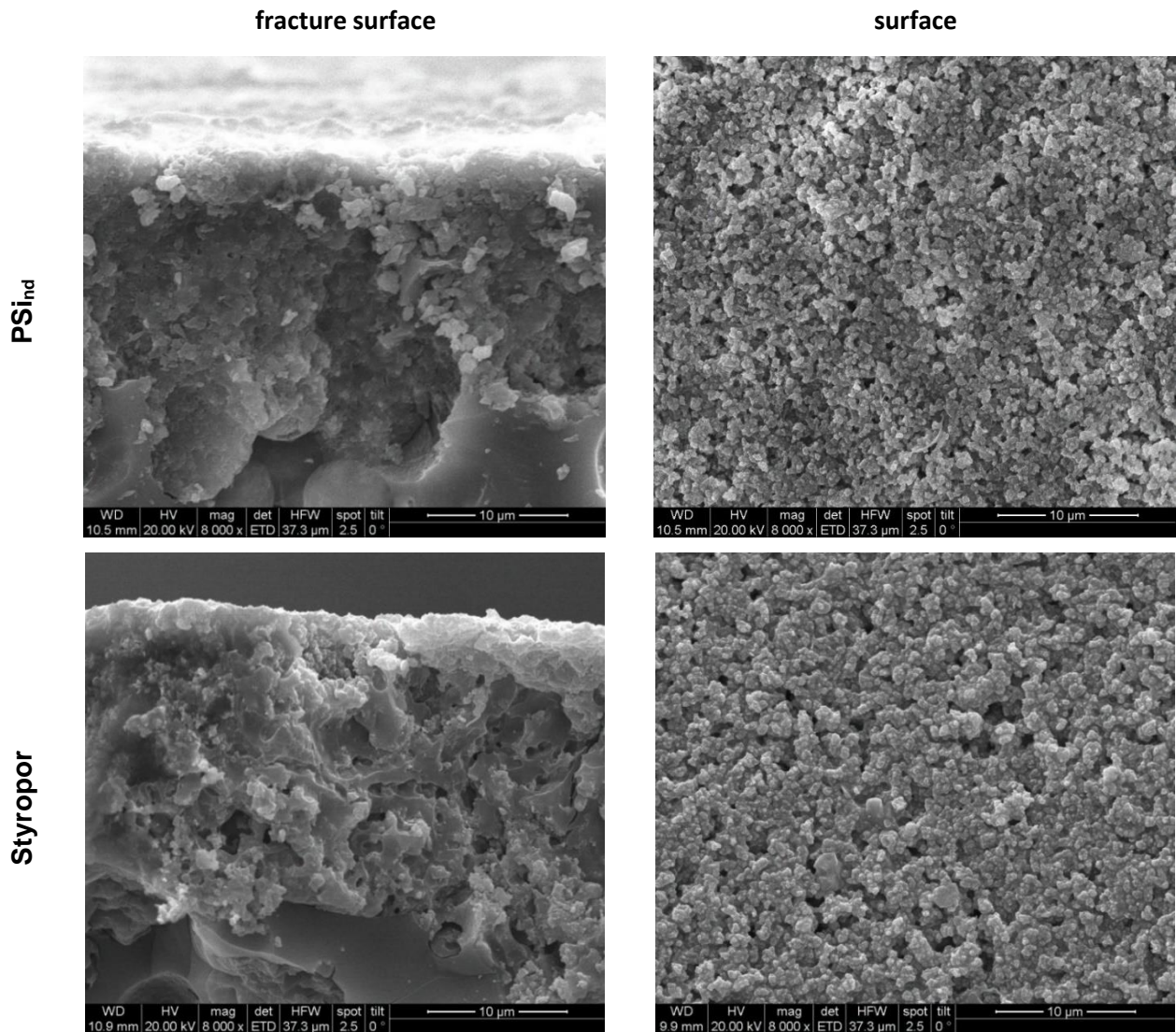


Figure 42: Comparison of the efficiency of the two polystyrene masking material types

4.3.4.3 Influence of the polystyrene concentration

The concentration used until now was always 1 wt%, which was shown to be too low to close the pores well enough to provide a good substrate for the top layer and hinder the polysilazane solution from penetrating the pores. The results for 10 wt% and 15 wt% on the slip cast supports can be seen below (Figure 43). The pictures of the sample masked with 1 wt% is added to make comparing easier.

Whereas for the lowest concentration the silicon nitride grains can still be identified and look bare, for the two higher concentrations, there are areas that are completely covered by a thin layer of polymer derived ceramic. All of the grains seem to have a coating of that former polymer, which makes them look smoother. When looking at the fracture surfaces, a thin layer at the top of the samples looks denser than the bulk for both the 10 wt% and the 15 wt% masked samples. As there are still big open pores, one run is likely not enough to obtain a dense layer.

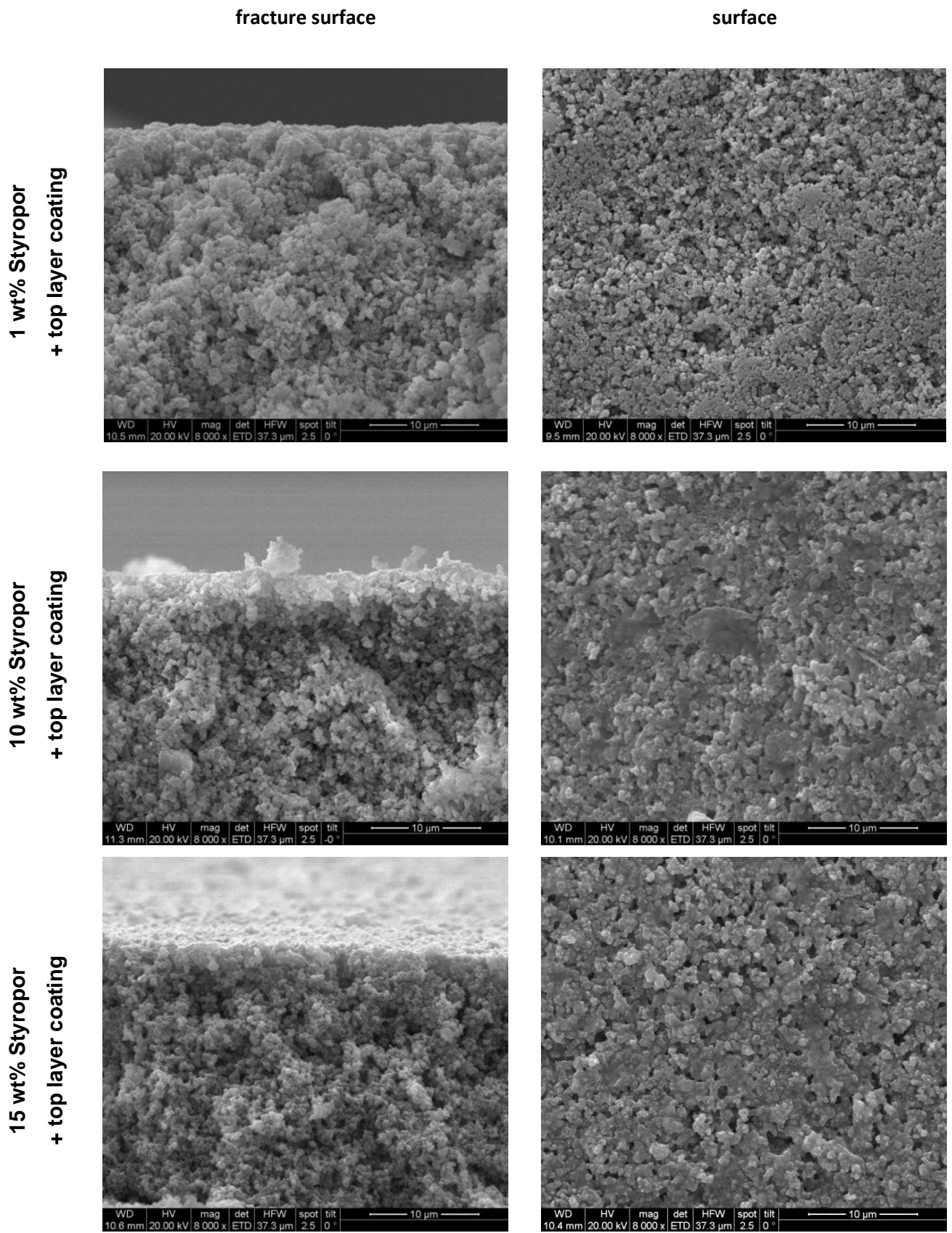


Figure 43: Influence of the PS concentration on the top layer formation (slip cast supports)

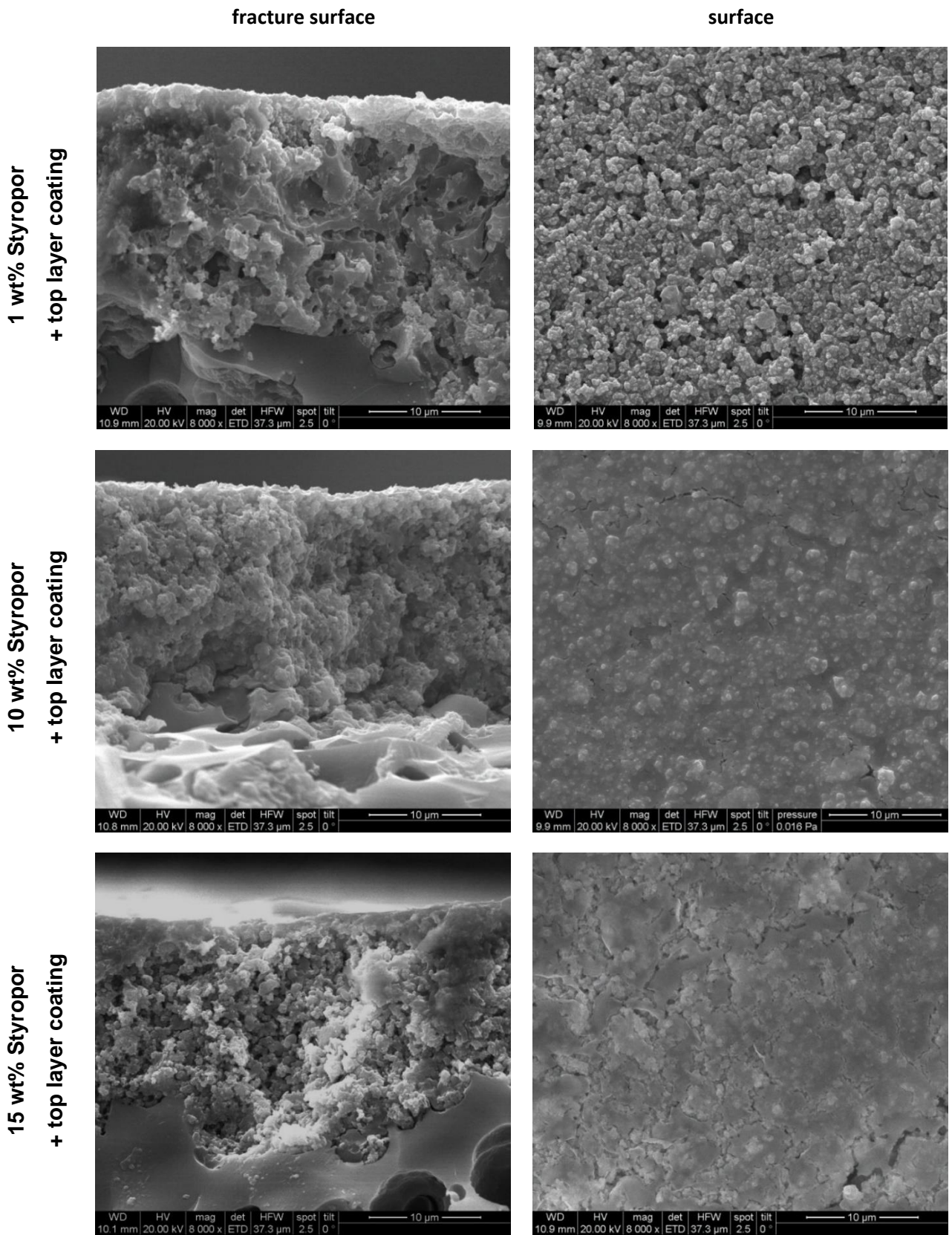


Figure 44: Influence of the PS concentration on the top layer formation (PDC-supports)

For the polymer derived supports, the results are shown in Figure 44.

When comparing them to the slip cast supports, a significant difference can be obtained: the surface images look similar to the desired, dense layer. That layer seems to be thin because the subjacent structures can be seen through the layer.

The surface looks smoother for the 10 wt% masking solution than for the 15 wt% masked sample, because it is more continuous. But when looking at the fracture surface, one can see that the intermediate layer is filled in a higher degree for the lower concentrated masking. The layer is not just on top of the sample – as it seems for the 15 wt% masked sample and would be desired– but filling the whole intermediate layer too.

15 wt% seems to be a good choice as concentration for the masking solution. Although a higher concentration may seem to be a logical next step, it wasn't tested, because the viscosity of the solution was already very high.

4.3.4.4 Influence of the dwelling time inside the masking solution

Until now the dwelling time inside the solution before removing was always 1 s. It was tested if a longer dwelling time – an extreme was chosen: 15 s – allows a more complete filling of the pores with the polystyrene by giving the solution more time to penetrate the sample.

Again first for the slip cast supports, but this time only the crosslinking step was done (Figure 45).

Against the expectations, the shorter time yielded better results. Larger areas were covered with a dense layer, partially looking like an independent layer and not just filling the upper part of the intermediate layer.

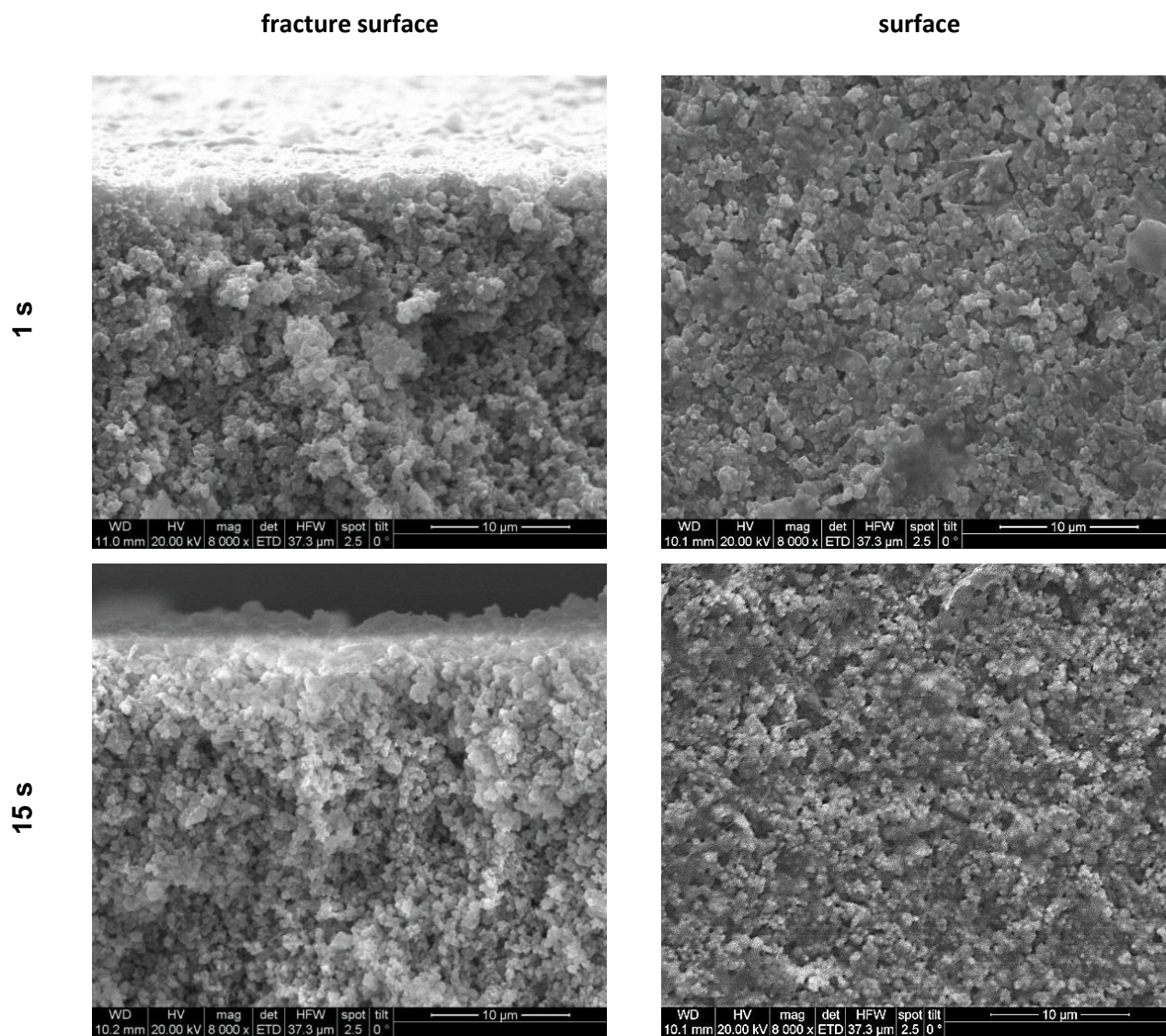


Figure 45: Influence of the dwell time inside the masking solution on the formation of the top layer (slip cast supports)

The difference between the two durations was less obvious for the polymer derived supports, which can be seen in Figure 46 (cross linked stage). There seem to be less cracks in the top layer of the sample kept in the masking solution for 15 s. The fracture surface looks similar.

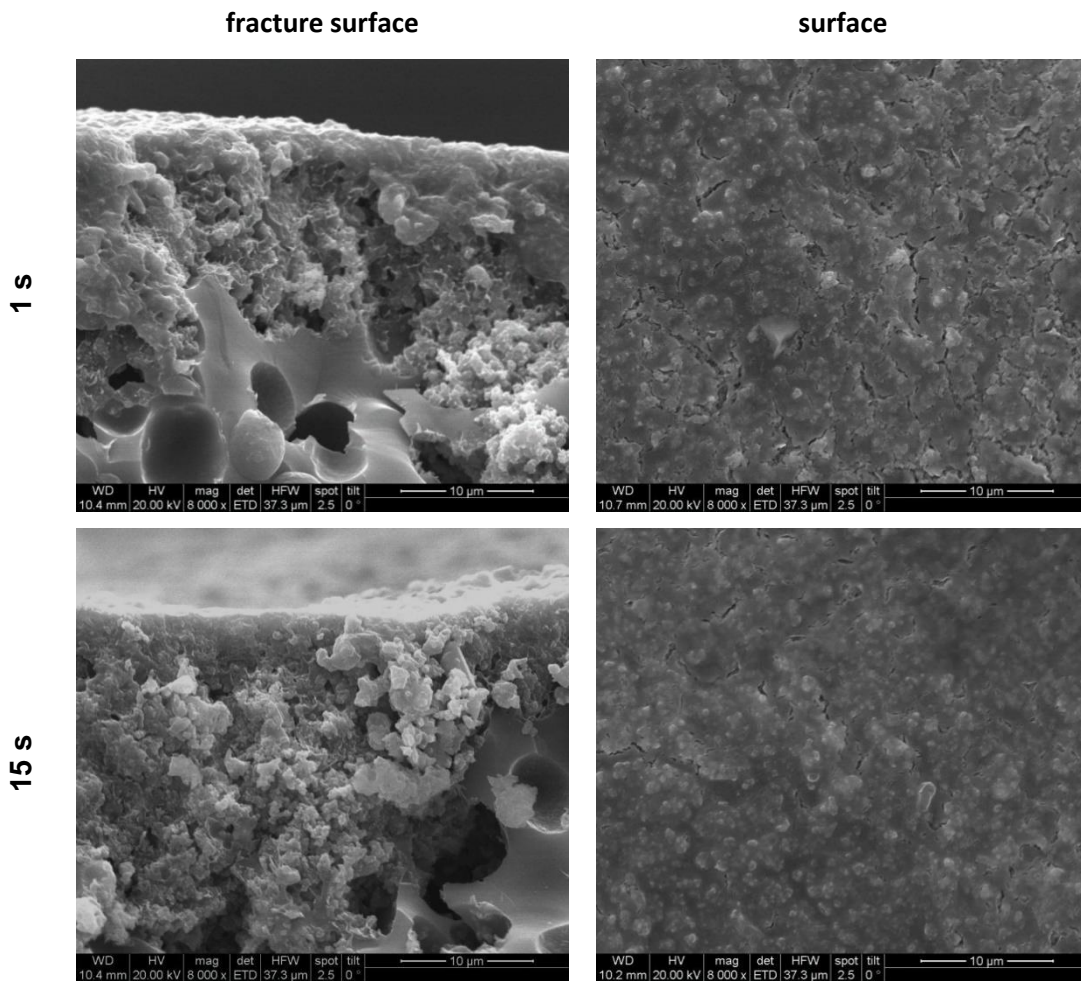


Figure 46: Influence of the dwell time inside the masking solution on the formation of the top layer (PDC-supports)

4.3.4.5 Multiple coating runs

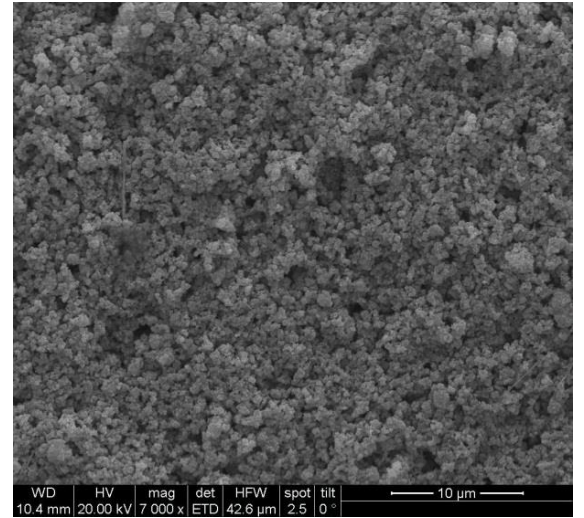
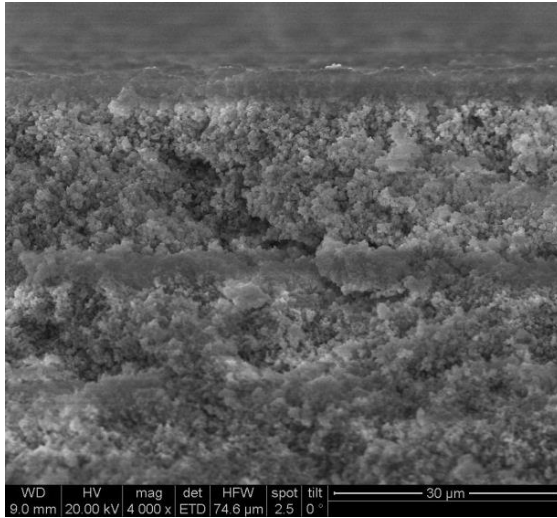
As before, first the results of the slip cast supports: 15 wt% achieved the best performance as masking solution, but still left open pores. The second run was done with different dipping parameters for the polysilazane coating; a withdrawal speed of 50 mm/min was used instead of the usually used 140 mm/min. The thought behind it was to get a thinner layer, because it should be enough to cover the existing cracks. The thicker a layer, the more likely it is to crack during pyrolysis and the more it reduces the permeability, which is negative for the desired application as membrane.

The pictures (Figure 47) show fracture surface and surface of the substrate (= support + intermediate layer), of the first coating step and of the second one, each in the pyrolysed stage. The second run helped to reduce the open porosity, although it didn't disappear completely.

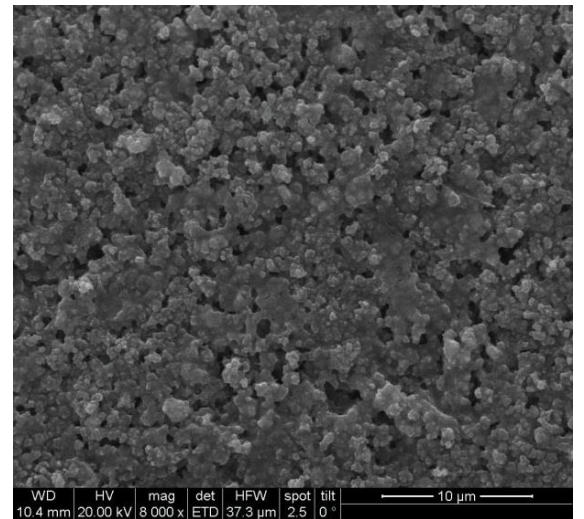
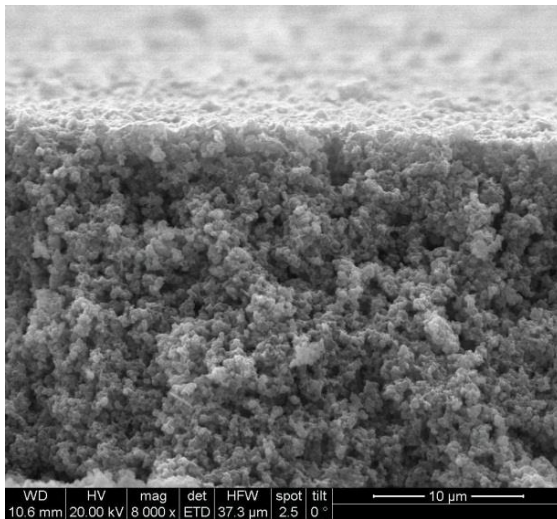
fracture surface

surface

support + intermediate layer



+ 1st top layer coating run
(140mm/min)



+ 2nd top layer coating run
(50 mm/min)

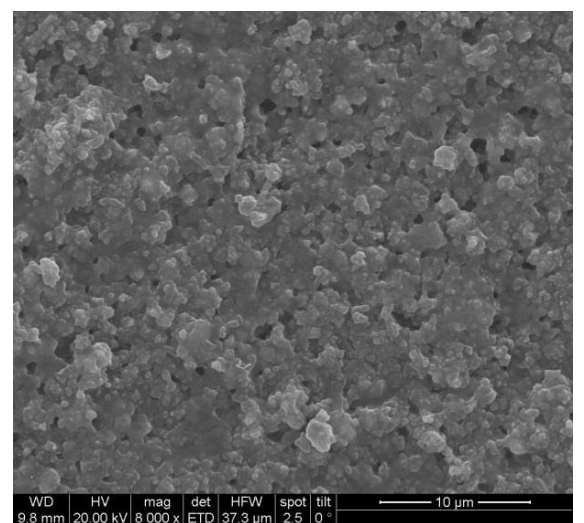
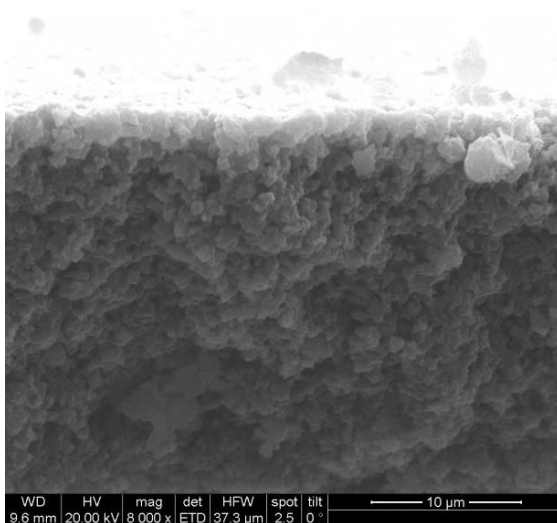


Figure 47: Multiple coating runs on slip cast supports

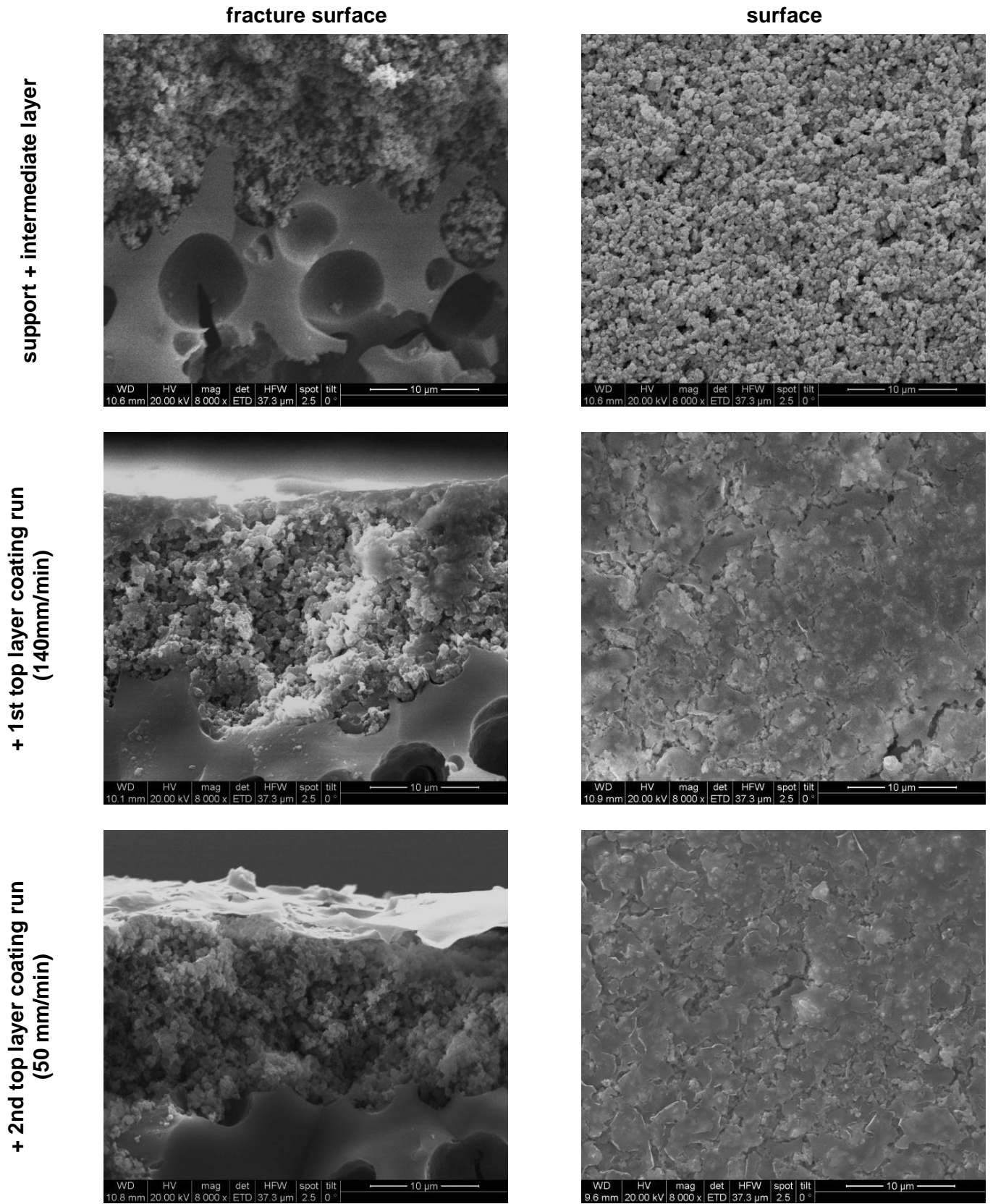


Figure 48: Multiple coating runs on PDC-supports

The same was done for the polymer derived samples (Figure 48). Again, the substrate itself (support+ intermediate layer) is shown for better comparability, the first coating step was already shown above too. The second coating run doesn't change the appearance much, there are still cracks in the surface. However, less of the structure beneath is visible and the size of the cracks decreased.

Based on these results, another variation of that was tried: the first coating step was carried out as before, but the second one was done without the masking step using a withdrawal speed of 140 mm/min again. The SEM-images can be seen in Figure 49. Three different layers can be seen after pyrolysis. The top layer is thin, the porosity of the layers underneath is still preserved. The surface showed less cracks than in the previous experiment.

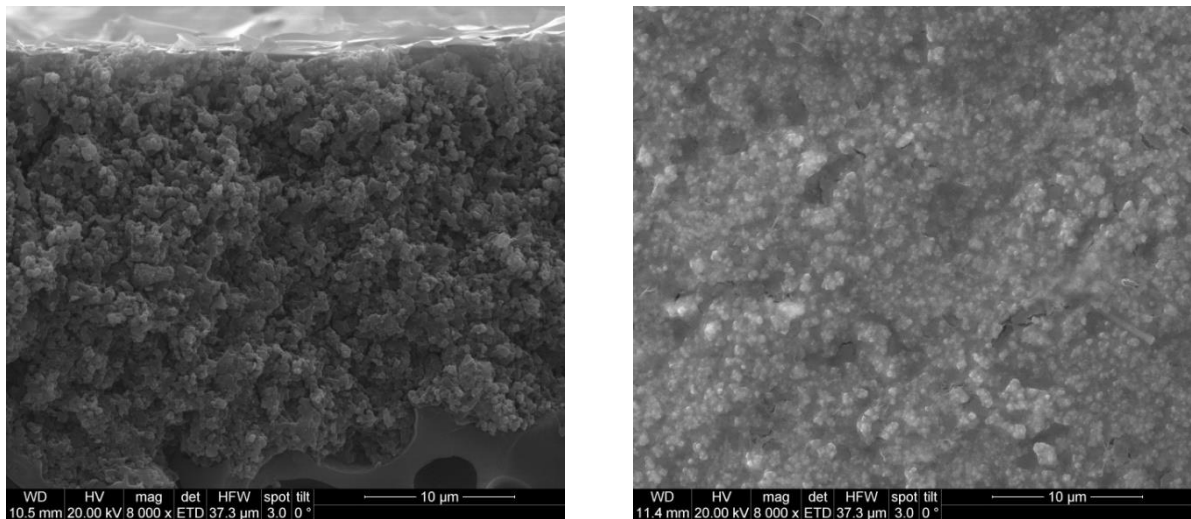


Figure 49: best results on PDC-support: PDC + intermediate layer (85 wt%) + two coating runs (first one including masking), pyrolysed, fracture surface (left) and surface (right)

4.3.4.6 Additional strategies for the slip cast supports

To make the polystyrene fill the pores close to and at the surface, the idea was to heat the sample directly before the masking step. The solvent was supposed to evaporate at the surface and prevent the solution from penetrating unnecessarily deep into the sample. This strategy wasn't successful – no layer could be found; the result was worse than for the normally masked samples.

Another attempt was to dip the sample twice in the masking solution without coating with polysilazane in between. A layer of polystyrene formed on top of the sample which made it possible to get a layer of preceramic polymer too. However, due to the lack of bonding to the intermediate layer, the top layer delaminates while decomposition of the polystyrene during

pyrolysis. The picture that was chosen here is just a small area where the offgoing layer can be still seen. on half of the surface, the layer did completely separate from the sample.

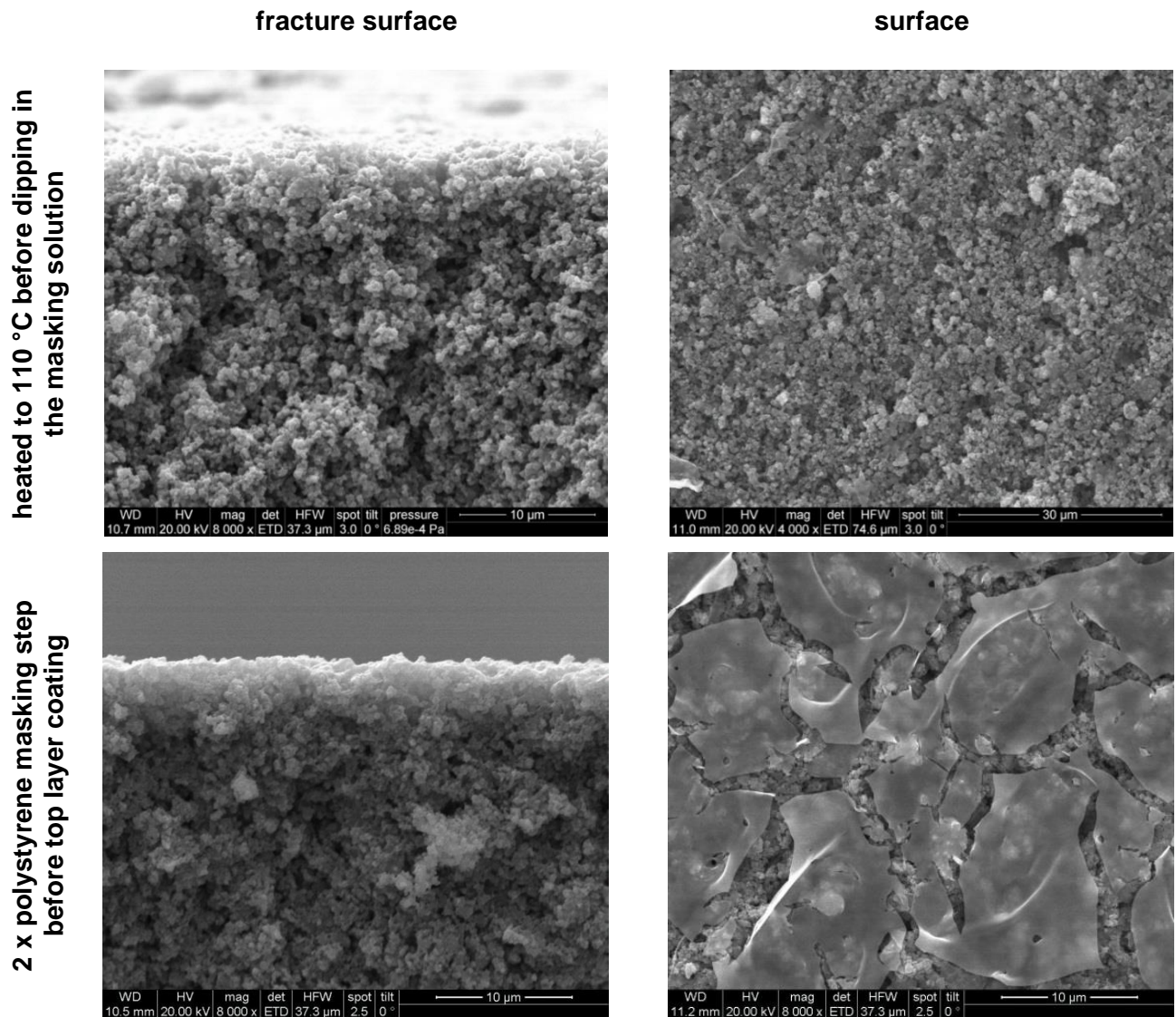


Figure 50: Results of additional strategies for the slip cast supports

As a consequence, another strategy was figured out: the polystyrene layer on top was prepared on purpose by dipping the sample in the masking solution for 15 s as often as it was necessary to obtain a continuous layer on top after drying. The resulting layer was ground off carefully with SiC-paper (#2000). The aim was to guarantee that the pores were completely filled by the polystyrene. As one can see in Figure 51 it was finally possible to get a dense polysilazane layer that was fully coating the surface of the substrate, at least in the

crosslinked stage. After pyrolysis, the layer shows cracks, but it is still connected well to the substrate.

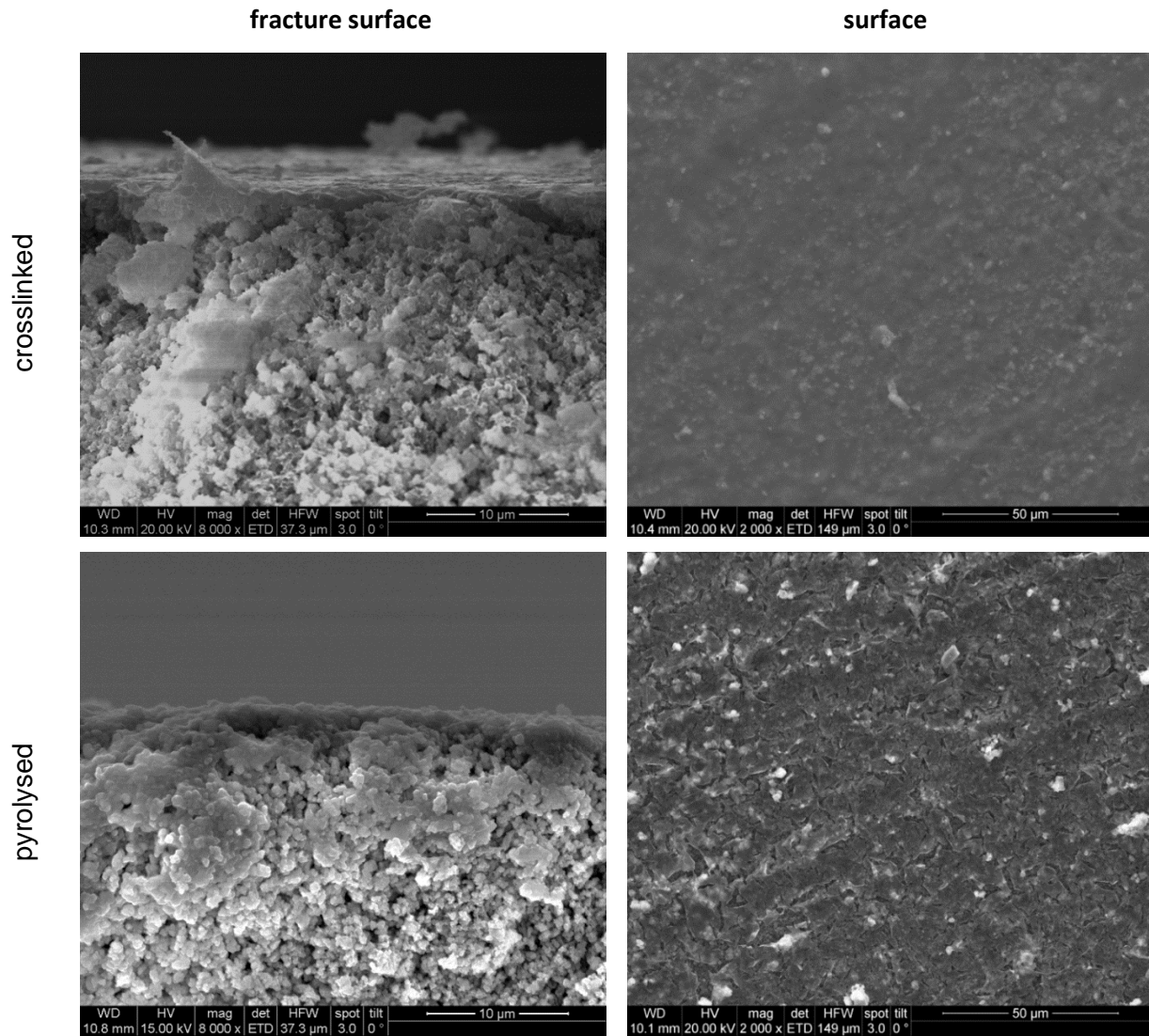


Figure 51: Oversaturation with masking solution and grinding the excessive PS off

4.4 TUBULAR STRUCTURES

The final experiments in this thesis were applying the so-far obtained results on tubular structures the shape of which is more realistic for possible applications. The support structures were prepared by other members of the research group.

4.4.1 Structures using slip cast supports

The tubular slip cast supports were prepared in a different way than the disc shaped samples used for the coating experiments. Sintering aids were used to yield a porosity between 30% and 40%. That leads to a different formation behaviour of the intermediate layer, because the filtration effects are lower. The resulting layer is lower for the same parameters and slips. This was only tested for two slips.

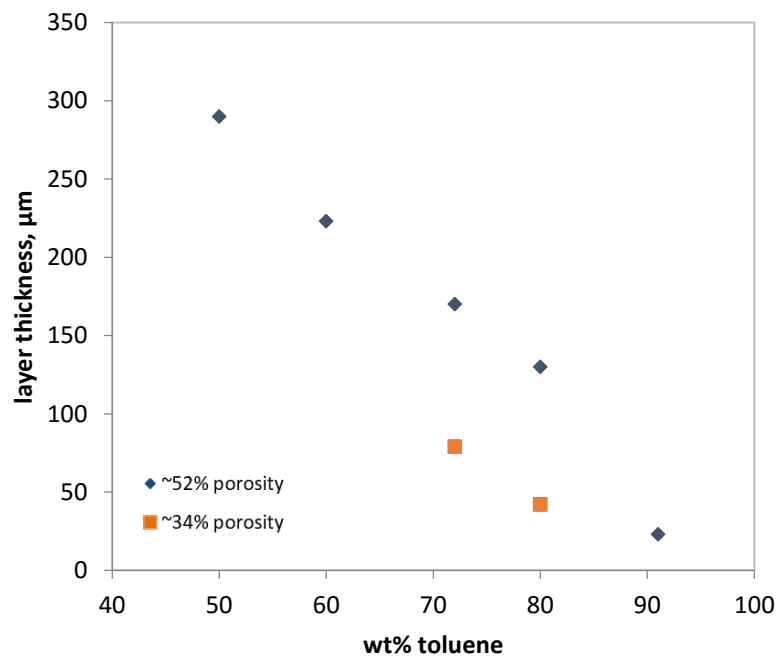


Figure 52: Thickness of the intermediate layer (determined by SEM) depending on the slip concentration for the two types of slip cast supports (52 % or 34 % porosity)

The layer thickness in relation to the slip concentration is shown in the diagram above (Figure 52), for the already known samples with a porosity of about 51 % and for disc shaped samples prepared in the same way as the tubular supports were prepared. The layer is much thinner than for the by now tested samples; one third/half of those with 51% porosity.

To coat the tubular structures, it was decided to use the 85 wt% slip to get a layer in the range of that on the until now investigated samples.

The resulted structure was analysed via electron microscopy (Figure 53).

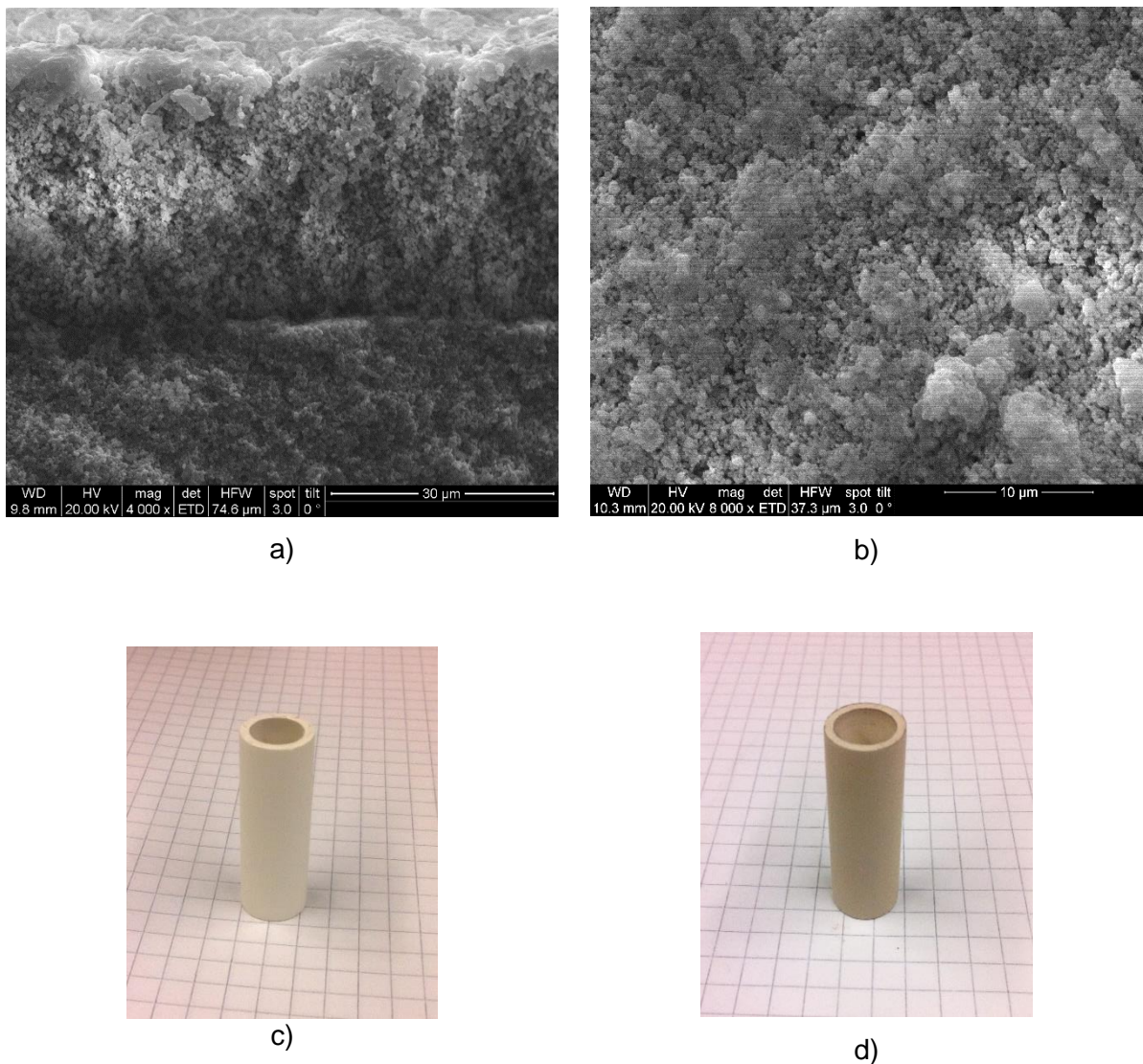


Figure 53: Pyrolysed intermediate layer 85wt% on a tubular slip cast support, fracture surface (a) and surface (b); c) shows the crosslinked sample, d) the pyrolysed sample

The layer thickness was in the range where it was expected: about 30 μm . It was homogenous almost all over the sample, except for a small part at the most upper part, where it was damaged while removing the wire.

A second sample prepared exactly the same way was then coated two times by first masking the sample with PS15wt% and a dwelling time of 1s and then applying the 50 vol% PSZ/n-hexane solution. To close small remaining cracks, a third coating step was conducted without using the PS-masking. The results are shown in Figure 54. When compared with the intermediate layer step, the first thing that can be seen is the change in colour from white to a dark brown due to the formation of the SiCN-coating on the outside.

When looking at the SEM-images, the intermediate layer seems slightly denser, but there also is a clearly visible top layer. The improvement in comparison to the previous stage can be seen from the surface-images too. Only very small pores are still remaining.

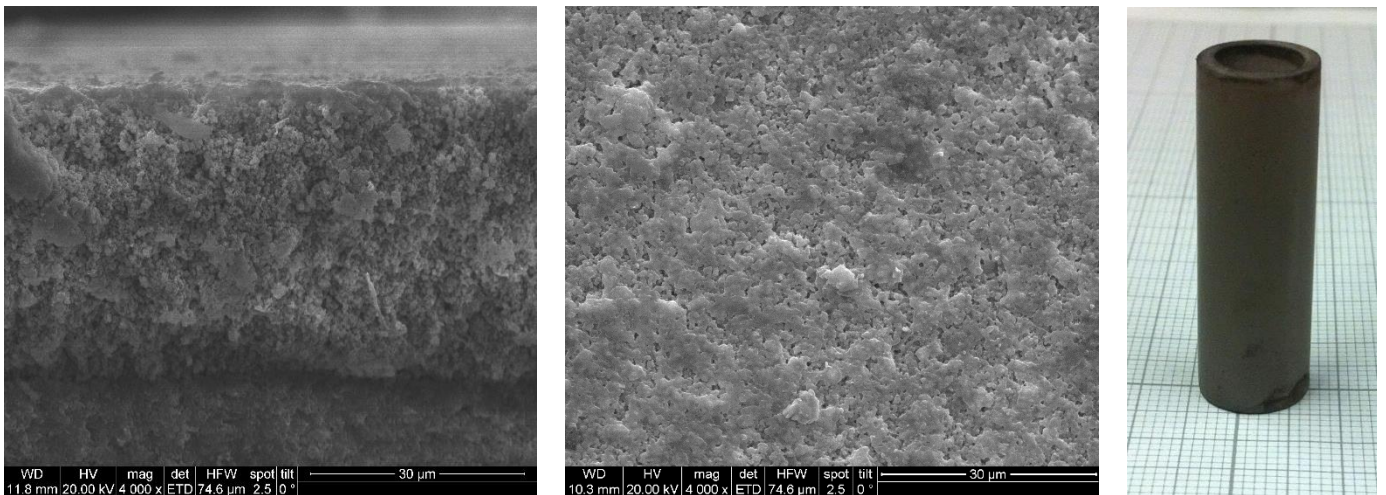


Figure 54: Slip cast tubular support with two masked top coating runs and one without masking; pyrolysed, fracture surface (left), surface (middle) and whole sample (right)

A last coating step without masking was performed using again the 50 vol% PSZ/n-hexane solution and the same parameters in order to close the remaining pores - unfortunately unsuccessful. As can be seen in Figure 55 the appearance of the top layer didn't improve when compared to the previous step. The permeation behaviour was thus investigated previous to this step.

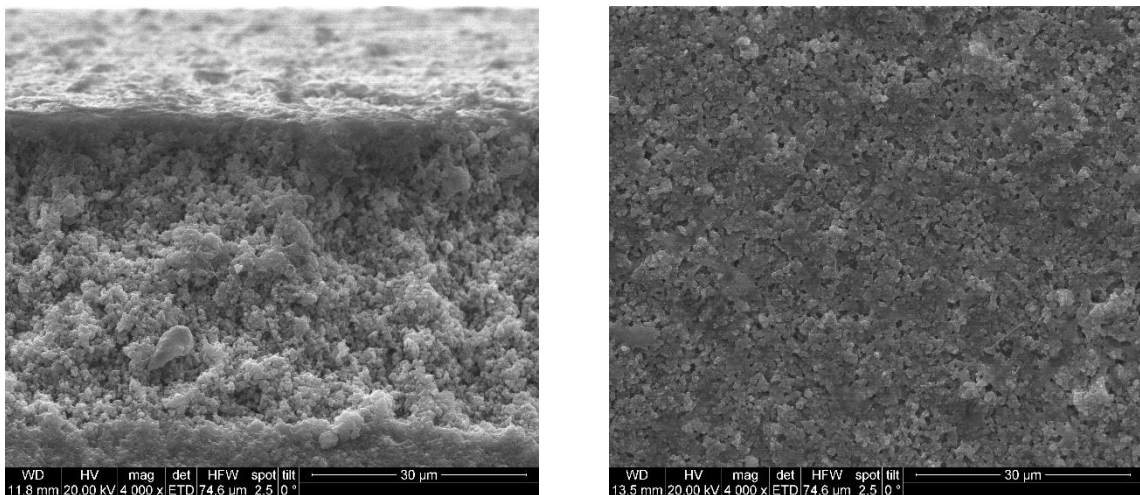
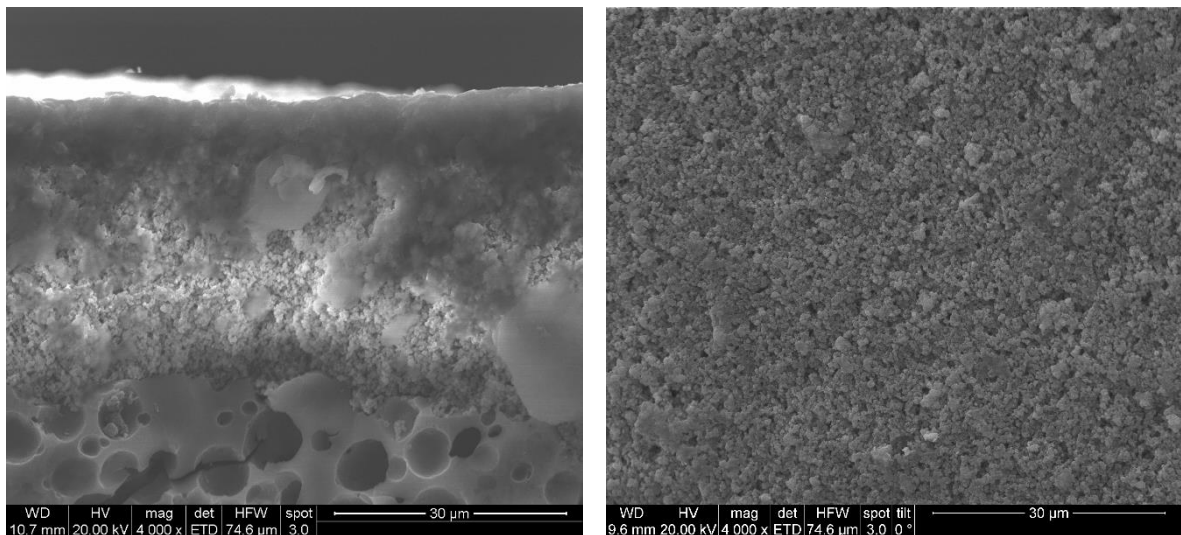


Figure 55: Slip cast tubular support with the final top layer coating, pyrolysed, fracture surface (left) and surface (right)

4.4.2 Structures using polymer derived supports

The intermediate layer deposition went as well as for the planar samples, except for the spots where defects were located on the support. A crack was running almost over the whole length of the tube and a pore was showing on the surface. Due to difficulties while removing the silicone parts, the most upper part is not coated as well as the rest.

The electron microscopy pictures of fracture surface and surface can be seen in Figure 56 in the pyrolysed stage as well as the overall appearance of the sample in the crosslinked and pyrolysed stage. At this stage (support + intermediate layer), a denser layer formed in the upper part of the intermediate layer and the surface looks smooth; it worked at least as well on the tubular supports as on the planar samples. The colour of the sample changed from the white crosslinked state to a light brown in the pyrolysed state, indicating the formation of the SiCN ceramic mostly on the surface which corresponds with the SEM-image.



a)

b)



c)



d)

Figure 56: Pyrolysed intermediate layer (85wt%) on a tubular PDC-support, fracture surface (a) and surface (b) of; c) shows the crosslinked sample d) the pyrolysed sample

Before applying the top layer, the sample was masked using the 15 wt% polystyrene solution and a dwelling time of 15 s. The top layer was applied using the 50 vol% polysilazane/n-hexane solution, a withdrawal speed of 140 mm/min and a dwelling time of 1 s. After that step, a second polysilazane coating step without previous masking was done to close the remaining cracks in the surface.

In the images below (Figure 57), the pyrolysed fracture surface and surface of the sample including the top layer(s) can be seen. When looking at the fracture surface, one can see that the pores of the support structure are almost unaffected by the application of the intermediate and the top layer. There is still porosity in the intermediate layer and although the top layer is partly included in it, there seems to be a layer above it as well.

The surface of the sample seems to be completely dense although the structure of the intermediate layer can be seen through the top layer almost everywhere.

The sample became almost black on the outside showing no difference to the support material anymore regarding colour.

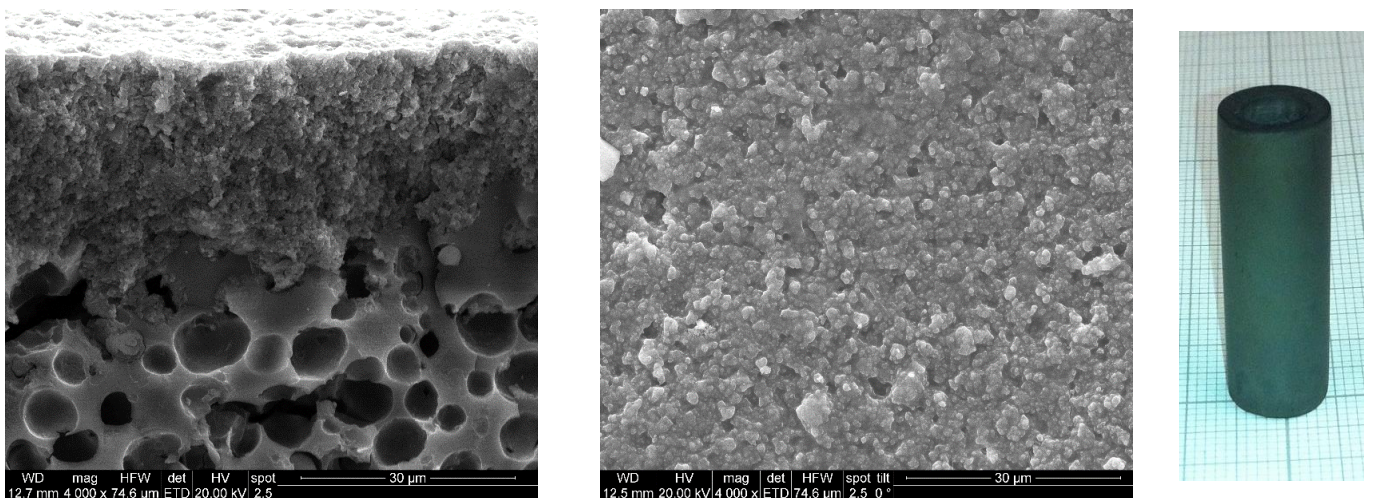


Figure 57: Tubular PDC- support with a masked top coating run and one without masking, after pyrolysis, fracture surface (left), surface (middle) and whole sample (right)

4.5 PERMEATION BEHAVIOUR

Only the PDC-supported planar samples were investigated. One bare support structure without further treatment after pyrolysis, one ground support structure, one with the pyrolysed intermediate layer (85 wt%) and one with the final choice of top layer coatings (one masked run with polystyrene concentration of 15wt% and a dwelling time of 15s using the 50 vol% PSZ/n-hexane solution with a withdrawal speed of 140 mm/min and a dwelling time of 1s for the top layer; a second coating run was done without masking) were measured. The permeated area A was 83 mm². The results are listed in Table 25.

Table 25: Permeation testing results of the planar PDC-supported samples

	Δp , bar	flow, cm ³ /s	thickness l, cm	$(p_i^2 - p_o^2)/(2p_o l)$	Q/A	
bare PDC-support	0.25	0.42	0.198	1.42E+07	5.07E-03	
	0.5	0.89	0.198	3.16E+07	1.08E-02	
	0.75	1.42	0.198	5.21E+07	1.71E-02	k_2 1.98E-10
	1	2.04	0.198	7.58E+07	2.46E-02	k_1 6.26E-15
	1.25	2.71	0.198	1.03E+08	3.27E-02	
	1.5	3.45	0.198	1.33E+08	4.16E-02	
	1.75	4.19	0.198	1.66E+08	5.06E-02	
	2	5.09	0.198	2.02E+08	6.15E-02	
grinded support	0.25	0.51	0.191	1.47E+07	6.12E-03	
	0.5	1.11	0.191	3.27E+07	1.34E-02	
	0.75	1.80	0.191	5.40E+07	2.17E-02	k_2 3.81E-10
	1	2.61	0.191	7.85E+07	3.15E-02	k_1 7.64E-15
	1.25	3.49	0.191	1.06E+08	4.22E-02	
	1.5	4.41	0.191	1.37E+08	5.33E-02	
	1.75	5.40	0.191	1.72E+08	6.52E-02	
	2	6.57	0.191	2.09E+08	7.93E-02	
support + intermediate layer (85 wt%)	0.25	0.25	0.194	1.45E+07	3.05E-03	
	0.5	0.56	0.194	3.22E+07	6.73E-03	
	0.75	0.88	0.194	5.32E+07	1.06E-02	k_2 5.33E-11
	1	1.26	0.194	7.73E+07	1.52E-02	k_1 3.87E-15
	1.25	1.67	0.194	1.05E+08	2.01E-02	
	1.5	2.10	0.194	1.35E+08	2.54E-02	
	1.75	2.56	0.194	1.69E+08	3.09E-02	
	2	3.08	0.194	2.06E+08	3.72E-02	
support + intermediate layer + final top layer coatings	0.25	too low to measure				
	0.5					
	0.75					
	1					
	1.25	0.0100	0.194	1.05E+08	1.21E-04	k_2 1.10E-15
	1.5	0.0121	0.194	1.35E+08	1.46E-04	k_1 2.42E-17
	1.75	0.0146	0.194	1.69E+08	1.77E-04	
	2	0.0175	0.194	2.06E+08	2.11E-04	

The permeability of the ground support is higher than the one of the untreated sample. The intermediate layer decreases the permeability to a lower level than that of the untreated support. The final structure shows a strong decrease in permeability, in the range of two orders of magnitude.

The final coated tubular structure was investigated too. The permeability is much higher than that of the planar sample treated the same way, although the SEM-images show good results (Table 26).

Table 26: Permeation testing results of the tubular PDC-supported sample after the final coating step

	Δp , bar	flow, cm^3/s	A, cm^2	thickness l, cm	$(p_i^2 - p_o^2)/(2p_o l)$	Q/A
support + intermediate layer + final top layer coatings	0.25	0.63	6.55	0.206	1.37E+07	9.54E-04
	0.5	1.34	6.55	0.206	3.04E+07	2.04E-03
	0.75	2.11	6.55	0.206	5.02E+07	3.21E-03
	1	3.01	6.55	0.206	7.30E+07	4.60E-03
	1.25	3.94	6.55	0.206	9.88E+07	6.01E-03
	1.5	4.97	6.55	0.206	1.28E+08	7.58E-03
	1.75	6.11	6.55	0.206	1.60E+08	9.32E-03
	2	7.30	6.55	0.206	1.95E+08	1.11E-02

k_2	5.95E-12
k_1	1.20E-15

The tubular slip cast supports were investigated as bare support structure, with the pyrolysed intermediate layer and with the final coatings (two times masking in 15wt% polystyrene solution for 1s and top coating, 1 additional top coating run without masking).

Whereas the permeability stays approximately the same after deposition of the intermediate layer, it increases after the final coating steps (Table 27).

Table 27: Permeation testing results of tubular samples with slip cast supports

	Δp , bar	flow , cm ³ /s	A, cm ²	thickness l, cm	$(p_i^2 - p_o^2)/(2p_o l)$	Q/A		
bare tubular PDC-support	0,25	0.61	8.59	0.150	1.88E+07	7.05E-04		
	0.5	1.20	8.59	0.150	4.17E+07	1.39E-03		
	0.75	1.84	8.59	0.150	6.88E+07	2.14E-03	k₂	4.73E-13
	1	2.42	8.59	0.150	1.00E+08	2.82E-03	k₁	6.40E-16
	1.25	3.08	8.59	0.150	1.35E+08	3.59E-03		
	1.5	3.79	8.59	0.150	1.75E+08	4.42E-03		
	1.75	4.55	8.59	0.150	2.19E+08	5.30E-03		
	2	5.22	8.59	0.150	2.67E+08	6.09E-03		
support + intermediate layer (85 wt%)	0.25	0.61	8.32	0.156	1.80E+07	7.27E-04		
	0.5	1.55	8.32	0.156	4.01E+07	1.87E-03		
	0.75	1.84	8.32	0.156	6.61E+07	2.21E-03	k₂	5.24E-13
	1	2.42	8.32	0.156	9.62E+07	2.91E-03	k₁	6.87E-16
	1.25	3.08	8.32	0.156	1.30E+08	3.70E-03		
	1.5	3.79	8.32	0.156	1.68E+08	4.56E-03		
	1.75	4.55	8.32	0.156	2.10E+08	5.47E-03		
	2	5.22	8.32	0.156	2.56E+08	6.28E-03		
support + intermediate layer + final top layer coatings	0.25	0.38	8.34	0.175	1.61E+07	4.59E-04		
	0.5	0.77	8.34	0.175	3.57E+07	9.17E-04		
	0.75	1.13	8.34	0.175	5.89E+07	1.36E-03	k₂	6.84E-14
	1	1.50	8.34	0.175	8.57E+07	1.80E-03	k₁	1.15E-15
	1.25	1.82	8.34	0.175	1.16E+08	2.18E-03		
	1.5	2.13	8.34	0.175	1.50E+08	2.55E-03		
	1.75	2.44	8.34	0.175	1.88E+08	2.92E-03		
	2	2.69	8.34	0.175	2.29E+08	3.23E-03		

5 DISCUSSION

5.1 SUPPORT STRUCTURES

The density of the slip cast supports could not be influenced by loading of the slip nor by the sintering temperature (Figure 22). As already mentioned during the result part, sintering didn't take place sufficiently, which is also confirmed by the lack of neck formation that can be seen when investigating the samples using a SEM. Sintering of silicon nitride is usually performed using Al_2O_3 and Y_2O_3 as sintering aids, as it was done for the tubular supports. These oxide additives remaining in the resulting support had initially been planned to be avoided, to get a resulting membrane module solely made of non-oxide ceramic.

The sometimes positive dimension change of the samples during the sintering process (Table 13) is to be interpreted with care, because of problems occurring when measuring the height of the samples. In many cases the samples had a curved topside due to meniscus forming of the slip during the casting process – an exact height thus could not be determined. The attempt to grind the samples to get planar discs failed due to the low mechanical stability of the samples, which led to parts breaking off the sample edges. When considering that, according to the SEM images, almost no sintering took place, one can assume that the dimension change is mostly due to the uncertainty of the measurement and not to the sintering process.

Except for the batches I, II & VII, the preparation of the PDC-supports worked well. The densities are in a range that was expected from previous work. Batches I and II were the first ones pyrolysed in a new furnace. Most likely the gas lines weren't completely tight, leading to oxygen contamination of the atmosphere and partial oxidation of the samples. Batch VII was pyrolysed in between a row of pyrolysis steps of tubular structures which have a higher PE content due to their higher volume, leading to an increasing amount of decomposition products which have to be removed by the N_2 -flow. They condense at the cooler gas outlet leading to a blockage of the same after a while. A reduced nitrogen flow was observed when taking the samples out of the furnace, which confirms the assumption that the gas outlet was partially closed. This could be an explanation for the different properties of the samples of this batch. The samples showing different porosities than expected weren't used for coating experiments.

5.2 INTERMEDIATE LAYER

Initially, N-6 and N-3 were anticipated to yield the best results as silanisation reagents for the stabilization of the slips prepared for the intermediate layer, because of their -NH groups similar to those of the polyvinylsilazane which already showed positive effect on the slip consistence and due to their longer chain length compared to 3-A. but the sedimentation tests showed better performance of the 3-A coated silicon nitride powder (Figure 25). One possible explanation could be that the silanisation reaction didn't work as well for the N-6 and N-3 silanes. This is assumed by the observation of the supernatant after silanisation being yellowish (N-6 has a light yellow colour) when coating the silicon nitride with the N-6 silane. The N-3 silane is colorless, thus nothing similar could be observed.

The 3-A silane was recently bought, whereas the other two chemicals were taken from a storage in the university, already being stored for over 5 years. Maybe this is a reason for the unexpectedly bad performance too.

Nevertheless, 3-A enhanced the stability of the slip enough to choose it for the further experiments.

The use of oleic acid for slip stabilisation didn't work at all. It even decreased the stability of the slip (Figure 24 and Figure 25). Again, the acid was already stored for several years, giving a possible explanation for the failure.

As already mentioned, the preceramic polymer that was used seemed to have a positive effect on the dispersion of the silicon nitride powder. The silicon nitride powder formed large agglomerates before addition of the polyvinylsilazane. The concentration of the polymer is lower in the slip prepared following Mori, apparently resulting in the lower stability of the slip.

In the first coating experiments on the PDC-supports it became obvious that the slip didn't wet the support surface properly, leading to a wavy surface which results in cracks after pyrolysis. Some parts of the surface were even almost uncoated. Grinding the surface showed a profound improvement which leads to the assumption that some decomposition products forming during pyrolysis remained on the surface, influencing the wetting behaviour (Figure 58).

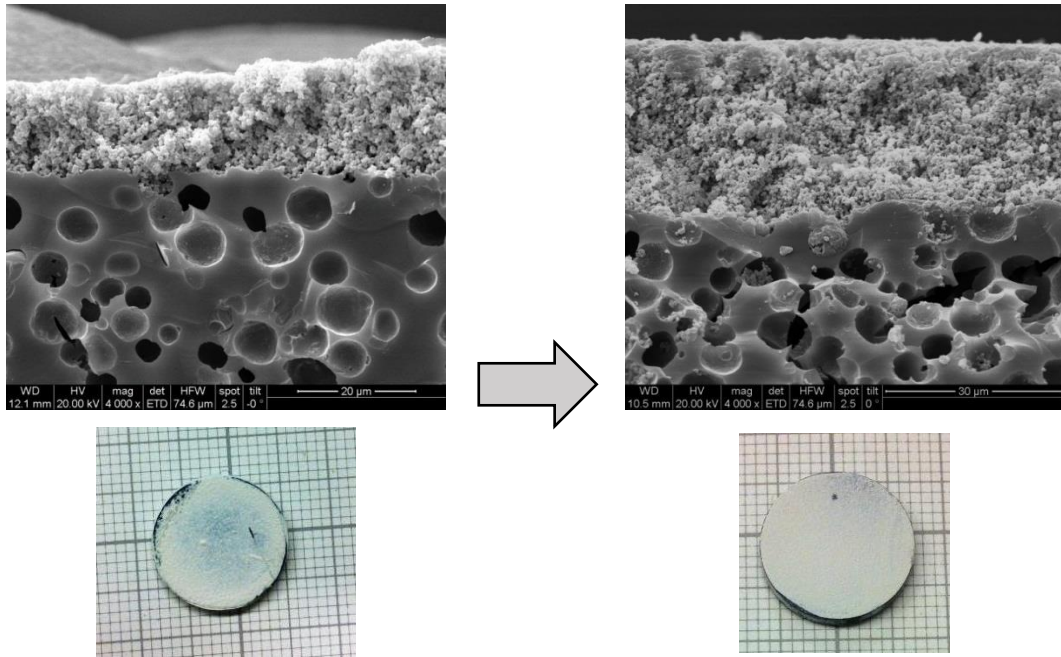


Figure 58: Untreated (left) and ground (right) PDC-support with an intermediate layer, fracture surface and whole sample

The intermediate layer formation behaved differently for the slip cast and the PDC-supports. This can be attributed to their different pore structure and porosity. Filtration effects occurred to a far higher degree for the higher porous slip cast supports with uniform pore structure than for the PDC-supports. A possible explanation could be the closure of the small pore channels connecting the larger spherical pores of the PDC-supports by the silicon nitride particles leading to a decrease in filtration and therefore thinner intermediate layers. In case of the slip cast supports, the silicon nitride powder can't get inside the pores and is therefore forming a structure similar to that of the support without slowing down the filtration process.

Once a concentration yielding a crack free layer was found for the slip cast supports, it could be used for the following samples without any problems.

For the PDC-supports, the chosen concentration of 80 wt% toluene showed promising results when preparing the first samples. When additional samples were coated under the same conditions for the use in further experiments regarding the top layer, cracks in the intermediate layer appeared after pyrolysis. A third batch of samples with the same intermediate layer were prepared, partially showing cracks. The resulting layer thickness when using this concentration seems to be very close to the critical thickness, making the preparation too unreliable.

5.3 TOP LAYER

Preliminary tests went well for the PSZ/toluene solutions. The dependency of layer coating thickness on withdrawal speed and concentration was coherent. A higher withdrawal speed caused a thicker coating because the solution has less time to drip down. A higher concentration leads to thicker coatings for obvious reasons.

The fitting to the Landau-Levich -model was satisfactory, making it possible to adapt it to solutions with different concentrations by measuring their viscosity and surface tension.

The experiments turned out to be more difficult for the PSZ/n-hexane solutions, which were necessary when using masked samples. N-hexane has a higher vapor pressure compared to toluene, making the coating step very sensitive to ambient conditions. For the same reason difficulties occurred during viscosity measurement. The viscosity increased with increasing shear rate which also means with increasing duration of the measurement. Because of the open experimental set up, evaporation of the n-hexane increasing the polymer content of the solution and therefore the viscosity could be a reasonable explanation.

The values calculated using the Landau-Levich-model were always higher than the experimental data, probably because of the difficulties during the coating step which were described previously.

To prove that some kind of barrier has to be put on the support to make the preparation of a dense top layer possible, bare supports were coated. No layer could be observed on none of the samples (Figure 39). The polymer solution penetrated the supports completely, because of capillary forces, and closed some of the pores of the support structures.

The prepared intermediate layer doesn't seem to be enough to prevent penetrating of the dipping solution, although better results could be achieved than for bare support. At first sight it seemed as if a second coating would be the solution on the PDC-supports, but it turned out that the preceramic polymer completely filled the intermediate layer (Figure 40). That would fulfill the separation aims, but is simply too thick (with about 30 μm instead of 1 μm) to also provide enough permeation for possible future application as gas separation membrane.

A promising additional strategy was masking of the samples with polystyrene following Elyassi et al. [53]. During the experiments it turned out that polystyrene concentrations of 15 times higher than those reported had to be used to reach decent results. When leaving aside that a different support material and preceramic polymer were used (SiC-membrane module), the support structure seems to be denser than the ones prepared in this thesis

which would explain why a lower concentration is already sufficient to fill the pores (comparing Figure 59 and Figure 51 below).

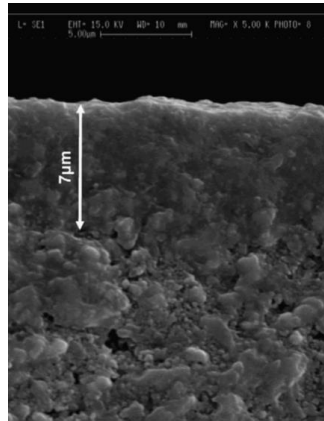


Figure 59: SiC-support after three alternating masking and coating steps prepared by Elyassi et al. (Figure 4 in [53])

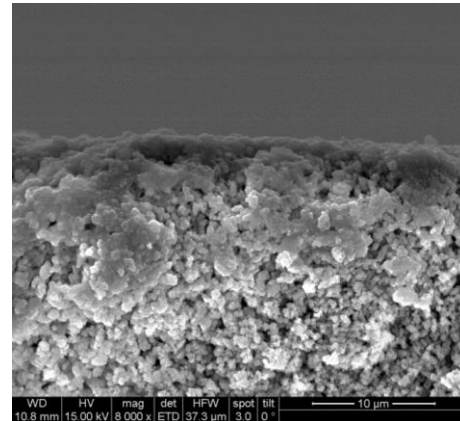


Figure 51: Oversaturation with masking solution and grinding the excessive PS off

Conventional styrofoam gave equally well/slightly better results compared to the purchased polystyrene, likely due to the extremely high molecular weight of styrofoam.

The use of intermediate layers of the same thickness on both support types would presume that the following coating steps can be carried out using the same parameters for both. When looking at the results, it is obvious that this isn't the case, probably for the same reason as during intermediate layer forming itself. The underlying support still influences the behaviour as already discussed in more detail above (5.2).

By using different dwelling times and masking steps, acceptable results could be achieved for both support types. For the PDC-support one masked step was enough, followed by a top layer coating to close remaining cracks. For the slip cast supports, two masked steps were necessary, followed by a one without masking to close remaining cracks.

5.4 COMPARISON OF PLANAR AND TUBULAR SAMPLES

The adaption of the chosen methods to the tubular support structures went very well. Already during intermediate layer formation, a denser part formed on the outer surface for both support types, which can be seen in the SEM-images as well as because of the colour change during pyrolysis (Figure 53 and Figure 56). This means that the method worked even better for the tubular samples than for the planar ones. The comparison of the intermediate layer on a planar and a tubular PDC-support is shown in Figure 60.

In case of the slip cast supports, this is most likely due to their denser support structure caused by the addition of sintering aids to the slips. However, for the same reason the use of such an intermediate layer becomes questionable; the support looks even denser than the intermediate layer. Directly masking the support would probably lead to even better results, while saving at least two days of preparation time (cross linking overnight and pyrolysis for 25 hours for the intermediate layer).

For the PDC-supports – the planar as well as the tubular ones – an intermediate layer is necessary because a masking technique like this can't close the pores formed by the sacrificial PE-fillers.

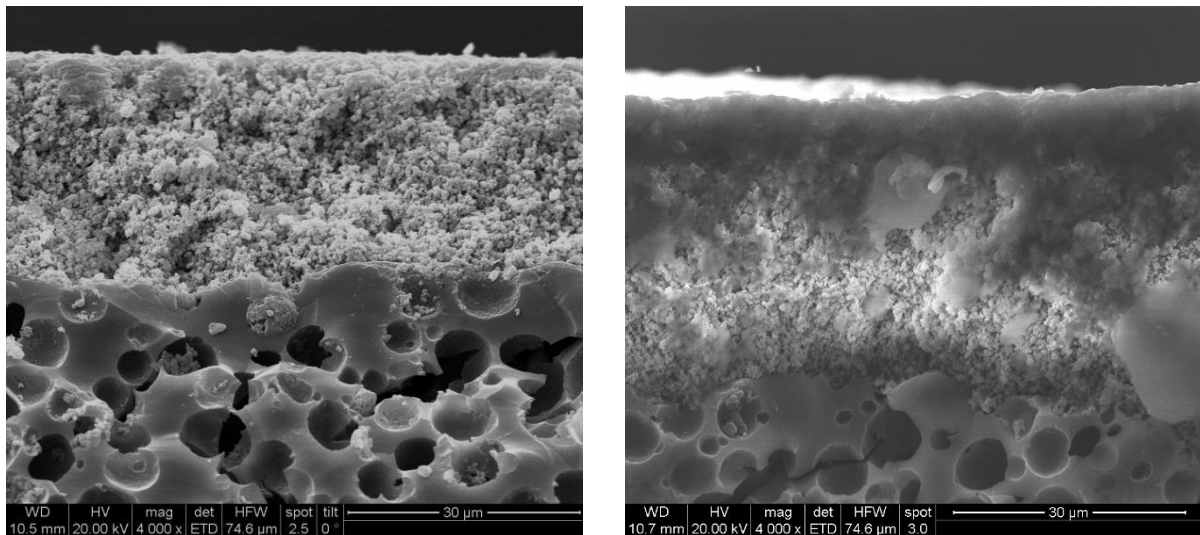


Figure 60: Planar (left) and tubular (right) PDC-support with intermediate layer, fracture surface

5.5 PERMEATION BEHAVIOUR

The results of the planar PDC-supported sample are consistent. The increase of permeability after the grinding step confirms the theory that decomposition products condensed at the surface, influencing the wetting behaviour when applying the intermediate layer. They are removed through the grinding step, opening the pores at the surface and therefore enhancing the permeability.

The intermediate layer decreases the permeability, which means that the layer is less porous than the support structure and is therefore the limiting factor for the permeability so far.

The top layer led to further decrease of the permeability, as expected, because of its almost dense structure.

The investigations on the tubular samples were only carried out for the final structure, because the support structure wasn't defect free showing, a large crack almost over the whole length of the sample, which couldn't be closed completely with the intermediate layer. This is an explanation for the good permeability of the final structure, too, which isn't consistent with the SEM-images that actually showed good layer formation.

Only the tubular and not the planar samples with slip cast supports were investigated. On the one hand because they couldn't be compared with each other because of the differently prepared support structure, on the other hand because no planar samples were left as whole ones.

The relatively similar permeabilities with and without intermediate layer show that the support structure seems to be the limiting part, which also means that it is denser than the intermediate layer. This again questions the necessity of an intermediate layer on the supports prepared with sintering aids as already mentioned above.

The top layer does not decrease the permeability; an explanation could be cracks occurring during fixation of the sample in the testing setup. Another possible explanation could be that another support was coated with the intermediate layer and the top layer than the one that was measured because the SEM investigations required cutting off a little piece of the sample and the quality of the remaining sample was reduced through the cutting process. Although the supports were sintered in the same batch, which usually means that they have the same porosity, little differences of the permeability of support and intermediate layer are likely.

The permeation testing can only be seen as rough impression of the actual behaviour of the samples. Only one sample was tested for each type of support structure; the tubular PDC-support structure did even show large defects. Nevertheless, some effects related to the different coating steps can be seen.

6 SUMMARY

Two of the three planned routes to manufacture the macroporous support structures were implemented successfully, namely slip casting of Si_3N_4 and pyrolysis of a polyvinylsilazane (preceramic polymer) with use of PE as sacrificial filler.

The third one - warm pressing - wasn't investigated further due to poor first results and time constraints.

The powder based route resulted in samples with a porosity of about 52 %, thus lying above the desired value of 30-40%. This was mainly due to the lack of sintering additives to avoid oxide impurities in the final support ($\text{Al}_2\text{O}_3/\text{Y}_2\text{O}_3$ are commonly used as sintering aid). Looking at the resulting support structures, sintering barely took place no matter which temperature or loading of the slip was used. Although the porosity was higher than desired, the coating experiments were nonetheless carried out on these supports.

The tubular support structures that were used, were prepared during another thesis of a member of the research group, whose focus was the support preparation. For the previously mentioned reason it was decided to use sintering aids; thus the tubular structures have lower porosity than the disc shaped samples, on which the actual coating experiments were carried out, leading to adaption of some parameters when testing the results on these tubular structures.

The polymer derived route resulted in samples with a porosity of approximately 44 %. The tubular supports were prepared in the same way. Therefore, the same conditions could be used as for coating of the disc shaped samples.

The pore structure of the two different types of support structures differed significantly. Whereas the slip cast support has a uniform pore size, the PDC-support has large pores due to the filler burnout which are connected via small channels resulting in different coating behaviour.

It was proven that direct coating of both support types was not successful. The polymer solution used for the top layer penetrated the supports, which led to partially closed pores after crosslinking and pyrolysis. No layer could be observed on top of the samples.

The preparation of an intermediate layer was the first step to solve that problem. To combine the structural and chemical properties of both the support structure and the top layer, a slurry containing Si_3N_4 powder and the polyvinylsilazane as well as toluene as a solvent was used.

Two different compositions were prepared, which both turned out to be highly unstable. Two strategies were chosen to enhance the stability: oleic acid as dispersion aid, and silanisation of the silicon nitride powder. In the latter one, three different silanisation reagents were tested. The stability of the slips was tested by investigating the sedimentation behaviour.

The polyvinylsilazane turned out to act as dispersion aid for the silicon nitride powder. Oleic acid didn't show any positive effect on the slip stability. Silanisation enhanced the stability – 3-Aminopropyltrimethoxysilane as silanisation reagent showed the best results. A ratio of 16.4:12 wt% of silicon nitride to polyvinylsilazane was chosen. Slips of different concentrations were prepared ranging from a toluene content of 45 wt% to 91 wt%.

The layer was deposited via dipcoating. Filtration effects due to the pore structure of the support resulted in higher layer thicknesses than expected. The slip with 91 wt% toluene was used for the slip cast supports, yielding in a homogenous, crackfree layer with a thickness of about 30 µm after pyrolysis.

The PDC-supports had to be ground before applying the intermediate layer, to allow sufficient wetting of the surface. In contrast to untreated supports, which showed a wavy layer with large cracks and uncoated parts, the ground samples showed a uniform thickness over the whole support. A concentration of 85 wt% toluene was used for the PDC-supports, yielding in a layer thickness of again approximately 30 µm.

The top layer coating on top of the intermediate layer didn't work as desired. The solution penetrated the intermediate layer as well, but especially for the PDC-supported samples not as much as the support structure. To obtain better results, the composition of the intermediate layer should probably be changed to get a denser structure, for example by increasing the preceramic polymer content.

Therefore, an additional step had to be added to the process. The samples were masked using polystyrene, which can be burned out during pyrolysis revealing the original pore structure. Another solvent has to be used for the top layer dip coating solution, because toluene would dissolve the polystyrene; n-hexane was chosen. Parameters such as polystyrene type (commercial available polystyrene or styrofoam), polystyrene concentration in the masking solution, dwelling time in the masking solution, as well as the necessity of an intermediate layer on the slip cast supports were investigated. Multiple coating runs of alternating masking and top layer coating steps turned out to be necessary.

Some extra steps were tested on the samples with slip cast supports: heating the sample before masking to assemble the polystyrene close to the surface or repeating the masking step before top layer coating. The latter one led to another idea, because a PS layer formed

on the surface of the sample resulting in a clearly visible top layer, which unfortunately didn't connect to the intermediate layer but only to the polystyrene layer and therefore detached during pyrolysis. The PS layer was formed on purpose by dipping the sample several times until the layer was visible followed by grinding off the excessive PS before coating with the preceramic polymer. A dense layer could be formed in the crosslinked stage but unfortunately showed crackformation during pyrolysis.

Styrofoam was the polystyrene of choice due to equally good results as the industrial polystyrene, but easier and cheaper access. The highest polystyrene concentration of 15 wt% in toluene gave the best results for both types of supports. While the samples with slip cast supports showed slightly better results for a dwelling time of 1 s, the samples using PDC-supports did for the longer dwelling time of 15 s.

Although the structure of the intermediate layer doesn't differ much from the structure of slip cast supports, the surface becomes smoother when applying the layer, providing a better substrate for the following coatings. Thus, samples with intermediate layer were used for both support types.

The best results for the samples with PDC-supports were achieved by masking the samples using the 15 wt% polystyrene solution and a dwelling time of 15 s. The top layer was applied using the 50 vol% polysilazane/n-hexane solution, a withdrawal speed of 140 mm/min and a dwelling time of 1 s. After that step, a second polysilazane coating step without previous masking was done to close the remaining cracks in the surface. The same procedure was followed for the tubular samples.

The best results for the samples with slip cast supports were the ones mentioned above where the samples are oversaturated with PS and excessive PS was grinded off before the top layer coating step. Good results were also achieved using two runs of masking in 15 wt% PS solution with a dwelling time of 1 s and top layer coating followed by one run without masking step. The second method was used for the tubular samples, because grinding curved samples leads to difficulties.

The coating of the tubular structures was successful for both types of supports. The results were even slightly better than those of the planar supports.

Dip coating parameters to obtain a top layer with a thickness of about 1 μm were found during preliminary tests on dense substrates investigating the dip coating behaviour of differently concentrated solutions of the preceramic polymer and varying withdrawal speeds. Viscosity and surface tension of the solutions were measured to find out if the Landau-

Levich-model can be applied to these solutions. When considering that the final coating is a solid and crosslinking takes place, by adding two parameters to the original Landau-Levich-equation, the model fits the experimental values very well for the PSZ/toluene solutions and sufficiently well for the PSZ/n-hexane solutions.

7 REFERENCES

1. Zhou, Y., M. Fukushima, H. Miyazaki, Y.-i. Yoshizawa, K. Hirao, Y. Iwamoto, and K. Sato, *Preparation and characterization of tubular porous silicon carbide membrane supports*. Journal of Membrane Science, 2011. **369**(1–2): p. 112-118.
2. Deng, W., X. Yu, M. Sahimi, and T.T. Tsotsis, *Highly permeable porous silicon carbide support tubes for the preparation of nanoporous inorganic membranes*. Journal of Membrane Science, 2014. **451**: p. 192-204.
3. Fukushima, M., Y. Zhou, H. Miyazaki, Y.-i. Yoshizawa, K. Hirao, Y. Iwamoto, S. Yamazaki, and T. Nagano, *Microstructural Characterization of Porous Silicon Carbide Membrane Support With and Without Alumina Additive*. Journal of the American Ceramic Society, 2006. **89**(5): p. 1523-1529.
4. Kikuchi, E., Y. Nemoto, M. Kajiwara, S. Uemiya, and T. Kojima, *Steam reforming of methane in membrane reactors: Comparison of electroless-plating and CVD membranes and catalyst packing modes*. Catalysis Today, 2000. **56**(1-3): p. 75-81.
5. Biesheuvel, P.M. and H. Verweij, *Design of ceramic membrane supports: permeability, tensile strength and stress*. Journal of Membrane Science, 1999. **156**(1): p. 141-152.
6. Verweij, H., Y.S. Lin, and J. Dong, *Microporous Silica and Zeolite Membranes for Hydrogen Purification*. MRS Bulletin, 2006. **31**(10): p. 756-764.
7. Elyassi, B., M. Sahimi, and T.T. Tsotsis, *Silicon carbide membranes for gas separation applications*. Journal of Membrane Science, 2007. **288**(1–2): p. 290-297.
8. <https://www.ceramtec.com/ceramic-materials/silicon-nitride/>; 15.5.2016
9. <http://www.azom.com/article.aspx?ArticleID=53> ; 08.08.2016
10. <http://accuratus.com/silinit.html>; 07.08.2016
11. Colombo, P., G. Mera, R. Riedel, and G.D. Sorarù, *Polymer-Derived Ceramics: 40 Years of Research and Innovation in Advanced Ceramics*. Journal of the American Ceramic Society, 2010. **93**(7): p. 1805-1837.
12. T. Konegger, R. Bordia: "Polymer-derived Ceramics with Multiscale Porosity for Gas Separation Applications"; Poster: CCOMC Fall Meeting 2014, Anderson; 23.09.2014 - 24.09.2014
13. Riedel, R., G. Mera, R. Hauser, and A. Klönczynski, *Silicon-based polymer-derived ceramics: Synthesis properties and applications-A review*. Nippon Seramikkusu Kyokai Gakujutsu Ronbunshi/Journal of the Ceramic Society of Japan, 2006. **114**(1330): p. 425-444.
14. Sarkar, S. and L. Zhai, *Polymer-Derived Non-Oxide Ceramic Fibers; Past, Present and Future*. Materials Express, 2011. **1**(1): p. 18-29.
15. Günthner, M., T. Kraus, A. Dierdorf, D. Decker, W. Krenkel, and G. Motz, *Advanced coatings on the basis of Si(C)N precursors for protection of steel against oxidation*. Journal of the European Ceramic Society, 2009. **29**(10): p. 2061-2068.
16. Konegger, T., C.-C. Tsai, and R.K. Bordia, *Preparation of polymer-derived ceramic coatings by dip-coating*. Materials Science Forum, 2015: p., in press.
17. Konegger, T., C.C. Tsai, and R.K. Bordia, *Preparation of polymer-derived ceramic coatings by dip-coating*, in *Materials Science Forum 2015*. p. 645-652.
18. Konegger, T., R. Patidar, and R.K. Bordia, *A novel processing approach for free-standing porous non-oxide ceramic supports from polycarbosilane and polysilazane precursors*. Journal of the European Ceramic Society, 2015. **35**(9): p. 2679-2683.
19. Konegger, T., L.F. Williams, and R.K. Bordia, *Planar, Polysilazane-Derived Porous Ceramic Supports for Membrane and Catalysis Applications*. Journal of the American Ceramic Society, 2015. **98**(10): p. 3047-3053.
20. Schulz, M., *Polymer derived ceramics in MEMS/NEMS – a review on production processes and application*. Advances in Applied Ceramics, 2009. **108**(8): p. 454-460.
21. Grossenbacher, J., M.R. Gullo, V. Bakumov, G. Blugan, J. Kuebler, and J. Brugger, *On the micrometre precise mould filling of liquid polymer derived ceramic precursor*

- for 300-mm-thick high aspect ratio ceramic MEMS. *Ceramics International*, 2015. 41(1): p. 623-629.
22. Mori, H., S. Mase, N. Yoshimura, T. Hotta, K. Ayama, and J.I. Tsubaki, *Fabrication of supported Si₃N₄ membranes using the pyrolysis of liquid polysilazane precursor*. *Journal of Membrane Science*, 1998. 147(1): p. 23-33.
 23. Tsubaki, J., H. Mori, K. Ayama, T. Hotta, and M. Naito, *Characterized microstructure of porous Si₃N₄ compacts prepared using the pyrolysis of polysilazane*. *Journal of Membrane Science*, 1997. 129(1): p. 1-8.
 24. Vakifahmetoglu, C., D. Zeydanli, and P. Colombo, *Porous polymer derived ceramics*. *Materials Science and Engineering: R: Reports*, 2016. 106: p. 1-30.
 25. Fooki, A.C.B.M., A.H. Aparecida, T.B. Fideles, R.C. Costa, and M.V.L. Fook, *Porous hydroxyapatite scaffolds by polymer sponge method*. *Key Engineering Materials*, 2009. 396-398: p. 703-706.
 26. Deisinger, U., *Generating porous ceramic scaffolds: Processing and properties*. *Key Engineering Materials*, 2010. 441: p. 155-179.
 27. Ben-Nissan, B., *Natural bioceramics: from coral to bone and beyond*. *Current Opinion in Solid State and Materials Science*, 2003. 7(4-5): p. 283-288.
 28. Hoffmann, C., B. Reinhardt, D. Enke, and S. Kaskel, *Inverse silicon carbide replica of porous glasses*. *Microporous and Mesoporous Materials*, 2014. 184: p. 1-6.
 29. Tancred, D.C., B.A.O. McCormack, and A.J. Carr, *A synthetic bone implant macroscopically identical to cancellous bone*. *Biomaterials*, 1998. 19(24): p. 2303-2311.
 30. Tang, L.Q., W. Ni, H.Y. Zhao, Q. Xu, and J.X. Jiao, *Preparation of macroporous TiO₂ by starch microspheres template with assistance of supercritical CO₂*. *BioResources*, 2009. 4(1): p. 38-48.
 31. Rodríguez-Lorenzo, L.M. and K.A. Gross, *Calcium Phosphate Porous Scaffolds from Natural Materials*. *Key Engineering Materials*, 2004. 254-256: p. 957-960.
 32. Vijayan, S., R. Narasimman, and K. Prabhakaran, *A urea crystal templating method for the preparation of porous alumina ceramics with the aligned pores*. *Journal of the European Ceramic Society*, 2013. 33(10): p. 1929-1934.
 33. Shi, Y., Y. Meng, D. Chen, S. Cheng, P. Chen, H. Yang, Y. Wan, and D. Zhao, *Highly ordered mesoporous silicon carbide ceramics with large surface areas and high stability*. *Advanced Functional Materials*, 2006. 16(4): p. 561-567.
 34. Shi, Y., Y. Wan, B. Tu, and D. Zhao, *Nanocasting synthesis of ordered mesoporous silicon nitrides with a high nitrogen content*. *Journal of Physical Chemistry C*, 2008. 112(1): p. 112-116.
 35. Kotani, M., K. Nishiyabu, S. Matsuzaki, and S. Tanaka, *Processing of polymer-derived porous SiC body using allylhydridopolycarbosilane (AHPCS) and PMMA microbeads*. *Nippon Seramikkusu Kyokai Gakujutsu Ronbunshi/Journal of the Ceramic Society of Japan*, 2011. 119(1391): p. 563-569.
 36. Schmalz, T., J.M. Hausherr, W. Müller, T. Kraus, W. Krenkel, R. Kempe, and G. Motz, *Analysis of polyethylene-particle filled SiCN precursor and the resulting porous ceramics with emphasis on using micro computed tomography*. *Nippon Seramikkusu Kyokai Gakujutsu Ronbunshi/Journal of the Ceramic Society of Japan*, 2011. 119(1390): p. 477-482.
 37. Sung, I.K., Christian, M. Mitchell, D.P. Kim, and P.J.A. Kenis, *Tailored Macroporous SiCN and SiC Structures for High-Temperature Fuel Reforming*. *Advanced Functional Materials*, 2005. 15(8): p. 1336-1342.
 38. Fukushima, M. and P. Colombo, *Silicon carbide-based foams from direct blowing of polycarbosilane*. *Journal of the European Ceramic Society*, 2012. 32(2): p. 503-510.
 39. Konegger, T., R. Felzmann, B. Achleitner, and D. Brouczek, *Mullite-based cellular ceramics obtained by a combination of direct foaming and reaction bonding*. *Ceramics International*, 2015. 41(7): p. 8630-8636.

40. Gaudillere, C. and J.M. Serra, *Freeze-casting: Fabrication of highly porous and hierarchical ceramic supports for energy applications*. *Boletín de la Sociedad Española de Cerámica y Vidrio*, 2016. 55(2): p. 45-54.
41. Tang, Y., S. Qiu, Q. Miao, and C. Wu, *Fabrication of lamellar porous alumina with axisymmetric structure by directional solidification with applied electric and magnetic fields*. *Journal of the European Ceramic Society*, 2016. 36(5): p. 1233-1240.
42. Deville, S., C. Viazzi, and C. Guizard, *Ice-Structuring Mechanism for Zirconium Acetate*. *Langmuir*, 2012. 28(42): p. 14892-14898.
43. Naviroj, M., S.M. Miller, P. Colombo, and K.T. Faber, *Directionally aligned macroporous SiOC via freeze casting of preceramic polymers*. *Journal of the European Ceramic Society*, 2015. 35(8): p. 2225-2232.
44. Hüsing, N. and U. Schubert, *Aerogels - Airy Materials: Chemistry, Structure, and Properties*. *Angewandte Chemie - International Edition*, 1998. 37(1-2): p. 22-45.
45. Soleimani Dorcheh, A. and M.H. Abbasi, *Silica aerogel; synthesis, properties and characterization*. *Journal of Materials Processing Technology*, 2008. 199(1-3): p. 10-26.
46. Bakumov, V., M. Schwarz, and E. Kroke, *Emulsion processing of polymer-derived porous Si/C(O) ceramic bodies*. *Journal of the European Ceramic Society*, 2009. 29(13): p. 2857-2865.
47. Vakifahmetoglu, C., M. Balliana, and P. Colombo, *Ceramic foams and micro-beads from emulsions of a preceramic polymer*. *Journal of the European Ceramic Society*, 2011. 31(8): p. 1481-1490.
48. Barg, S., B.P. Binks, H. Wang, D. Koch, and G. Grathwohl, *Cellular ceramics from emulsified suspensions of mixed particles*. *Journal of Porous Materials*, 2012. 19(5): p. 859-867.
49. Binks, B.P., *Macroporous Silica From Solid-Stabilized Emulsion Templates*. *Advanced Materials*, 2002. 14(24): p. 1824-1827.
50. Ciora, R.J., B. Fayyaz, P.K.T. Liu, V. Suwanmethanond, R. Mallada, M. Sahimi, and T.T. Tsotsis, *Preparation and reactive applications of nanoporous silicon carbide membranes*. *Chemical Engineering Science*, 2004. 59(22-23): p. 4957-4965.
51. Elyassi, B., W. Deng, M. Sahimi, and T.T. Tsotsis, *On the Use of Porous and Nonporous Fillers in the Fabrication of Silicon Carbide Membranes*. *Industrial & Engineering Chemistry Research*, 2013. 52(30): p. 10269-10275.
52. Hedlund, J., F. Jareman, A.-J. Bons, and M. Anthonis, *A masking technique for high quality MFI membranes*. *Journal of Membrane Science*, 2003. 222(1-2): p. 163-179.
53. Elyassi, B., M. Sahimi, and T.T. Tsotsis, *A novel sacrificial interlayer-based method for the preparation of silicon carbide membranes*. *Journal of Membrane Science*, 2008. 316(1-2): p. 73-79.
54. Wang, C., L. Ling, Y. Huang, Y. Yao, and Q. Song, *Decoration of porous ceramic substrate with pencil for enhanced gas separation performance of carbon membrane*. *Carbon*, 2015. 84: p. 151-159.
55. Khosravi, A., J.A. King, H.L. Jamieson, and M.L. Lind, *Latex Barrier Thin Film Formation on Porous Substrates*. *Langmuir*, 2014. 30(46): p. 13994-14003.
56. Xomeritakis, G., C.M. Braunbarth, B. Smarsly, N. Liu, R. Köhn, Z. Klipowicz, and C.J. Brinker, *Aerosol-assisted deposition of surfactant-templated mesoporous silica membranes on porous ceramic supports*. *Microporous and Mesoporous Materials*, 2003. 66(1): p. 91-101.
57. Tseng, H.-H., K. Shih, P.-T. Shiu, and M.-Y. Wey, *Influence of support structure on the permeation behavior of polyetherimide-derived carbon molecular sieve composite membrane*. *Journal of Membrane Science*, 2012. 405-406: p. 250-260.
58. Wach, R.A., M. Sugimoto, A. Idesaki, and M. Yoshikawa, *Molecular sieve SiC-based membrane for hydrogen separation produced by radiation curing of preceramic polymers*. *Materials Science and Engineering: B*, 2007. 140(1-2): p. 81-89.
59. <http://www.aurelautomation.com/special-equipments/dip-coating-unit/>; 08.08.2016

60. L. Landau, B. Levich, Dragging of a Liquid by a Moving Plate, *Acta Physicochim. URSS* 17 (1942), 42-54.
61. Iijima, M., N. Okamura, and J. Tatami, *Polyethyleneimine–Oleic Acid Complex as a Polymeric Dispersant for Si₃N₄ and Si₃N₄-Based Multicomponent Nonaqueous Slurries*. *Industrial & Engineering Chemistry Research*, 2015. 54(51): p. 12847-12854.
62. Yan, L., W. Si, S. Lin, H. Miao, and L. Qi, *Influence of coupling agents on the chemical compatibility between ultrafine Si₃N₄ powders and organic binders*. *Key Engineering Materials*, 2002. 224-226: p. 691-696.
63. http://www.amchro.com/uct/Silane_Coupling_Agents_2014_4101-32-03.pdf; 09.08.2016
64. <http://www.gelest.com/product/3-aminopropyltrimethoxysilane/>; 03.09.2016
65. <http://www.gelest.com/product/n-2-aminoethyl-3-aminopropyltrimethoxysilane-tech-95/>; 03.09.2016
66. <http://www.kruss.de/products/tensiometers/force-tensiometer-k6/> ; 9.5.2016
67. T.Konegger, T.Prochaska, R.Obmann, *Journal of the Japanese Ceramic Society* (2016), in press.
68. Innocentini M, Sepulveda P, Ortega F, Permeability, in: Scheffler M., Colombo P. (Eds.), *Cellular Ceramics*, Wiley-VCH, Weinheim, 2005, pp. 313-41.